

Environmental Research Center Papers

Number 11

1987

Environmental Research Center
The University of Tsukuba

VARIATIONS IN THE URBAN HEAT ISLAND INTENSITY AFFECTED BY GEOGRAPHICAL ENVIRONMENTS*

By Hye-Sook PARK**

(received March 5, 1987)

ABSTRACT

The main object of this research was to examine the urban influence and the topographical effects on the heat island intensity.

First, influences caused by the urban structures on the heat island intensity were discussed. The relationships between the maximum heat island intensity and the urban population are approximately linear and proportional, and regression lines can be represented as linear lines for American and European cities (Oke, 1973). By contrast, in Japanese and Korean cities the relationship changes at around 300,000 population. At that level the regression lines bend so that, in effect, there are lines in two directions, one for cities smaller than 300,000 population, another for larger cities. The increments of the maximum heat island intensity for cities with populations over 300,000 are larger than those for cities with populations under 300,000. That means that in Japan and Korea, the function and structure of cities above a population of 300,000 are different from those with smaller populations. In order to quantify and relate the differences of urban function and structure to the heat island intensity, the author has employed the urban population as an index of urban function and the sky view factor and the impermeable surface coverage ratio as indices of urban structure. Although the relationship between the sky view factor and the urban population did not alter remarkably at around 300,000 in population in Japanese and Korean cities, Japanese cities can be divided into two groups. One includes the cities which have a sky view factor that accords with their populations, the other the cities which have a larger sky view factor than expected from their populations. On the other hand, the relationships between the impermeable surface coverage ratio and the urban population were represented by a biphasic regression line for cities in both countries, with a slope transition occurring at the 500,000 population level. It is considered that the impermeable surface coverage ratio is probably not the only factor involved in this biphasic correlation, but is probably a key to understanding it.

As a next step, the physical meanings of each index were discussed based on the heat balance at the ground surface. The results are as follows. The sky view factor (an index of urban geometry) and the impermeable surface coverage ratio (an index of the thermal structure of the ground surface) are closely correlated with the radiation and heat balance at the ground surface which are related to radiative cooling during the clear and calm nights.

Second, the topographical factors of location on the coast, location on a plain inland from the coast, and location in a basin, which affected the heat island intensi-

* A dissertation submitted in partial fulfilments for the degree of Doctor of Science in Doctoral Program in the University of Tsukuba.

** Address from April 1, 1987 is the Institute of Geoscience, the University of Tsukuba.

ty, were discussed. A basin city does not seem to be much influenced by advection. On the other hand, the advection by sea-breezes in a coastal city seems very strong all day long during daytime in summer. Particularly, the cooling amounts of temperature (ΔT_{t-s}) and cooling rates ($\Delta T/\Delta t$) from sunset until sunrise in a basin city are higher than those of inland and coastal cities. These differences influence the nocturnal heat island intensity. Climatic analyses show that the heat island intensity is remarkably developed in winter nighttime, but is weak in summer daytime.

Furthermore, the heat island intensity is affected by the difference between the intensity of the nocturnal surface inversion in the urban area and the nocturnal surface inversion in the nearby rural area. In a basin city, the surface inversion layer is highly notable and is caused by radiative cooling, which produces a strong heat island intensity. On the other hand, in a coastal city, a surface inversion layer does not form because there is much advection effect caused by cool sea-breezes, and the heat island intensity is negative or slightly positive.

Finally, the urban influences and the topographical effects on the heat island intensity are summarized and schematic models are presented.

CONTENTS

ABSTRACT	1
LIST OF FIGURES	5
LIST OF TABLES	7
LIST OF SYMBOLS	8
CHAPTER I INTRODUCTION	9
1.1 Previous studies	9
1.2 Purpose of this study	12
CHAPTER II DATA AND METHODS	13
2.1 Flow of this study	13
2.2 Field observation data	13
2.2.1 Data on the heat island intensity	13
2.2.2 Data on the sky view factor	15
2.2.3 Special observation data	15
2.3 Published data	16
2.4 AMcDAS data	17
CHAPTER III RELATIONSHIPS BETWEEN URBAN STRUCTURES AND THE HEAT ISLAND INTENSITY	20
3.1 Statistical analyses of the relationships between the indices of urban structures and the maximum heat island intensity	20
3.1.1 City size and the maximum heat island intensity	20
3.1.2 Relationships between the indices of urban structure and the maximum heat island intensity	22
3.1.3 Interrelationships between the indices of urban structures, urban population and the maximum heat island intensity	25
3.2 Thermal characteristics induced by urban structures	28
3.2.1 Heat balance at the ground surface	28
3.2.2 Urban canyon geometry and long-wave radiation	30
3.2.3 Thermal admittance and the heat island intensity	39
CHAPTER IV TOPOGRAPHICAL EFFECTS ON THE HEAT ISLAND INTENSITY	43
4.1 The heat island intensity and city size classification based on topographical factors	43
4.2 Contrasting phenomena in the heat island intensity among the three types of cities	43
4.2.1 City located on an inland plain	44
4.2.2 City located in a basin	50
4.2.3 Coastal city	50
4.2.4 Comparing the cities from the topographical perspective	53
4.3 Spatial and temporal aspects of the heat island intensity in the three types of cities	54

4.3.1	Diurnal variations of the heat island intensity	54
4.3.2	Annual variations of the heat island intensity	57
4.4	Characteristics of the surface inversion layer in two different topographical locations	60
4.4.1	Surface inversion layer in a basin city	60
4.4.2	Surface inversion layer in a coastal city	62
4.4.3	Comparing features of the surface inversion layers in the two cities	64
4.5	Schematic models of urban influences and topographical effects on the urban heat island	67
CHAPTER V CONCLUSIONS		70
ACKNOWLEDGEMENT		73
REFERENCES		74

LIST OF FIGURES

FIGURE	PAGE
1 Flow of this study	14
2 Distribution of settlements for which climatological and geographical data were obtained	18
JAPAN : 1. Tokyo 2. Osaka 3. Nagoya 4. Kyoto 5. Sapporo 6. Hiroshima	
7. Sakai 8. Kumamoto 9. Sendai 10. Niigata 11. Shizuoka 12. Kanazawa	
13. Gifu 14. Asahikawa 15. Nagano 16. Hakodate 17. Toyama 18. Aomori	
19. Maebashi 20. Fukui 21. Akita 22. Morioka 23. Takada 24. Tsuchiura	
25. Isezaki 26. Tatebayashi 27. Wakkanai 28. Shinjoh 29. Akikawa	
30. Mitsukaido 31. Shimozuma 32. Shin-machi 33. Tamamura-cho	
KOREA : 1. Seoul 2. Taegu 3. Taejon 4. Seongnam 5. Kwangmyung	
6. Euijeongbu 7. Shindo	
3 Relationships between the maximum heat island intensity and the urban population for Japanese, Korean, North American and European cities	20
4 Relationships between the maximum heat island intensity and the sky view factor for Japanese, Korean, North American and European cities	23
5 Relationships between the maximum heat island intensity and impermeable surface coverage ratio for Japanese and Korean cities	24
6 Relationships between sky view factor and the urban population for Japanese, Korean, North American and European cities	25
7 Relationships between impermeable surface coverage ratio and the urban population for Japanese and Korean cities	27
8 Flow of heat balance at the ground surface	29
9 Distribution of ground surface temperatures in and near Mitsukaido City (1986. 4. 14. 04 : 00-05 : 30)	30
10 Distribution of air temperatures in and near Mitsukaido City (1986. 4. 14. 04 : 00-04 : 30)	31
11 Distribution of sky view factors in and near Mitsukaido City (1986. 4. 14)	32
12 Distribution of the ground surface temperature, the air temperature, the cooling amounts of the ground surface temperature, the diurnal range of the ground surface temperature, and the sky view factor at the observation points along A to B spanning a suburban area	33
13 Relationship between the sky view factor and the ground surface temperature (04 : 00-05 : 30) at designated points in the urban area	33
14 Fish-eye lens photographs taken from (a) ground surface and (b) roof surface levels illustrating the reduction of the sky view factor by buildings. Sky view factor 0.51 for (a) and 0.94 for (b)	34
15 Hourly changes of surface temperatures and air temperatures for three observation points	35
16 Decrease after sunset of the ground surface temperature and of the roof surface temperature in the urban area	36

17	Hourly mean in the long-wave radiation components of the ground surface and the roof surface level	37
18	Comparison of the downward long-wave radiation at the ground surface ($L_g \downarrow$) with the sum of the downward long-wave radiation at the roof surface level ($L_r \downarrow$) and the long-wave radiation from the wall surface ($L_w \downarrow$)	38
19	Mean hourly urban-rural cooling rates (A) and heat island intensities (B). Urban area has two surface levels, ground surface and roof surface	39
20	Surface temperature decrease after sunset in urban (two levels, ground surface and roof surface) and rural areas	41
21	Variation of surface temperature decrease from sunset, net long-wave radiation at the surface and their ratio, versus time from sunset between urban and rural areas	41
22	Relationships between the maximum heat island intensity and the urban population are compared in three categories, basin, inland plain, and coastal cities	44
23	Surface weather maps of days for which data were collected. Upper is summer and lower is winter	45
24	Diurnal variations of air temperature, cooling and warming rates, heat island intensity, wind, and sunshine duration in Gifu City for Aug. 1-2, 1981	46
25	Same as Fig. 24, but for Jan. 30-31, 1981	47
26	Diurnal variations of air temperature, cooling and warming rates, heat island intensity, wind, and sunshine duration in Asahikawa City for Aug. 20-21, 1984	48
27	Same as Fig. 26, but for Jan. 6-7, 1984	49
28	Diurnal variations of air temperature, cooling and warming rates, heat island intensity, wind, and sunshine duration in Niigata City for Aug. 9-10, 1982	51
29	Same as Fig. 28, but for Jan. 7-8, 1983	52
30	Diurnal variations of the heat island intensity in Asahikawa, Gifu, and Niigata during the summer (1981-1984 ; 23 times)	55
31	Frequency distribution of the heat island intensity of Gifu City in summer. The chosen days same as Fig. 30	56
32	Same as Fig. 31, but for Asahikawa City	57
33	Same as Fig. 31, but for Niigata City	58
34	Annual change of the daily variation in the heat island intensity of Gifu City (1981-1984 ; the average value for each hour on selected days in every month ; °C)	59
35	Same as Fig. 34, but for Asahikawa City (°C)	59
36	Same as Fig. 34, but for Niigata City (°C)	60
37	Comparison of temperature profiles between Asahikawa City and its surrounding area on Jan. 18-19, 1983	61
38	Comparison of temperature and wind profiles between Akita City and its surrounding area on June 9, 1974	63
39	Same as Fig. 38, but for Oct. 14, 1974	64
40	Schematic models of the heat island phenomenon	68

LIST OF TABLES

TABLE	PAGE
1 Latitude, longitude, and elevation of the AMeDAS stations of the chosen cities ...	18
2 Maximum heat island intensity ($\Delta T_{u-r(max)}$), sky view factor, and impermeable surface coverage ratio for Japanese and Korean settlements. Ordered according to population (P)	19
3 Mean of each long-wave radiation component (Wm^{-2}) (April 13-14, 1986, 18:00-05:00)	37
4 Diurnal range of temperature, wind speed, sunshine duration, cooling amounts of temperature from sunset until sunrise (ΔT_{t-s}), and the maximum heat island intensity ($\Delta T_{u-r(max)}$) among the three types of cities	53
5 Characteristics of the surface inversion layer, lapse rate of temperature (γ), wind and the maximum heat island intensity ($\Delta T_{u-r(max)}$) in each city	65

LIST OF SYMBOLS

Roman alphabet

AMeDAS	Automated Meteorological Data Acquisition System
C	specific heat capacity
C_r, K	thermal admittance
H	sensible heat flux
h	building heights
IE	latent heat flux
G_o	ground heat flux
K	heat conductivity
$L \uparrow$	upward long-wave radiation
$L \downarrow$	downward long-wave radiation
$L_r \downarrow$	downward long-wave radiation at the roof surface
$L_s \downarrow$	downward long-wave radiation at the ground surface
$L_w \downarrow$	long-wave radiation from the wall
P	urban population
Q	anthropogenic heat
R_n	net radiation flux
T	surface temperature
T_r	rural air temperature
T_{rn}	rural air temperature in flat land
T_u	urban air temperature
t	time from sunset
X	impermeable surface coverage ratio
w	width of the urban canyon
Z	ground depth

Greek alphabet

α	albedo
γ	lapse rate of temperature
$\Delta T / \Delta t$	cooling and warming rates
ΔT_a	advection
ΔT_r	temperature deviation
ΔT_{r-r}	heat island intensity on the urban roof surface
ΔT_{s-r}	heat island intensity on the urban ground surface
ΔT_{t-s}	cooling amounts of surface temperature from sunset to sunrise
ΔT_{u-r}	heat island intensity
$\Delta T_{u-r(max)}$	maximum heat island intensity
Ψ_s	sky view factor
λ	soil conductivity
ρ	density of the ground surface material
π	circular constant

CHAPTER I

INTRODUCTION

1.1 Previous studies

The urban heat island is an example of man-made climate, and has been intensively studied. The heat island intensity (ΔT_{u-r}) is the difference between the highest urban temperature figure from among all figures for places in the city at any time and lowest background rural temperature figure from among all figures for places in the area surrounding the city at the same time. Therefore, it is the temperature rise caused by the urban influences. The factors that promote the growth of the heat island intensity are complicated. Factors that have been considered to cause the heat island include 1) the anthropogenic heat released by the urban inhabitants, 2) the thermal characteristics of the urban fabric and the urban geometry, and 3) changes of the radiative fields caused by air pollution in the urban area (Kawamura, 1968, 1977 ; Nishizawa, 1973 ; Oke, 1974, 1979 ; Chandler, 1976 ; Landsberg, 1981 ; Lee, 1984 ; Goldreich, 1984).

Generally, the urban population can be considered an integrated measure of urban characteristics, including the physical city size, the geometry and material of the urban surface and anthropogenic energy consumption. The relationship between population and urban functions is well known (Smith, 1965). Large cities have complex urban morphologies. In this study, population is being used as a surrogate variable in place of structure and form. Indeed, Mitchell (1961) produced a model which related urban warming and population growth based on the idea that the amount of warming can be considered to be proportional to the travel distance of air moving from the urban-rural boundary to the urban center. Thus, as a city grows outward as a result of population pressure, its heat island intensity rises. Summers (1965) revealed that the mixing depth produced is proportional to the square root of the heat input in the simplest case of zero wind shear, and that the magnitude of the heat island effect, as defined by the excess city center temperature, is proportional to the square root of the city's length parallel to the wind direction.

Most previous studies conducted from this view-point have been directed at evaluating the effect of a city's growth over time on its heat island (Arakawa, 1937, 1968 ; Mitchell, 1953 ; Fukui, 1957, 1968, 1969 ; Chandler, 1964 ; Moffitt, 1972 ; Yoshino, 1981 ; Yoshino and Kai, 1973_a ; Kikuchi, 1974 ; Macjima *et al.*, 1980). However, some studies have examined the heat islands of many different sizes of settlements in the same period (Duckworth and Sandberg, 1954 ; Oke, 1973 ; Eagleman, 1974 ; Fukuoka, 1983 ; Park, 1986_a, 1986_b ; Jauregui, 1986). Duckworth and Sandberg (1954) suggested that the heat island intensity increases with increasing city size (population, population density and built-up area) using data for San Francisco, San Jose and Palo Alto in the United States. Oke (1973) revealed that there is a linear proportionality between the logarithms of the populations of cities and their maximum heat island intensities ($\Delta T_{u-r(max)}$) in North American and European cities. The slope of the regression line is different for North American and European cities. The reason for this difference in slope was explained by Oke in terms of differences in the urban morphology of European and North American cities, the European having fewer tall buildings. Jauregui (1986) reported similar relationships in tropical cities. However, he suggested that the relationship between the maximum heat island intensity and population in tropical cities seems to display a different slope for cities larger than about 1,000,000 inhabitants than for the smaller cities. This difference in slope could imply that some tropical cities experi-

ence a marked change in their morphology (larger slum areas, reduced proportion of green areas, taller central city buildings, etc.) once they reach a certain size. The present writer (Park, 1986_a) found this same relationship in Korean cities except that the dividing population size was 300,000 rather than 1,000,000. The research pointed to a strong interrelationship between the maximum heat island intensity, the urban population, and the impermeable surface coverage ratio. Fukuoka (1983) indicated a nonlinear relationship for Japanese cities where the slope of the regression line was steeper for cities with a population exceeding 300,000 than for similar North American cities, and smaller for small Japanese cities (population below 300,000) than for similar European cities. He speculated that those differences were caused by differences in urban structure, urban functions, and climatic zone. However, he did not describe how and why they should cause the difference.

As cities increase in size, their influence on the atmosphere grows. Hence, we must examine the processes within the urban boundary layer as an aid to understanding the radiative and thermal environment. According to Oke (1976), an important distinction in the scale of investigations in urban climatology exists between the urban canopy layer and the urban boundary layer. The distinction allows differentiation between processes operating at the microscale, below building height (the canopy layer), and those operating at the mesoscale, generally above building height. The interaction between these two scales of investigation is complicated, but despite the undoubted complexity of the radiative environment in the microscale canopy layer, the radiative fluxes through the top of the building /air column have proved to be remarkably smooth diurnally, and are consistent with fluxes observed at about roof level (Nunez and Oke, 1977). Recent studies of energy balances from a variety of different surfaces have produced a much clearer picture of the nature of energy exchange in the urban environment, both at the microscale (*e.g.*, Nunez and Oke, 1977, 1980 ; Oke, 1978) and the macroscale (*e.g.*, Yap and Oke, 1974 ; Landsberg and Maisel, 1972 ; Landsberg, 1979).

Within the canopy layer, there will obviously be a large range of moisture availabilities depending on the precise structure of the urban canopy unit. Although individual faces of the urban canopy produce a complex pattern of energy partitioning, Nunez and Oke (1977) give values of smoothed heat fluxes for the whole unit as percentages of net radiation flux (R_n) of 10–15% for latent heat flux (LE), 25–30% for ground heat flux (G_o) and 60% for sensible heat flux (H).

Within the boundary layer, remote sensing of radiative surface temperatures by satellite in conjunction with a one-dimensional boundary layer model allowed Carlson *et al.* (1981) to calculate energy balance terms for entire cities. They concluded that urban centers are areas of distinct maxima of sensible heat flux (H) and minima of latent heat flux (LE).

At night, long-wave flux divergence should lead to cooling of elevated layers and increased instability. Observational evidence is limited, but Fuggle and Oke (1976) in Montreal measured radiative cooling rates three times greater than actual cooling rates and concluded that the lower urban atmosphere is cooled mainly by radiative flux divergence, the cooling being retarded by sensible heat transfer from the surface. Within the urban canopy layer, the radiative environment is quite different. Nunez and Oke (1976) found that radiative cooling rates are much less below roof level than above roof level and are similar to actual cooling rates. They attributed this largely to the decreased sky view factor below roof level which reduces radiative loss and also reduces turbulent transfer in the almost calm canyon air. Kobayashi (1979) made an observation of the long-wave radiation near and on a building in Tokyo. He observed that the long-wave radiation from the ground surface of the urban area was about half as much as that from the roof of the

building when the ground surface and the roof surface were composed of the same material. He pointed out that this was due to the interception of long-wave radiation from the urban ground surface by the walls of nearby buildings, which reflected some of it back to the ground surface. Particularly at nighttime, the heat-energy supplies to the ground surface only the ground heat flux (G_o), and it is balanced by the net radiation (R_n). Oke *et al.* (1981) outlined the difficulties of obtaining representative values of the heat storage term by direct measurement using heat flux plates, mainly because of the wide variety of urban surface materials and the necessity to integrate these on a city scale. Although these factors explain how and why heat islands form in cities, there is no study that shows precisely how these factors affect the heat island intensity, and how they relate to city size.

Even in a city on a 'flat' site, there are likely to be some topographical features which can be ignored during the day, but due to nocturnal air drainage play an important role by night. This fact causes the topographical factor to become a substantial obstacle when attempting to isolate the synthetic urban climate. Some preliminary studies on the classification of urban climates according to topography have been conducted by Tyson *et al.* (1972), Nkemdirim (1980_a) and Goldreich (1984).

The nocturnal urban heat excess can not be isolated for cities in valleys. It can not be isolated because of the cooling induced by katabatic air drainage towards the city center located in a valley (Nkemdirim, 1980_b). The influence of topography can be so strong that the magnitude of the heat island may depend more on the local terrain than on the urban complex (Chandler, 1964). Most of the studies of topographic influences have dealt with cities located in valleys. These studies have tended to focus on the interaction of nocturnal air drainage from the surrounding slopes with the urban heat island. The concept of the 'urban valley' was introduced by Paterson and Hage (1979). In contrast to cases of cities in valleys, such as Sheffield, Reading and Pretoria, the urban valley can be defined as a valley within a city center. It seems that three factors dominate the North Saskatchewan River Valley (50m deep) where it crosses the city of Edmonton in Alberta, Canada : a) the valley is a sink for cool air drainage, b) with moderate wind conditions, a shelter effect exists which results in calm conditions at the valley bottom, and c) the snow cover persists on the ice in the valley much longer than on the urban and rural plains. The resulting features include a very strong nocturnal inversion in the valley.

Some references to sea and lake breeze can be found in Landsberg's (1981) review. During the daytime the sea breeze pushes the heat island landward, as was reported for Durban (Preston-Whyte, 1970), and at night the heat island migrates towards the coast. This nocturnal migration is pronounced during wintertime when the sea is warmer than the land, as detected in Tel-Aviv by an airborne infrared image (Goldreich, 1984). Near the coastline, the mesoscale influence of a sea breeze circulation is strong enough to weather an urban-induced country breeze, a well-known phenomenon of continental cities. In Japan, no country breeze has been reported, except for Asahikawa because land and sea breezes and mountain and valley circulations are strong (Yoshino, 1975 ; Kawamura, 1975, 1977).

Atkinson (1983), in his review of thermally driven mesoscale numerical modelling, stated that only a few such models exist in the urban climate field, while for mountain and valley wind circulations such modelling has hardly begun. While Atkinson's review was in press an important advance was registered in topoclimate modelling. Whiteman and McKee (1982) modelled the dissipation of the nocturnal inversion in mountain valleys. Bader and McKee (1983) converted the multidimensional cloud/mesoscale Colorado State University model to simulate nocturnal inver-

sion destruction in a mountain valley. It seems that it would not be difficult to add an urban-induced heat source to examine its interaction with the topographically induced circulation.

The fact that the heat island intensity is greatly affected by the shapes of the land surface has been observed. Some previous research has examined the heat island of cities on plain surfaces. Other research has concerned the heat islands of coastal cities. Still other research has examined the heat islands of basin cities. However, no previous study has examined and compared the heat islands of cities in all three of those types of topographical locations. The present study does so.

1.2 Purpose of this study

Urban heat islands have been intensively studied, and the mechanisms or processes of heat islands are partly understood. Especially understood is the relationship between the maximum heat island intensity ($\Delta T_{u-r(max)}$) and urban population, as revealed by Oke (1973). However, there are regional differences in the relationship, for the slopes of the regression lines are different one from another. In Japanese and Korean cities, the relationship can be represented by a biphasic regression line, with a slope transition occurring at the 300,000 population level (Fukuoka, 1983 ; Park, 1986_a).

The present study aims to explain why the relationship is different in different regions such as North America, Europe, Japan and Korea, and especially why the regression lines are bent at approximately 300,000 population for Japanese and Korean cities. In other words, the primary concern of this study is to explain the present writer's earlier finding (Park, 1986_a) that the maximum heat island intensity of Japanese and Korean cities with over 300,000 population is disproportionately greater than the maximum heat island intensity of Japanese and Korean cities with under 300,000 population. The study also examines and analyzes the effect of topography on the heat islands using basin, inland plain, and coastal cities of Japan as examples. The results are summarized in schematic models.

CHAPTER II

DATA AND METHODS

2.1 Flow of this study

The general objective of this study is to examine the urban and topographical influences on the heat island intensity (ΔT_{u-r}). First, the urban influences will be considered, then the topographical effects. Finally there will be discussion of the conclusions of the study and the geographical environmental influences on the heat island intensity will be clarified. Therefore, this research will consist of three principal parts.

In the first part, the influences of the urban structures on the heat island intensity will be discussed. By using data from observations made from automobiles, the relationships between the maximum heat island intensity and the urban population will be examined, and by focusing on interregional comparisons, regional differences will be statistically observed. Furthermore, by using the sky view factor and the impermeable surface coverage ratio as the leading factors to explain the regional differences, it will be possible to observe the physical meanings of the link between the heat island intensity and the urban population. Thereafter, the indices of the sky view factor and the impermeable surface coverage ratio will be described in physical terms by using special observation data for Mitsukaido City based on a heat balance model at the ground surface.

The second part will examine the effect of topographical factors on the heat island intensity. Three cities were chosen for case studies in this regard. Gifu, Asahikawa and Niigata. Gifu is a city located on an inland plain surface. Asahikawa is located in a topographical basin. Niigata is a coastal city. The cities were selected from stations for which AMeDAS data, which is homogeneous in time and covers a long time period, are available. For each city, the spatial and temporal aspects of the heat island intensity will be reviewed in accordance with its landscape. Then assuming that variations of the heat island intensity are due to differences in the nocturnal surface inversion layer in the nearby rural area, the differences will be observed by using special observation data for Asahikawa, a basin city, and for Akita, a coastal city. To conclude the second part, there will be a discussion of the urban influences and topographical effects on the heat island intensity, and schematic models will be presented. The third part will summarize the results of the study. Figure 1 shows the general pattern of flow of the study.

2.2 Field observation data

2.2.1 Data on the heat island intensity

In order to examine regional aspects of the relationship between the heat island intensity and the urban population, it is necessary to calculate accurately the heat island intensity of each city. For that purpose, observational data for many sites in and out of the city are needed. Such data collected by persons riding in automobiles are available for many cities. However, the number of cities for which such data have been collected through an entire year is yet limited.

For this study, twenty Japanese cities were selected for which sets of automobile observation data on temperatures had been collected by scientific methods during the nighttime in autumn and winter when the heat island intensity is likely to be strongest. The data sets each had temperature figures for many locations in and surrounding a city, and for many times of a day and days of a month. A number representing the maximum heat island intensity for each city was obtained by

Chapter

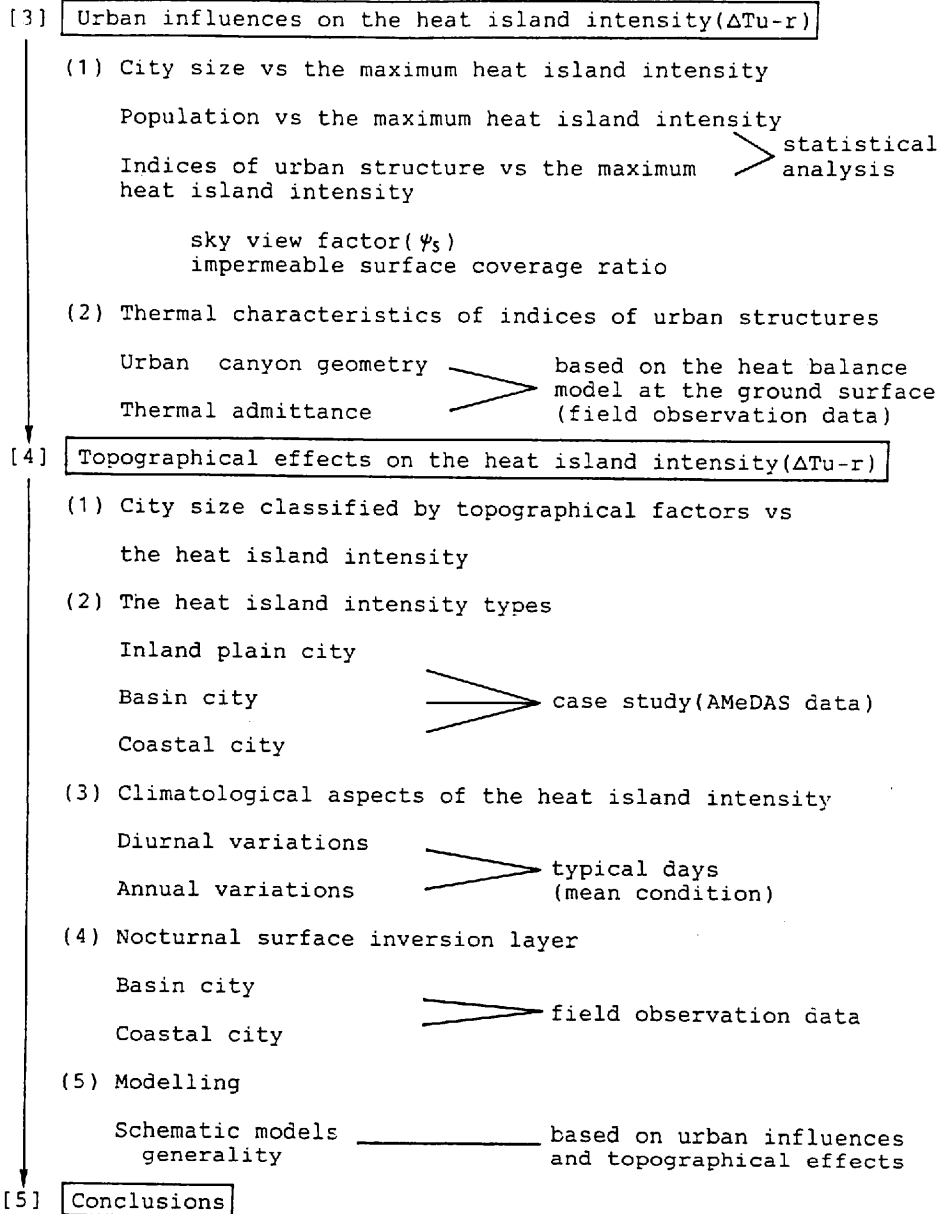


Fig. 1 Flow of this study

identifying the day and time at which the difference between the highest temperature in the urban area and the lowest temperature in the nearby rural area was greatest. The figure representing that difference was used to represent the maximum heat island intensity of the city. In any area and for any city, the heat island intensity is highest at night in clear and calm weather. The weather conditions under which the above mentioned temperature data sets were obtained, whether

under clear or cloudy skies, or under calm or windy conditions, are not known to the present winter. By using only the maximum heat island intensity figure, the question of weather conditions becomes unimportant, for it may be assumed that the temperature figures which yield the maximum heat island intensity ($\Delta T_{u-r(max)}$) were collected on a clear and calm night.

Automobile observations were available for only a few Korean cities. The present writer (Park, 1986a) produced some automobile observation data, collected during summer nights in June, July and August of 1982 in five Korean cities. Those data were used in the present study. Data collected by Kim (1976) during summer nights in one city were also used. It was assumed that the heat island intensity values for the Korean cities would be low since the automobile observations were carried out only in summer. Therefore, it would be impossible to compare the Korean values with those for cities in other regions. However, it was possible to compare the relationships between heat island intensity and urban population.

For twenty-one North American cities and fourteen European cities, data provided by Oke (1973, 1981) were used. Much of the data in his study was derived from sources in the literature. His own automobile observation data concerned nine cities in Quebec during nighttime in winter.

2.2.2 Data on the sky view factor

There is a close relationship between the formation of the heat island intensity and the geometrical unevenness of the urban canyon. The sky view factor is an index of the urban geometry.

Park and Kawamura (1986) calculated the sky view factors for twenty-three Japanese cities, including the above mentioned thirteen cities, and for seven Korean cities including the already mentioned six cities. The number representing the sky view factor for each city was derived in the following manner. A leveled camera with a fish-eye lens (a CANON 7.5mm, picture angle 180°) took whole-sky pictures at thirty-six different points. All points were within the central business district (C.B.D.) of the city, and all were in the center of a road. See Fig. 14 for examples of pictures. Then, with Ito's sky view factor calculation diagram (Ito, 1977), the percent of each picture which is occupied by sky (rather than by buildings) was calculated. Thereafter, the mean of the thirty-six percentage values for the city was determined, and that mean percentage figure became the sky view factor for the city.

For eighteen North American cities and eleven European cities, Oke's data (1981) were used. Oke's first empirical equation for the sky view factor was based on the $0.5m \times 0.5m \times 12.5mm$ hardware scale model. Later, he calculated the sky view factor for each city by revising the empirical equation with values measured from fish-eye lens photographs. Although, the method of calculating the sky view factors of Japanese and Korean cities differs from the method used for North American and European cities, both methods give approximate values and they satisfy the need for comparing the regional differences of the sky view factors in accordance with city size.

2.2.3 Special observation data

1) The present writer made some special observation for data in Mitsukaido City (41,000 population). The data were desired in order to examine the characteristics of the heat flow processes affecting the impermeable surface coverage ratio and relating to the sky view factor.

Mitsukaido City is located on a flat plain surface and has an urban area of $1km^2$. Most buildings are wooden and one or two stories high. A number of three or four story concrete buildings are clustered in the center of the urban area. Nearby rural areas are composed of fields and farms.

Measurements were taken from 09:00 on April 13 to 10:00 on April 14, 1986. During this period, Mitsuikaido City was in a high pressure zone, and the weather was clear (cloud cover $< 2/10$) and calm (average wind speed $< 0.2\text{m/s}$). The weather was ideal for heat island formation. Measurements of ground surface temperatures and of air temperatures at 1.5m above the surface was made three times (04:00 – 05:30, 13:30 – 15:30, 22:30 – 24:00) at thirty-four observation points mostly in the city but also in the surrounding rural area. Long-wave radiation, surface temperature, air temperature, wind direction, wind speed and cloud cover were measured hourly at one rural location and in the center of the city. At the city center location, the hourly measurements were made both at the ground surface (1.5m) adjacent to the tallest building in the city (the 16m high Masuda store) and on the roof of the building (17.5m). Also, the surface temperature of the building at a height of 6.3m was measured hourly. The ground surface near the building, and the wall and roof surfaces of the building, are concrete. Long-wave radiation was automatically recorded by a radiometer (Eiko-seiki CN – 11 and CN – 40) beginning at 10:00 on April 13 and until 10:00 on April 14. Surface temperatures were observed every hour using an infrared radiation thermometer (Matsushita Tsushin Kogyo ER – 2008). Wind direction and wind speed were measured every hour at the ground surface and on the roof surface by a Naka-asa type wind vane and anemometer. The wind direction and the average speed observed during a 5 minute interval in the hour were used to represent the hour. The cloud cover was estimated at the roof surface by visual inspection.

2) Because the heat island intensity and its diurnal variations are affected by the topography of the area in which the city is located, the cities studied were categorized into three kinds, inland plain, basin, and coastal. The author chose Asahikawa as an example of a basin city and Akita as an example of a coastal city, and collected special observation data about them for an examination of the differences between their inversion layers. Air temperature data for Asahikawa city and for the nearby rural area of Higashiasahikawa during the winter (January 18 – 19, 1983) were provided by the city office in Asahikawa. These data were recorded every 3 hours at 100m elevation intervals starting at 1.5m from ground surface and extending up to 900m. Data for Akita City and the nearby area of Takasu came from the Special Project of Atmospheric Environment in Akita Bay Region conducted by the Japan Meteorological Agency (1975, 1976). Takasu is located 30km from the coast. The temperature observation data for Akita City and Takasu were recorded at 09:00, 15:00, and 20:00 on June 9 and on October 14, 1974. They were recorded at 25m intervals from ground level to 100m in altitude and at 100m intervals between the altitudes of 50 and 950m.

2.3 Published data

1) The structure of a city affects its heat island intensity. Three indices of urban structure were chosen : the urban population, the sky view factor, and the impermeable surface coverage ratio. For the sky view factor, there were no published data. Sky view factor data were obtained as described in section 2.2.2. Data for the impermeable surface coverage ratio were obtained for twenty-three Japanese cities, including nineteen already mentioned, from the Japan Geographical Survey Institute. The Institute had 1 : 25,000 land use maps. The Institute had overlaid the maps with a 100m \times 100m grid and calculated the percentage of each grid square that is in each type of land use. The present writer then calculated the impermeable surface coverage ratio. It is the ratio of the total area occupied by buildings, roads, parking lots, driveways, and other structures made of artificial materials to the total city area.

For the six Korean cities, the present writer divided a 1:50,000 land use map into 0.5km \times

0.5km squares. Then the percent of a square occupied by each land use type was measured. Thereafter, the impermeable surface coverage ratio was calculated as described above for Japanese cities.

2) Population data for the North American and European cities were obtained from the UN statistical book, and for Japanese and Korean cities from recent censuses. Population data were used corresponding to the year when the estimation of the variables were made.

2.4 AMeDAS data

The heat island intensity is affected not only by population but also by the topographical and climatological environments of the cities. Chapter IV examines not only the heat island intensity of the topographically different cities but also compares their diurnal temperature variations. The Automated Meteorological Data Acquisition System (AMeDAS) recorded the data. AMeDAS is a regional system of climatological stations created by the Meteorological Agency of Japan in November 1974. Stations occur in a network at regular intervals of 17 or 21km. Meteorological observations at most stations include hourly rainfall (mm), hourly wind directions (16 directions) and hourly wind speed (m/s), hourly sunshine duration (0.1hr.), and hourly temperature (0.1°C). At some stations, only rainfall is recorded. There are 1317 AMeDAS stations throughout Japan. Six stations were chosen for this inquiry, three in cities and three in locations outside the cities. They were chosen according to the following criteria.

- 1) The observation station in the city should be within the built-up area.
 - 2) The observation station in the surrounding area should be on flat pastoral land.
 - 3) The observation stations both inside and outside the city should be within the same topographical environment, within the same basin and almost at the same elevation, for example.
 - 4) The distance between the urban station and the station in the surrounding area should be less than 50km. This criterion was based upon suggestions by Omoto and Hamotani(1982).
- With those criteria in mind, three cities were selected for their topographical locations.

- 1) Gifu City was chosen as an inland city on flat land.
- 2) Asahikawa City was picked as a basin city surrounded by the mountains, which would therefore have the characteristics of a basin climate, including cold air drainage and a cold air lake.
- 3) Niigata City was selected as a coastal city which would have a climate prominently including sea and land breezes.

The latitudes, longitudes, and elevations of the AMeDAS stations in the chosen cities and their surrounding areas are shown in Table 1. Table 2 lists the values of the maximum heat island intensity ($\Delta T_{u-r(max)}$), the sky view factor, and the impermeable surface coverage ratio for the Japanese and Korean settlements. Figure 2 shows the locations of the settlements for which data were obtained.

Table 1. Latitude, longitude, and elevation of the AMeDAS stations of the chosen cities

AMeDAS Stations	No.	latitude (°N)	longitude (°E)	elevation (m)	others
Asahikawa	12441	43.77	142.37	112	urban
Pippu	12396	43.52	142.29	167	rural
Gifu	52586	35.24	136.46	13	urban
Ibigawa	52511	35.29	136.34	45	rural
Niigata	54232*	37.55	139.03	2	urban
Niitsu	54296	37.47	139.05	3	rural

* Before Oct. 1, 1981, the number was 54231, but the location of the station was the same.

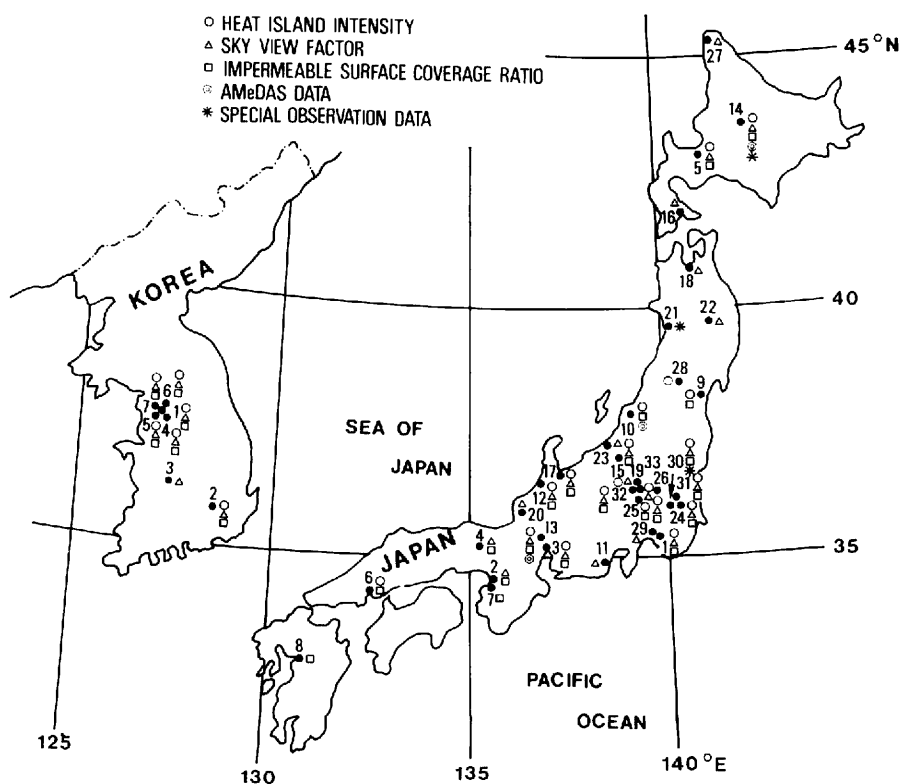


Fig. 2 Distribution of settlements for which climatological and geographical data were obtained

JAPAN : 1. Tokyo 2. Osaka 3. Nagoya 4. Kyoto 5. Sapporo 6. Hiroshima
 7. Sakai 8. Kumamoto 9. Sendai 10. Niigata 11. Shizuoka 12. Kanazawa
 13. Gifu 14. Asahikawa 15. Nagano 16. Hakodate 17. Toyama 18. Aomori
 19. Maebashi 20. Fukui 21. Akita 22. Morioka 23. Takada 24. Tsuchiura
 25. Isezaki 26. Tatebayashi 27. Wakkanai 28. Shinjoh 29. Akikawa
 30. Mitsukaido 31. Shimozuma 32. Shin-machi 33. Tamamura-cho
 KOREA : 1. Seoul 2. Taegu 3. Taejon 4. Seongnam 5. Kwangmyung
 6. Fuijeongbu 7. Shindo

Table 2. Maximum heat island intensity ($\Delta T_{u-r(max)}$), sky view factor, and impermeable surface coverage ratio for Japanese and Korean settlements. Ordered according to population (P).

Settlement	Year **	P ($\times 10^3$)	$\Delta T_{u-r(max)}$ ($^{\circ}C$)	Sky view factor (Ψ_s ; %)*	Impermeable surface coverage ratio (%)*	
JAPAN						
1. Tokyo	1977	8650	9.0	25	72	
2. Osaka	1986	2540		30	72	
3. Nagoya	1977	2080	5.5	34	55	
4. Kyoto	1986	1473		45	54	
5. Sapporo	1980	1400	5.9	50	40	
6. Hiroshima	1978	850	4.5		21	
7. Sakai	1986	810			42	
8. Kumamoto	1986	530			24	
9. Sendai	1968	480	4.0		29	
10. Niigata	1980	460	2.5		24	A
11. Shizuoka	1986	460		38		
12. Kanazawa	1983	420	3.4	53	20	
13. Gifu	1980	410	3.3	40	25	A
14. Asahikawa	1983	360	4.9	58	17	AO
15. Nagano	1983	325	3.0	48	13	
16. Hakodate	1986	320		65		
17. Toyama	1980	310	2.8	50	22	
18. Aomori	1986	290		52		
19. Maebashi	1975	250	2.5		22	
20. Fukui	1986	240		49		
21. Akita	1974	236				O
22. Morioka	1986	230		47		
23. Takada	1986	130		54		
24. Tsuchiura	1982	113	2.0	61	20	
25. Isezaki	1982	106	1.8		21	
26. Tatebayashi	1982	70	1.4	66	15	
27. Wakkanai	1986	53		73		
28. Sinjoh	1980	43	2.4			
29. Akikawa	1986	43		72		
30. Mitsuikaido	1986	41	2.1	70	15	O*
31. Shimozuma	1985	31	1.1	72	9	
32. Shin-machi	1982	15	1.2	78	13	
33. Tamamura-cho	1982	15	1.0		11	
KOREA						
1. Seoul	1982	8400	7.2 #	36	41	
2. Taegu	1977	1600	5.2	60	21	
3. Taejon	1986	620		61		
4. Seongnam	1982	380	2.3 #	65	14	
5. Kwangmyung	1982	150	1.5 #	72	13	
6. Euijeongbu	1982	140	1.3 #	72	12	
7. Shindo	1982	60	1.0 #	86	9	

A : AMeDAS data were also used for this settlement

O : Special observation data

* : Estimated by the author in 1986

** : Year of P ($\times 10^3$) and $\Delta T_{u-r(max)}$ data

: Estimated by the author in 1982

CHAPTER III

RELATIONSHIPS BETWEEN URBAN STRUCTURES AND THE HEAT ISLAND INTENSITY

3.1 Statistical analyses of the relationships between the indices of urban structures and the maximum heat island intensity

3.1.1 City size and the maximum heat island intensity

The population of a city is an index of the level of activity in the city and reflects the anthropogenic heat production of the city. Figure 3 shows the relationships between the logarithms of population and the maximum heat island intensity in Japanese, Korean, North American, and

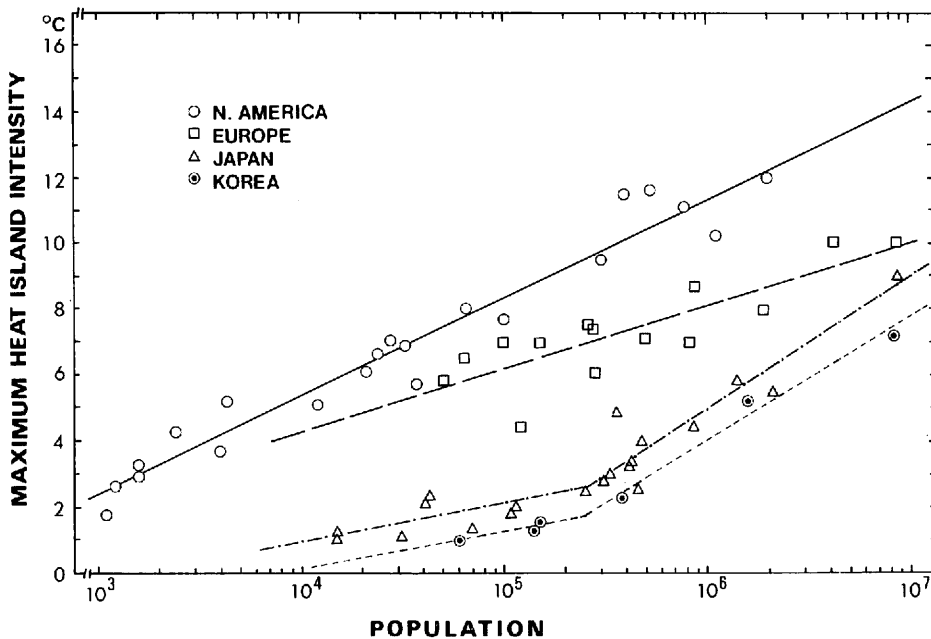


Fig. 3 Relationships between the maximum heat island intensity and the urban population for Japanese, Korean, North American and European cities

European cities. The heat island intensity values for the Japanese, North American, and European cities were the maximum values of observations which were carried out throughout a year in each city. The heat island intensity values for the Korean cities were derived from summertime temperature data. For the North American and European cities, the data on the maximum heat island intensity were obtained from the study by Oke (1973, 1981). Data for the Japanese and Korean cities were obtained as described in Chapter II.

Although the heat island intensity is greater the larger is the urban population in every country, there are regional differences in the relationships. For North American and European cities, the relationships are apparently linear proportionally and the regression lines can be represented as straight lines. For Japanese and Korean cities, the relationships are better represented by two

lines because the regression lines bend at around 300,000 in population. In other words, the increment of the maximum heat island intensity for cities with a population over 300,000 is larger than for cities with a population less than 300,000.

With P representing urban population and $\Delta T_{u-r(max)}$ representing the maximum heat island intensity, the regression equations of Japanese and Korean cities can be given as follows.

Japanese cities :

$$\Delta T_{u-r(max)} = 1.21 \log p - 3.92$$

$$(r^2 = 0.74 ; \text{population} < 300,000) \quad (1)$$

$$\Delta T_{u-r(max)} = 4.01 \log P - 19.09$$

$$(r^2 = 0.87 ; \text{population} > 300,000) \quad (2)$$

Korean cities :

$$\Delta T_{u-r(max)} = 1.19 \log P - 4.73$$

$$(r^2 = 0.97 ; \text{population} < 300,000) \quad (3)$$

$$\Delta T_{u-r(max)} = 3.74 \log P - 18.44$$

$$(r^2 = 0.98 ; \text{population} > 300,000) \quad (4)$$

The data on North American and European cities were obtained from Oke's work (1973, 1981). Based on those data, regression equations of North American and European cities can be represented as follows.

North American cities :

$$\Delta T_{u-r(max)} = 2.96 \log P - 6.46 \quad (r^2 = 0.95) \quad (5)$$

European cities :

$$\Delta T_{u-r(max)} = 1.92 \log P - 3.41 \quad (r^2 = 0.81) \quad (6)$$

These two equations were created as part of the present study and are different from Oke's earlier equations (1973).

Oke (1973) suggested that the European and North American regression lines are different for the following reasons ; 1) The heat capacity of European cities is smaller than of North American cities. 2) The difference in heat capacities is the result of differences in the amounts of anthropogenic heat produced and differences in the qualities of the buildings in the cities. 3) The rate of evaporation is larger in European cities than in North American cities. Fukuoka (1983) speculated that the differences in the regression lines were caused by differences in urban structure, differences in the functions of cities, and differences in climates. He also speculated that Japanese cities could better be represented by two regression lines than by one because the structure and the functions of cities with under 300,000 inhabitants are different from those of cities with more than 300,000 people. Korean cities, like the Japanese cities, can be represented by two regression lines because their structure and functions, and their climates, more closely resemble those of Japanese cities than of European or American cities.

Various studies on the classification and development of Japanese cities (Ogasawara, 1954 ; Ishimizu, 1965 ; Hattori, 1979) indicate that most cities with populations under 250,000 are "standard type" cities, while most cities with over 250,000 people are standard type cities and/or cities differentiated to have certain functions. Ogasawara (1954) identified the percentage of the popula-

tion of each city within each occupation and arranged occupations in order from the highest to the lowest values. He called the cities which had one third of the total data "standard type" cities. The studies also suggest that cities which have about 300,000 people are district centers that serve as the political, economic, and cultural centers of their respective districts. Tonuma (1980) classified Japanese cities into several categories based on their populations. His categories are small cities (over 10,000 but 100,000 in population), middle cities (over 100,000 but under 300,000), large cities (over 300,000 but under 1,000,000), and megalopolises (over 1,000,000 people). He also pointed out that the cities which had 300,000 people were on the boundary between middle cities and large cities, that the cities which had over 300,000 people were the centers of their districts, and that these district centers were characterized by having central business districts with tall buildings.

Sung (1977) and Joo (1982) studied the development of cities in Korea. They classified Korean cities into developing large cities and stagnant cities. Developing large cities have 200,000 to 500,000 people and their annual increments of population are above average. They are typical industrial cities. Their functions become more focused with greater development. As a result, the differences between the functions and structure of the developing large cities and the functions and structure of stagnant cities become large. These ideas do not explain why the relationship between the heat island intensity and the urban population is different for cities with under 300,000 than for cities with over 300,000 people. However, they do suggest that the functions and structures of the two sizes of Japanese and Korean cities are much different one from the other.

Figure 3 shows that there are several cities with heat island intensity levels that are significantly different from those in the great majority of cities. These cities are affected by their geographical conditions. The coastal cities have much smaller heat island intensity levels and the basin cities have much larger heat island intensity levels. Therefore the heat island intensity of a city is potentially affected not only by city functions and structure but also by the geographical conditions of the city. The latter will be discussed in Chapter IV.

3.1.2 Relationships between the indices of urban structure and the maximum heat island intensity

As mentioned above, in Japan and Korea the relationship between the maximum heat island intensity and population is different for cities with under 300,000 people than for cities with over 300,000 people. There is no direct explanation of this phenomenon in the scholarly literature to date. But each city has a structure ; and the structure of each city is different from that of other cities. Each city also has functions, and the functions often occur in distinct areas, each area with a different primary function. Commonly the centers of large cities are busy areas with tall buildings. In order to quantify and relate the features of a city's structure to the city's heat island intensity, the sky view factor (Oke, 1981) and the impermeable surface coverage ratio (Yamashita, 1981) are used as indices of the features.

The sky view factor is as reflection of the unevenness of a city's surface which in turn is related to the radiation balance and sensible heat flux in the urban canyons. The sky view factor is the ratio of the height of buildings (h) to the width of urban canyons (w). Figure 4 shows the relationships between the maximum heat island intensity and the sky view factor in Japanese, Korean, North American, and European cities.

The sky view factor data for the North American and European cities are from the report by Oke (1981). Those for the Japanese and Korean cities were measured by the present writer. The method of measurement is described in Chapter II.

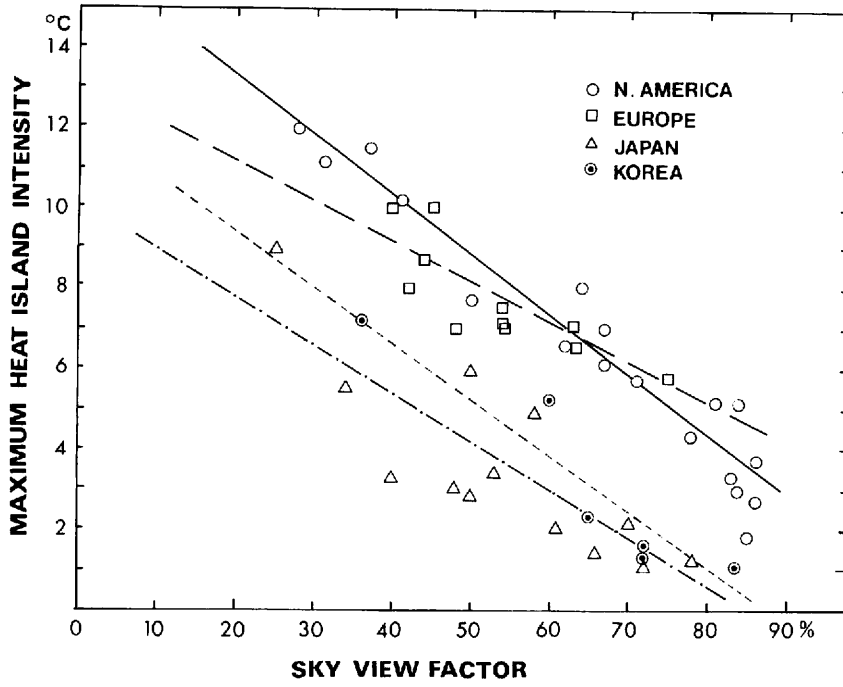


Fig. 4 Relationships between the maximum heat island intensity and the sky view factor for Japanese, Korean, North American and European cities

The regression equations that relate the maximum heat island intensity ($\Delta T_{u-r(max)}$) to the sky view factor (Ψ_s) for Japanese, Korean, North American, and European cities are as follows.

Japanese cities :

$$\Delta T_{u-r(max)} = -0.12 \Psi_s + 10.15 \quad (r = -0.83) \quad (7)$$

Korean cities :

$$\Delta T_{u-r(max)} = -0.14 \Psi_s + 12.23 \quad (r = -0.93) \quad (8)$$

North American cities :

$$\Delta T_{u-r(max)} = -0.15 \Psi_s + 16.34 \quad (r = -0.96) \quad (9)$$

European cities :

$$\Delta T_{u-r(max)} = -0.10 \Psi_s + 13.20 \quad (r = -0.82) \quad (10)$$

There is a negative relationship between the maximum heat island intensity and the sky view factor and it has a high coefficient of correlation. This means that the sky view factor is closely related to the formation of the heat island. Although to elucidate the effect of the sky view factor on the formation of the heat island is not an objective of this chapter, the following ideas are apparent.

As urbanization proceeds, the ratio of building area to sky area increases (*i.e.*, the sky view factor decreases) due to an increase in the number of tall buildings. This causes the air between the buildings to absorb more energy due to the short-wave radiation reflected from the surfaces of the buildings. The decrease in the sky view factor causes a decrease in the upward long-wave radiation due to an interruption by the buildings at night. This in turn makes the inside of the city

maintain a high temperature and produces the heat island phenomenon (Parry, 1967 ; Yap and Oke, 1974 ; Fuggle and Oke, 1976 ; Nunez and Oke, 1976, 1977 ; Kobayashi, 1979 ; Barring and Mattsson, 1985 ; Yamashita *et al.*, 1986). Other researchers have reported that in urban areas which are crowded with buildings, the latent heat flux is suppressed due to a decrease in the wind speed which in turn results in the urban canyons maintaining a high temperature (Nishizawa, 1958 ; Nunez and Oke, 1976). These scholars also reported that when inversion layers come to an urban area, the layers are disrupted due to the unevenness of the city surface and hence are neutralized.

As the city grows, the increase in the number of buildings results in an increase in the surface area which is covered with impermeable materials such as concrete and asphalt. Consequently there are changes in the heat balance of the ground surface and in the heat island intensity. The present study uses the impermeable surface coverage ratio as an index of the alteration of heat flux created by the differences in the composition of the ground surface. The impermeable surface coverage ratio is defined as the ratio of the area which is covered with artificial materials to the total urban area.

The impermeable surface coverage ratio was calculated as shown in Chapter II. The data are only approximate values, but the errors where they exist are probably small and do not affect the results of this chapter. The impermeable surface coverage ratios for the Korean cities and for the Japanese cities were obtained in different ways so that they can not be compared directly. Yet they allow clarification of the relationship between the heat island intensity and the impermeable surface coverage ratio within each country. Figure 5 shows the relationships between the maximum heat island intensity ($\Delta T_{u-r(max)}$) and the impermeable surface coverage ratio (X) in Japanese and Korean cities. These relationships can be represented by the following regression equations.

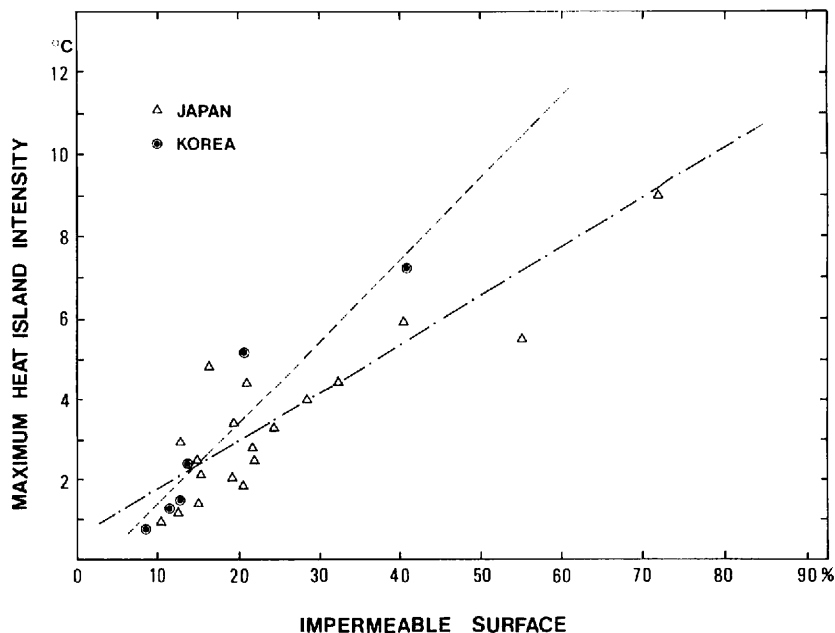


Fig. 5 Relationships between the maximum heat island intensity and impermeable surface coverage ratio for Japanese and Korean cities

Japanese cities :

$$\Delta T_{u-r(max)} = 0.11X + 0.50 \quad (r = 0.88) \quad (11)$$

Korean cities :

$$\Delta T_{u-r(max)} = 0.20X - 0.65 \quad (r = 0.95) \quad (12)$$

The very high coefficients of correlation mean that the impermeable surface coverage ratio is highly correlated with the formation of the heat island. The relationship can be explained as follows : 1) Increasing the area of impermeable surface causes decreases in evapotranspiration as well as loss of latent heat from the ground. This elevates the temperature inside the city. 2) Because impermeable materials have a high heat capacity and a high heat conductivity, the decrease in air temperature during the nighttime is lessened, maintaining a high temperature inside the city (Kawamura, 1964 ; Myrup and Morgan, 1972 ; Oke, 1981).

In conclusion, the heat island intensity is highly correlated with the sky view factor and with the impermeable surface coverage ratio and these relationships are linearly proportional.

3.1.3 Interrelationships between the indices of urban structures, urban population and the maximum heat island intensity

As demonstrated above, the maximum heat island intensity is highly correlated with the sky view factor and with the impermeable surface coverage ratio. In this section, the relationship between the sky view factor, which is an index of urban structure, and the impermeable surface coverage ratio will be discussed.

Figure 6 shows the relationships between the sky view factor (Ψ_s) and urban population (P) in

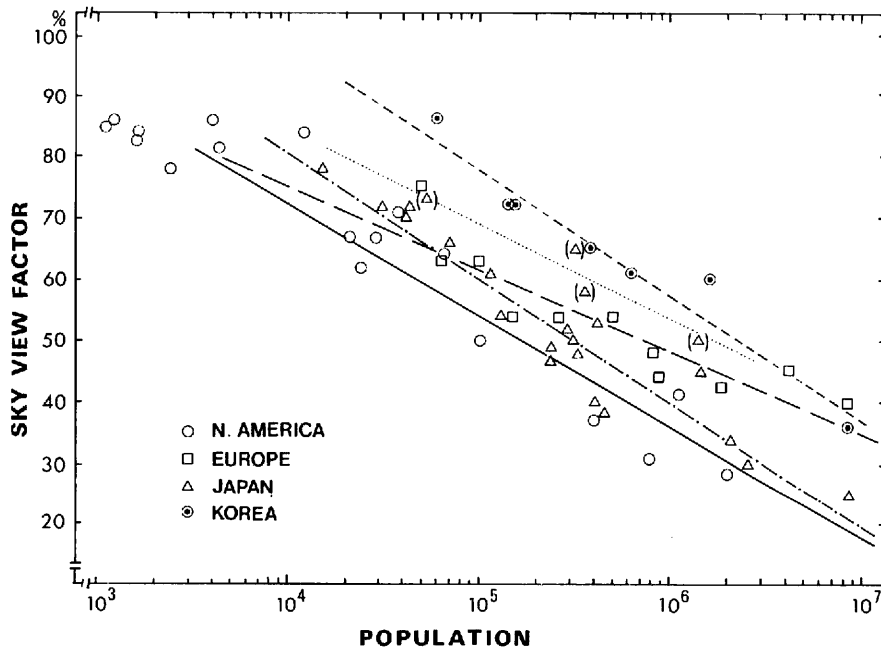


Fig. 6 Relationships between sky view factor and the urban population for Japanese, Korean, North American and European cities

Japanese, Korean, North American, and European cities. The sky view factor decreases with an increase in the urban population, demonstrating a negative correlation. This means that the sky view factor decreases with an enlargement of the urban area and with increases in the number of tall buildings. This relationship within each region is shown in the following regression equations.

Japanese cities :

$$\Psi_s = -20.36 \log P + 162.06 \quad (r^2 = 0.92) \quad (13)$$

Korean cities :

$$\Psi_s = -20.67 \log P + 181.50 \quad (r^2 = 0.94) \quad (14)$$

North American cities :

$$\Psi_s = -18.09 \log P + 144.71 \quad (r^2 = 0.91) \quad (15)$$

European cities :

$$\Psi_s = -13.35 \log P + 128.62 \quad (r^2 = 0.83) \quad (16)$$

These regression lines are regionally different, and the slope for North American cities is steeper than that for European cities. This can be attributed to the extreme unevenness of urban canyons in North American cities as compared to European cities in spite of the similar population size. Therefore, the effect of the buildings on heat island formation is larger in North American cities. This is very similar to the relationship between urban population and the maximum heat island intensity (*see* Fig. 3). The slopes of the regression lines for Japanese and Korean cities are similar to the slope for North American cities and different from that for European cities. This owes to the similarity of Japanese and Korean cities to North American cities, in contrast to European cities. In the case of Korean cities, the regression line has a larger intercept than that for Japanese cities. In other words, Korean cities have a larger sky view factor than Japanese cities. This is the result of the shorter buildings in the centers of cities in Korea compared to those in Japan and the narrower roads in Korean cities than those of Japanese cities.

There are two other striking features in Fig.6. The first is that for Japanese cities, the relationship between the sky view factor and urban population is best represented by two lines. The cities in Hokkaido, whose symbols are bracketed as () in Fig. 6, have populations as follows : Wakkanai (53,000), Hakodate (320,000), Asahikawa (352,000) and Sapporo (1,420,000). These cities have a larger sky view factor than the other cities in Japan, and their values are above the regression line that represents all Japanese cities (Equation (13)). The regression equation for the cities in Hokkaido can be represented as follows :

$$\Psi_s = -15.44 \log P + 146.41 \quad (r^2 = 0.94) \quad (17)$$

This regression line is similar in its slope to that for European cities (*cf.* Equation (16)). Therefore, it is suggested that urban canyons in Hokkaido are similar to those in Europe. Considering these features, Japanese cities can be divided into two groups. One includes the cities which have a sky view factor in accordance with their population, and the other the cities which have larger sky view factors than expected from their population (*i.e.*, cities in Hokkaido). The second striking feature is that there are no significant differences in the sky view factors of the North American cities which have populations under 10,000. Though the data are lacking to support the conclusion, one can speculate that the same phenomenon could well be observed in

other countries.

Figure 7 shows the relationships between urban population (P) and the impermeable surface coverage ratio (X) in Japanese and Korean cities. The impermeable surface coverage ratio increases with an increase in the urban population. This relationship can be represented by a biphasic regression line in both countries, with a slope transition occurring at a 500,000 population level. For Korea, the relationship is possibly biphasic, but because there are few cities above 300,000 in population, it is not possible to say that the relationship is definitely biphasic. This is very similar to the relationship of urban population to the maximum heat island intensity observed in Fig. 3. The regression lines can be given by the following equations :

for Japanese cities which have populations under 300,000,

$$X = 9.85 \log P - 30.77 \quad (r^2 = 0.78) \quad (18)$$

for Japanese cities which have populations over 300,000

$$X = 44.89 \log P - 230.13 \quad (r^2 = 0.87) \quad (19)$$

for Korean cities which have populations under 300,000

$$X = 6.11 \log P - 19.60 \quad (r^2 = 0.87) \quad (20)$$

for Korean cities which have populations over 300,000, based however on data for only three cities.

$$X = 20.98 \log P - 105.47 \quad (r^2 = 0.95) \quad (21)$$

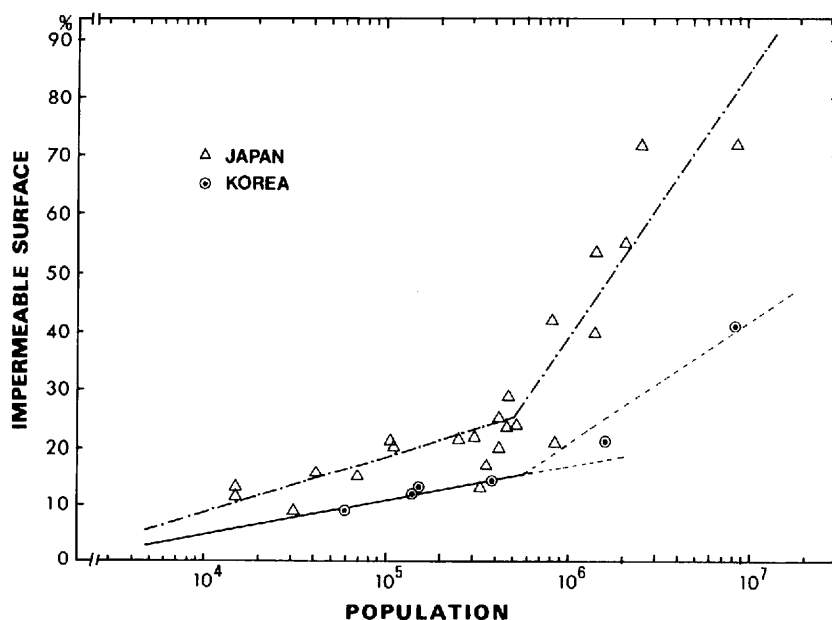


Fig. 7 Relationships between impermeable surface coverage ratio and the urban population for Japanese and Korean cities

Thus, the impermeable surface coverage ratio is one of the indices which explains why the relationship between the heat island intensity and the urban population can better be represented with two regression lines than with one simple regression line. Although the impermeable surface coverage ratio may not be the only factor involved in this biphasic correlation, it is probably a key to understanding it. As indicated above, Equation (21) is based on only on three cities. If it were based on a larger sample, its slope number (20.98) would probably be different. However, the upward trend of the line (*see* Fig. 7) would remain.

3.2 Thermal characteristics induced by urban structures

3.2.1 Heat balance at the ground surface

According to the principles of energetics, the heat balance on the ground surface can be given by the equation :

$$R_n = H + IE + G_o \quad (22)$$

where R_n stands for the net radiation flux which is absorbed by the ground surface, H stands for sensible heat flux, IE stands for latent heat flux, and G_o stands for the heat conducted from the surface into the ground heat flux. In the urban area, as the heat balance is affected by anthropogenic heat (Q), the heat balance equation is the following :

$$R_n + Q = H + IE + G_o \quad (23)$$

Horizontal heat conduction is not considered in this type of one dimensional model of heat balance. In other words, this equation describes the hypothetical state of the vertical heat balance in a specific area of the city. Therefore, in order to consider the structure of the heat island, which is a phenomenon of three dimensions, it would be better to consider a model with three dimensions. However, if there is no wind (*i.e.*, if calm conditions prevail), the horizontal heat balance is negligibly small and therefore we can use the one dimensional model.

The heat balance on the ground surface should be considered in the daytime and at night. In the daytime, the ground surface absorbs the heat energy from the sun and attains a higher temperature than does the air. Hence, in Equation (22), sensible heat flux becomes larger and heats the atmosphere. Furthermore, the atmosphere in the urban canyon absorbs the direct heat energy from the sun in addition to the heat energy reflected by the buildings. This phenomenon makes the albedo (α) of the city lower and consequently increases the urban temperature (Kung *et al.*, 1948 ; Terjung and Louie, 1973 ; Dabberdt and Davis, 1974 ; Yamashita, 1975 ; Lunde, 1977 ; Aida and Goto, 1978 ; White *et al.*, 1978). Furthermore, the proportion of the area covered with impermeable materials such as concrete and asphalt is higher in the urban area than in the surrounding area. This makes the latent heat flux (IE) smaller and hence the urban temperature is elevated (Myrup and Morgan, 1972 ; Landsberg, 1972 ; Carlson *et al.*, 1981 ; Oke, 1982).

With sunset, a decline in the temperature of the impermeable material begins and the temperature differential between this material and the atmosphere decreases. After sunset, the ground surface does not absorb the heat energy from the sun, while its infrared radiation becomes greater than its absorption from the atmosphere ; hence cooling proceeds. The atmosphere starts to cool from the bottom, which is close to ground surface, and proceeds upwards. This phenomenon induces the formation of a stable layer of air over the ground surface, a decline in the activity of turbulence, and a decline in the sensible heat flux. Therefore, the heat energy supplied to the ground surface comes only from the ground heat flux (G_o) which radiates upward from inside the

ground. This heat is balanced with the net radiation flux (R_n). This is the simplest case of the heat balance.

The heat balance can be given by the equation :

$$R_n = G_o = - \lambda \left(\frac{\partial T}{\partial Z} \right)_{Z=0} \quad (24)$$

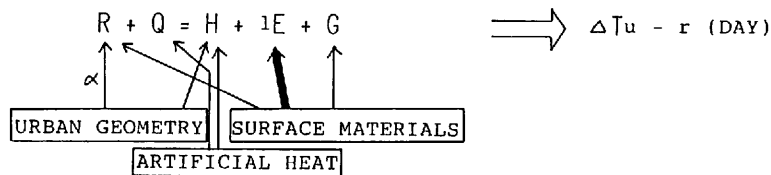
where λ stands for the conductivity of the soil. T stands for the temperature of the ground, and Z stands for the depth of the ground. When the heat energy radiates from the ground, R_n becomes negative, and when the heat energy is supplied to the ground, R_n becomes positive. The heat island intensity in nighttime is affected considerably by the conducted heat of ground heat flux (G_o) which is related to the net radiation flux (R_n), the heat capacity (C_p) of the materials composing the ground surface, and their conductivity (K).

According to studies mentioned above, the heat island phenomenon appears predominantly during the nighttime rather than the daytime (Chandler, 1970 ; Oke, 1974, 1979 ; Landsberg, 1981 ; Lee, 1984). Therefore, this study has focused on the heat island phenomenon during the night. As demonstrated previously, the heat island intensity is closely related to the sky view factor and to the impermeable surface coverage ratio.

In this section, the physical meaning of each index will be clarified based on the heat balance equation of the ground surface. First, the effect of buildings interrupting the long-wave radiation into the urban ground surface will be discussed using the sky view factor which is a geometrical index of the ground surface. Second, the thermal features of the materials composing the urban surface will be discussed using the impermeable surface coverage ratio which is the index of the structure of the ground surface based on the equation of Brunt (1941) which shows the cooling during the night. The urban population was used instead of the anthropogenic heat consumption

HEAT BALANCE AT THE GROUND SURFACE

(1) DAY TIME



(2) NIGHT TIME

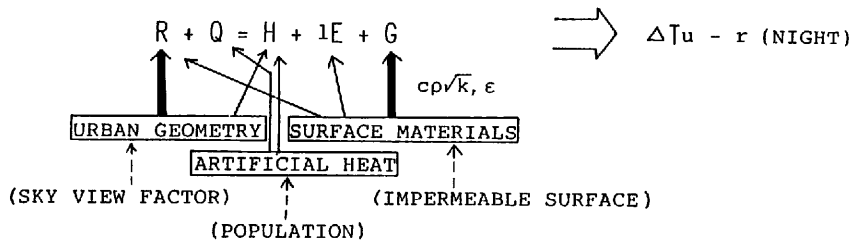


Fig. 8 Flow of heat balance at the ground surface

(Q). Generally, the urban population is an integrated measure of urban characteristics such as the physical size of the city, the geometry and materials of the urban surface, and anthropogenic energy consumption. Anthropogenic energy consumption in an urban area depends on factors such as geographical location, prevailing climate, population, wasted heat from transportation, and industrial and commercial activities (Bach, 1970 ; East, 1971 ; Torrance and Shum, 1976 ; Landsberg, 1981).

Figure 8 is a flow chart which summarizes information on the heat balance of the ground surface.

3.2.2 Urban canyon geometry and long-wave radiation

Long-wave radiation measurements were carried out in Mitsukaido City, a small city on the Kanto Plain, for the purpose of elucidating the effect of the interruption of long-wave radiation by buildings, which is closely related to the formation of the heat island at night. The temperature of the ground surface and the air temperature were measured by automobile observation, and the relationship of these data to the sky view factor was studied. Furthermore, the components of long-wave radiation on the surface of the tallest building (on the ground surface, roof surface, and

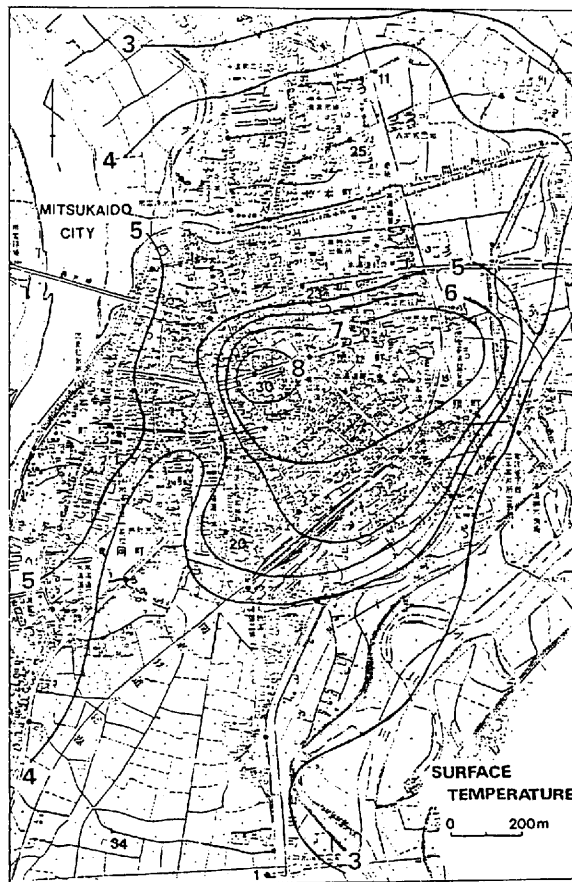


Fig. 9 Distribution of ground surface temperatures in and near Mitsukaido City (1986. 4. 14. 04 : 00 - 05 : 30)

wall surface) in the center of the city were measured, and the effect of the buildings on the long-wave radiation into the urban ground surface was studied.

In Mitsukaido City, the distribution of ground surface temperatures (Fig. 9) is similar to the distribution of air temperatures (Fig. 10) in that the ground surface temperatures and air temperatures in the urban area are higher than those in the surrounding area. However, the distribution of the sky view factors is just the reverse, for the sky view factors in the urban area are smaller than those in the rural area (Fig. 11). In other words, it is evident that the sky view factor is smaller at the center of the city than in the surrounding area, while the ground surface temperature and the air temperature are higher in the urban area than in the surrounding area.

Figure 12 shows the distribution of the ground surface temperature, the air temperature, the cooling amounts of the ground surface temperature, the diurnal range of the ground surface temperature, and the sky view factor at observation points along a line A to B spanning Mitsukaido City and its surrounding area (shown in Fig. 11). The ground surface temperature was higher for concrete and asphalt than for soil. A similar pattern was observed in the air temperature. Thus the ground surface temperature and air temperature are considerably affected by the materials which compose the ground surface. The distribution of the ground surface temperature

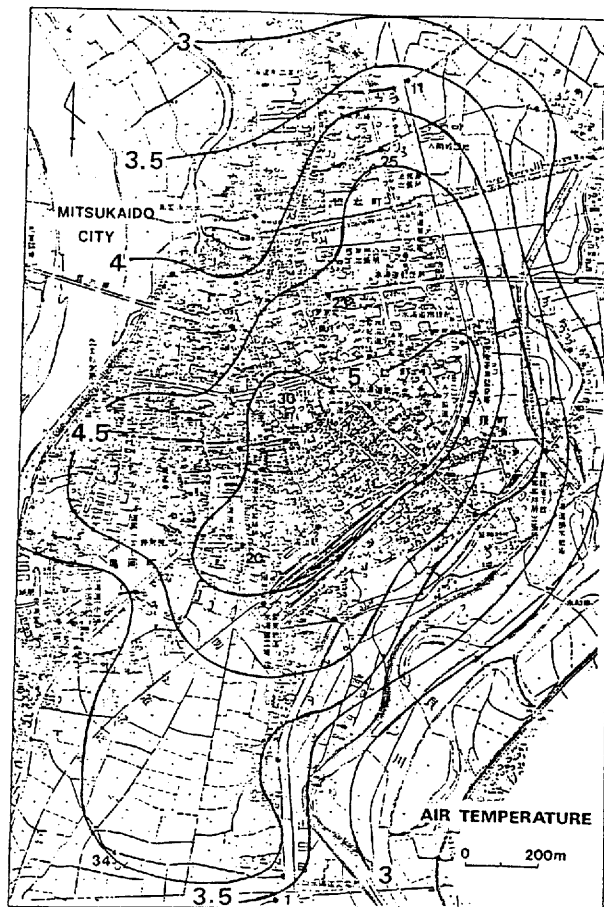


Fig. 10 Distribution of air temperatures in and near Mitsukaido City
(1986. 4. 14. 04 : 00 - 04 : 30)

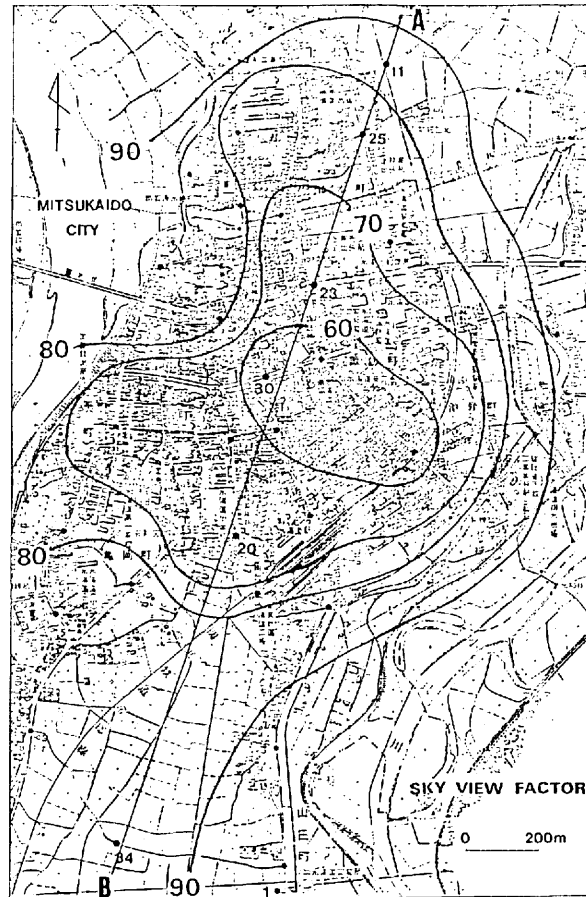


Fig. 11 Distribution of sky view factors in and near Mitsukaido City
(1986. 4. 14)

and air temperature on street surfaces, which were composed of the same material, depended on the sky view factor. These temperatures were lower at the points where the sky view factor was large, and were higher at the points where the sky view factor was small.

The points where the decrements of the ground surface temperatures were small and the points where the diurnal ranges of the ground surface temperature were small coincided with the points where the sky view factor was small. This means that places where the sky view factor is small, such as in the centers of cities where buildings are taller and close together, maintain higher temperatures during nighttime than places farther from the centers where buildings are shorter.

Figure 13 shows the relationship between the ground surface temperature and the sky view factor at selected points in the urban area. The figure indicates that there is a negative relationship between the sky view factor and the ground surface temperature ($r = -0.74$).

In order to elucidate the effect of the sky view factor on the distribution of ground surface temperatures and of air temperatures, time-courses of these temperatures were observed on the ground surface and the roof surface. Also the surface temperature was measured on a wall. The sky view factor of the ground was 51% and that of the roof surface was 94% (Fig.14).

Figure 15 shows the hourly changes of the air temperature and the ground surface tempera-

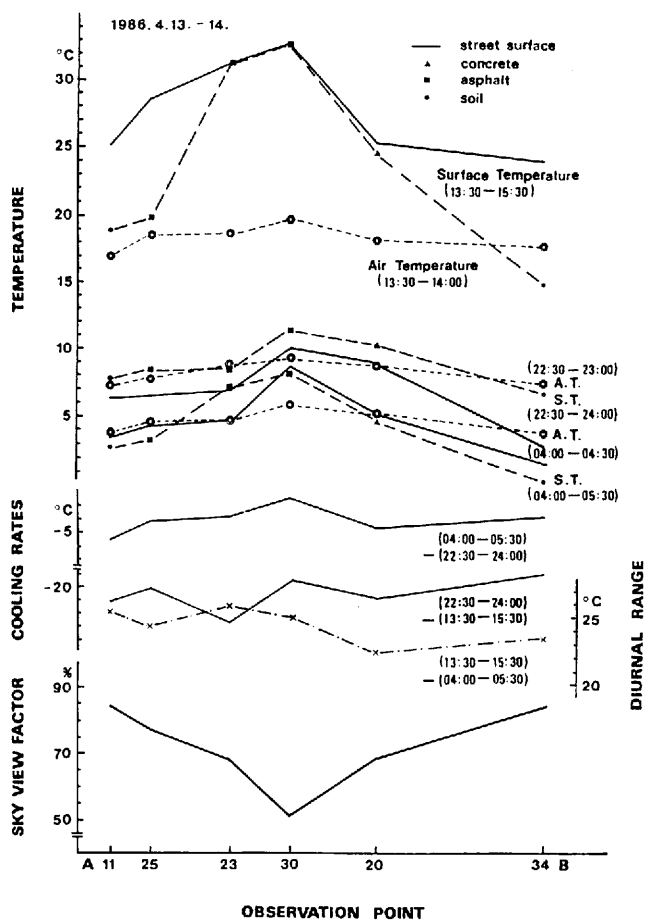


Fig. 12 Distribution of the ground surface temperature, the air temperature, the cooling amounts of the ground surface temperature, the diurnal range of the ground surface temperature, and the sky view factor at the observation points along A to B spanning a suburban area

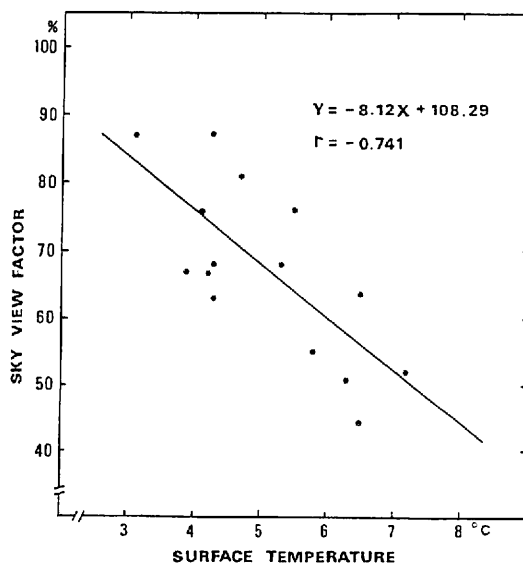
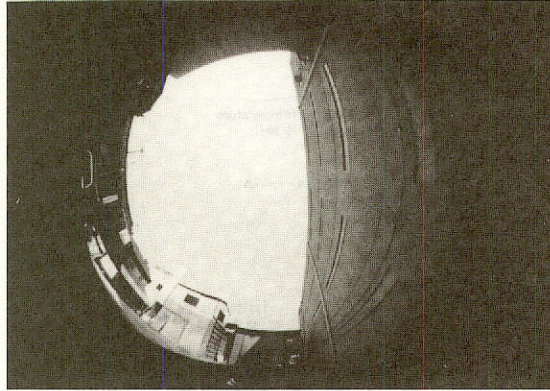


Fig. 13 Relationship between the sky view factor and the ground surface temperature (04 : 00 - 05 : 30) at designated points in the urban area

(A)



(B)

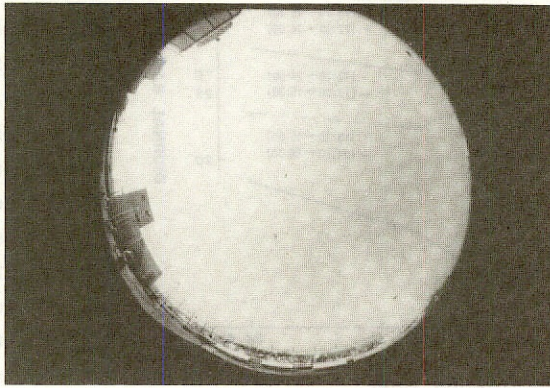


Fig. 14 Fish-eye lens photographs taken from (a) ground surface and (b) roof surface levels illustrating the reduction of the sky view factor by buildings.
Sky view factor 0.51 for (a) 0.94 for (b)

ture on the ground surface, the roof surface and the wall surface. A reversal of the relative temperatures of the roof surface and the ground surface was observed as the day became night. The temperature of the roof surface was higher, at times considerably higher, than that of the ground surface until about 17:00. However, the former was lower than the latter between 17:00 – 07:00. In other words, the roof surface temperature was higher than the ground surface temperature in the daytime, but lower at night. The wall surface temperature was mostly lower than the ground surface temperature and the roof surface temperature during the daytime, but was between those two values in the nighttime. The rate of change in the ground surface temperature was higher than that of the roof surface in both the daytime and the nighttime. This means that the ground surface is slower to cool down than the roof surface.

If the net long-wave radiation is approximately constant through the nighttime (as in the case of a calm and clear night), the cooling of the ground surface can be represented by the following equation, according to Brunt (1941) :

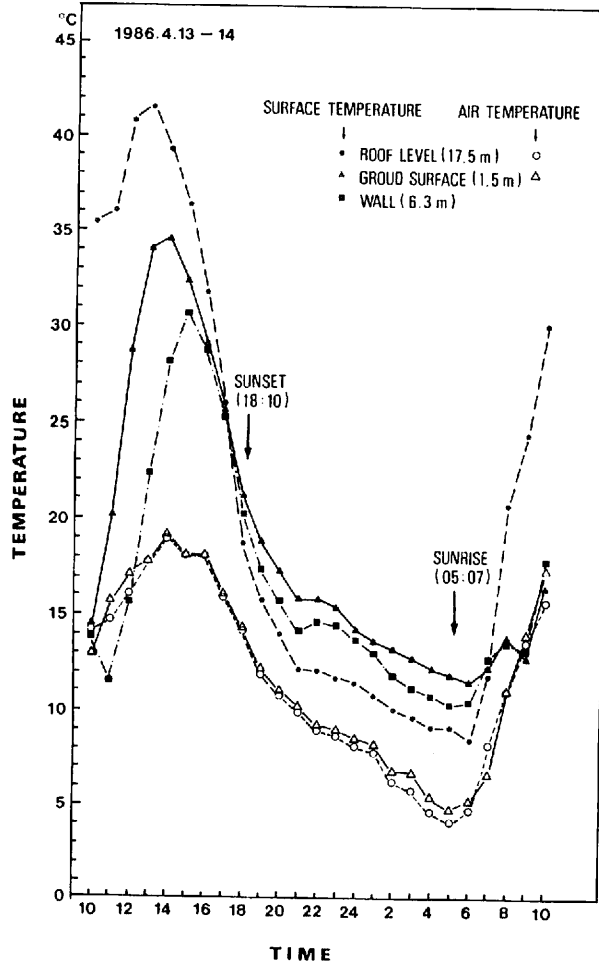


Fig. 15 Hourly changes of surface temperatures and air temperatures for three observation points

$$\Delta T_{t-s} = -\frac{2}{\pi^{1/2}} \frac{R_n}{C \rho K^{1/2}} t^{1/2} \quad (25)$$

where ΔT_{t-s} stands for the cooling amount of the surface temperature from sunset to sunrise, R_n stands for the net long-wave radiation, π stands for the circular constant, C stands for the specific heat capacity of the ground surface material, ρ stands for the density of the ground surface material, and K stands for the heat conductivity of the ground surface material. Since the ground surface and the roof surface where the observation were performed were both made of concrete, the $C \rho K^{1/2}$ in the above equation is constant, and the change of temperature by cooling is determined by R_n and $t^{1/2}$.

While the measurements were made, the weather was clear (cloud cover < 2/10) and calm (average wind speed < 0.2 m/s), and the net long-wave radiation (R_n) was approximately constant during the night. Figure 16 shows the cooling amounts from sunset until sunrise of the ground surface temperature and of the roof surface temperature. For calculation of Brunt's curve, a R_n value of 69 Wm^{-2} was used for the ground surface and 113 Wm^{-2} for the roof surface. A value of 2380

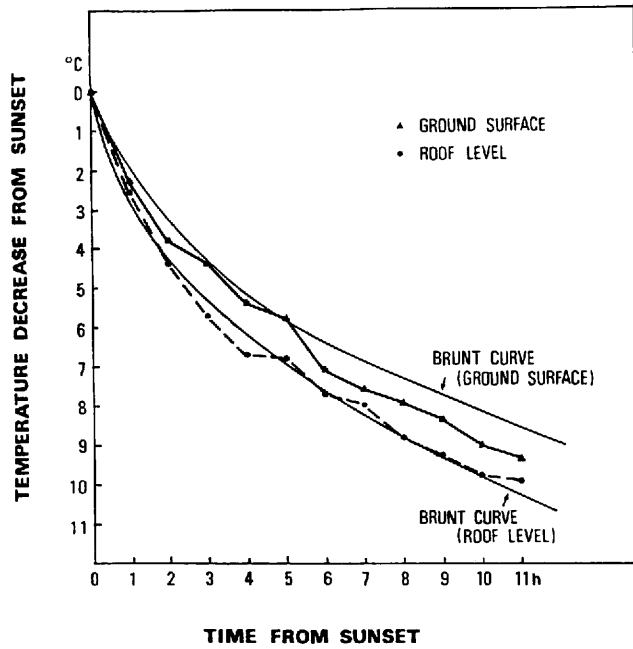


Fig. 16 Decrease after sunset of the ground surface temperature and of the roof surface temperature in the urban area

$\text{Wm}^{-2}\text{S}^{1/2}\text{K}^{-1}$, which is the value for a concrete surface, was used for $C_p\text{K}^{1/2}$ (Ingersoll *et al.*, 1948). Brunt's theoretical curve and the measured curve of changes in surface temperatures during the night are slightly different. However, the theoretical curve for roof surface temperature fits very well with the measured curve. Thus, the changes in the surface temperature during the night can be adequately represented by Brunt's equation. This suggests that the difference between the changes in roof surface temperatures and changes in ground surface temperatures depends largely on R_n .

Figure 16 also shows that the surface temperatures on both the ground and the roof surface changed rapidly just after sunset and gradually thereafter. The slope of the Brunt curve is larger for the change of roof surface temperatures than for ground surface. In other words, the temperature declines more rapidly on the roof surface than on the ground surface. As mentioned above, the diurnal range of ground surface temperatures is small where the sky view factor is small. This suggests that the ground surface maintains a high temperature during both the daytime and the nighttime due to the presence of the building which absorb the short-wave radiation in daytime and decrease the long-wave radiation in nighttime.

The components of the long-wave radiation which affect the cooling of the surface during the night will be discussed next. Figure 17 shows the hourly changes in the long-wave radiation components at the ground surface and the roof surface from 18:00 on April 13 to 05:00 on April 14. The vertical axis represents the amount of radiation every hour in Wm^{-2} . The absorption of energy on the surface is represented by a positive value and the emission of energy is represented by a negative value. Therefore, downward long-wave radiation ($L \downarrow$) is positive, while upward long-wave radiation ($L \uparrow$) is negative. R_n was a measured value. $L \uparrow$ was a calculated value from the surface temperature according to the principle of Stefan-Boltzmann. $L \downarrow$ was determined by the following equation.

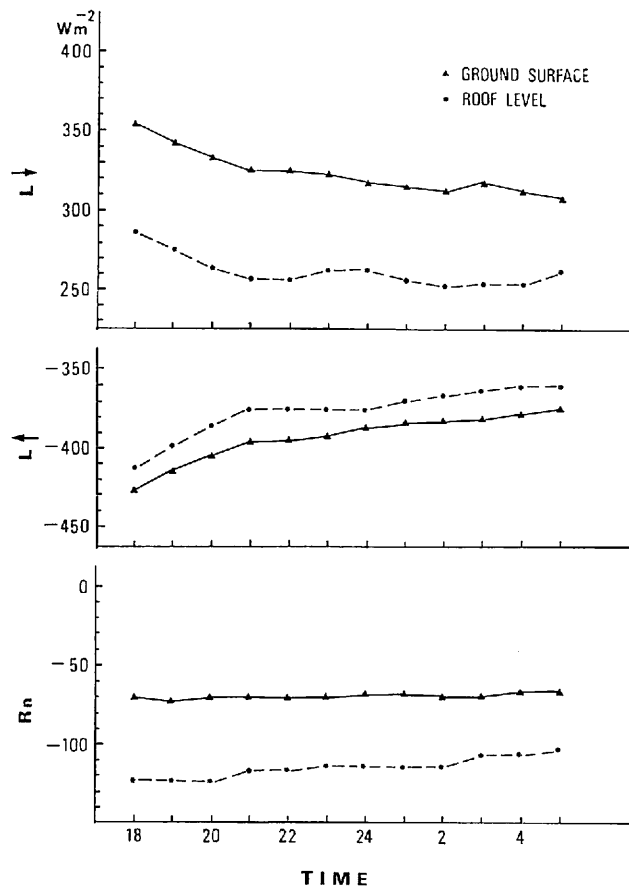


Fig. 17 Hourly mean in the long-wave radiation components of the ground surface and the roof surface level

Table 3. Mean of each long-wave radiation component (Wm⁻²)
(April 13-14, 1986, 18:00-05:00)

	long-wave radiation (Wm ⁻²)		
	$L \downarrow$	$L \uparrow$	R_n
roof surface	263	-376	-113
wall		(L_w) 386	
ground surface	324	-329	-69

$$L \downarrow = R_n - L \uparrow$$

(26)

Table 3 shows the average values of the various components of the long-wave radiation from the roof surface and the ground surface during the night. The long-wave radiation from the wall surface ($L_w \downarrow$) is also shown in this table. As sunrise approached, $L \downarrow$ gradually decreased, the absolute value of $L \uparrow$ gradually decreased, and the absolute value of the R_n of the roof surface gradually decreased. The R_n of the ground surface was approximately constant during the night. The R_n of the roof surface was always larger than that of the ground surface. As show in Table 3,

the average values of the R_n of the roof surface and of the ground surface were 113 Wm^{-2} and 69 Wm^{-2} respectively. Therefore, the radiative cooling on the ground surface was merely 0.6 times of that on the roof surface. This could explain the phenomenon that the cooling on the ground surface is smaller than on the roof surface as shown in Fig. 16.

Next, differences in the net long-wave radiation (R_n) of the ground surface and the roof surface will be discussed, with its components $L \downarrow$ and $L \uparrow$. The $L \downarrow$ of the ground surface was larger than that of the roof surface, and the difference was always about 61 Wm^{-2} . The absolute values of the $L \uparrow$ of both the ground surface and the roof surface decreased gradually until sunrise (*i.e.*, the radiative energy which was emitted from the surface decreased.). The difference between the $L \uparrow$ of the ground surface and that of the roof surface was approximately 16 Wm^{-2} , an amount smaller than the difference between their $L \downarrow$. The difference between the R_n of the ground surface and that of the roof surface was approximately 44 Wm^{-2} . Therefore, this difference of R_n was due to the difference of $L \downarrow$. In other words, the interruption of the long-wave radiation by the buildings made the $L \downarrow$ larger than $L \uparrow$ and stabilized the temperature of the ground surface.

Figure 18 was made to evaluate the interruption effect of the buildings. The vertical axis shows the downward long-wave radiation at the ground surface ($L_s \downarrow$) and the horizontal axis shows the sum of the long-wave radiation from the wall surface ($L_w \downarrow$) and the downward long-wave radiation on the roof surface ($L_r \downarrow$). These two correspond with each other on one to one basis. Therefore the downward long-wave radiation on the ground surface can be explained by the downward long-wave radiation on the roof surface and that from the wall surface. In conclusion, the sky view factor is closely correlated with the long-wave radiation which is related to the

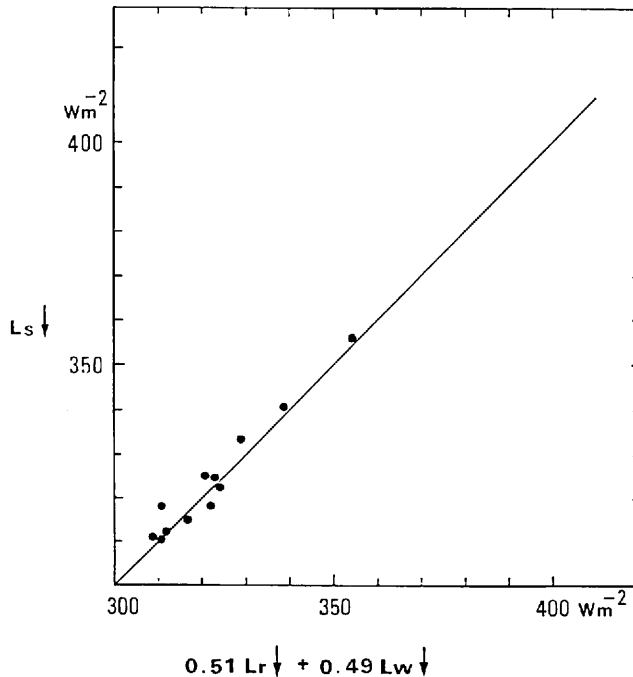


Fig. 18 Comparison of the downward long-wave radiation at the ground surface ($L_s \downarrow$) with the sum of the downward long-wave radiation at the roof surface level ($L_r \downarrow$) and the long-wave radiation from the wall surface ($L_w \downarrow$)

radiative cooling at night. Therefore the sky view factor, which is one of the indices of urban structure, is one of the main factors causing the nocturnal heat island phenomenon.

3.2.3 Thermal admittance and the heat island intensity

As demonstrated in the previous section, the heat island intensity is greatly affected by the net long-wave radiation (R_n) and the upward conducted heat from the ground (ground heat flux, G_o) as shown in Equation (25). In this section, the thermal characteristics of the surface coverage materials, which affect the heat island, are discussed based on measurements of the ground surface temperature, the air temperature, and the components of long-wave radiation in Mitsukaido City. The measurements were performed on concrete surfaces at the center of the city (observation point 30) and on a surface of soil in the surrounding area (observation point 1). The methods

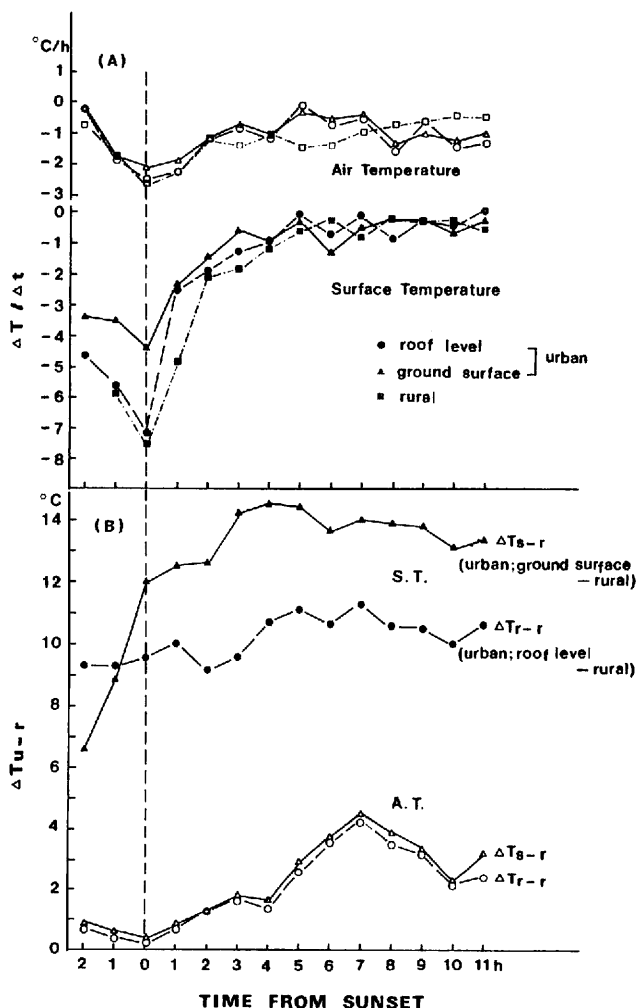


Fig. 19 Mean hourly urban-rural cooling rates (A) and heat island intensities (B).
Urban area has two surface levels, ground surface and roof surface

and periods of measurements were the same as those described in the previous section (shown in Chapter II).

Figure 19 (A) shows the cooling rates ($\Delta T/\Delta t$) of the surface temperature and the air temperature from two hours before sunset until sunrise at the ground and roof surface levels in the city and at the ground level in the rural area. Figure 19 (B) shows the differences between the urban surface and air temperatures and the rural surface and air temperatures. In order to consider the effect on temperature of the surface coverage materials, the effect of the interruption of the long-wave radiation by the building must be excluded. Therefore, the data on the roof surface which are not interrupted by the buildings, are compared with the data of the rural area. In the two hours before sunset, the rural surface temperature cooled markedly ($> 5^\circ\text{Ch}^{-1}$). At the same time, the urban surface temperature cooled only a little ($< 5^\circ\text{Ch}^{-1}$). Presumably this was a result of strong rural surface long-wave radiation and cooling of the lower atmosphere. The urban roof surface temperature cooled moderately. These trends continued until about three or four hours after sunset. The cooling rates of the urban ground surface were about 40 to 50% of those in the rural area. The cooling rates of the urban roof surface were about 30 to 40% of those for the rural area. Later in the night the cooling rates became similar in the three locations and remained fairly constant until sunrise. During the period from sunset to almost midnight, the heat island intensity (ΔT_{u-r}) steadily increased to its maximum value in response to the differing urban and rural cooling rates. Presumably during this period the urban area expended much of its stored heat, and rural surface temperatures became low so that outgoing losses were reduced. Then, the heat island diminished gradually until sunrise.

There are two striking features in Figure 19 (B). First, the difference in the temperature between the roof surface in the urban area and the ground surface in the rural area depends on the differences in the thermal features of the surface coverage materials. The roof surface which is made of concrete has a larger thermal admittance than the soil surface in the rural area. This causes the roof surface in the urban area to maintain a high temperature while the ground surface becomes cool in the rural area. Thus the difference in their temperatures appears. Second, the ground surface of the urban area maintains a high temperature compared to the roof surface due to the interruption of the long-wave radiation by the buildings. Therefore, the ground surface temperature in the urban area is very high because it is greatly affected by the urban geometry and the thermal admittance level. This enhances the heat island intensity. As indicated in Fig. 19 (A) and (B), the temporal trends of air temperatures were similar to those of the surface temperatures described above.

Figure 20 shows the relationship between the cooling amounts of the surface temperature (ΔT_{t-s}) from sunset until sunrise and the net long-wave radiation (R_n) of the ground surface, of the roof surface at the center of the urban area and of the ground in the rural area during the nighttime. The values for the urban area are those shown in Fig. 15 and those for the rural area were calculated from the special observation data. In calculating the Brunt curves (Equation (25)) for the area, $R_n = 110 \text{ Wm}^{-2}$ and $C\rho K^{1/2} = 1600 \text{ Wm}^{-2} \text{ S}^{1/2} \text{ K}^{-2}$ were used based on the special observation data collected by the present writer and on the published data by Oke and Maxwell(1975) respectively. These Brunt curves have the shape of the standard decay function and agree with the field measurements qualitatively. The slope of the Brunt curve is steepest in the rural area and is progressively less steep for the roof surface and then the ground surface in the urban area. In other words, the rural area is liable to cool while the urban area retains the heat.

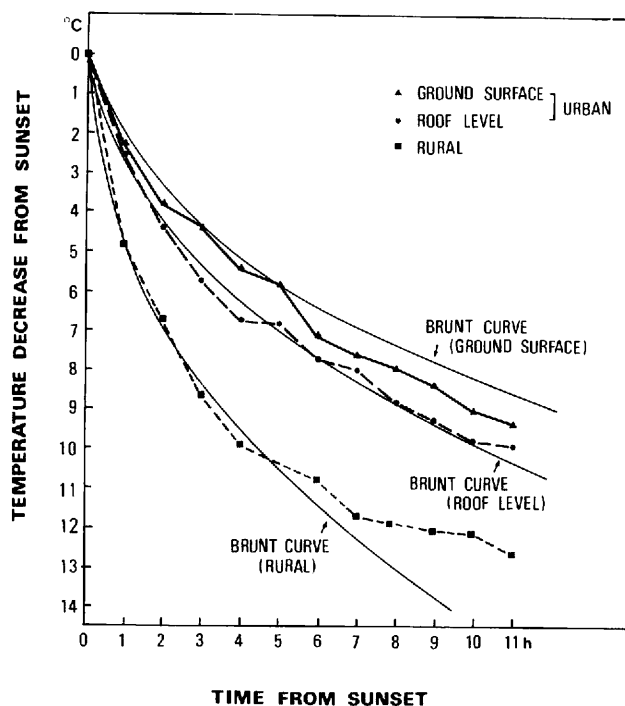


Fig. 20 Surface temperature decrease after sunset in urban (two levels, ground surface and roof surface) and rural areas

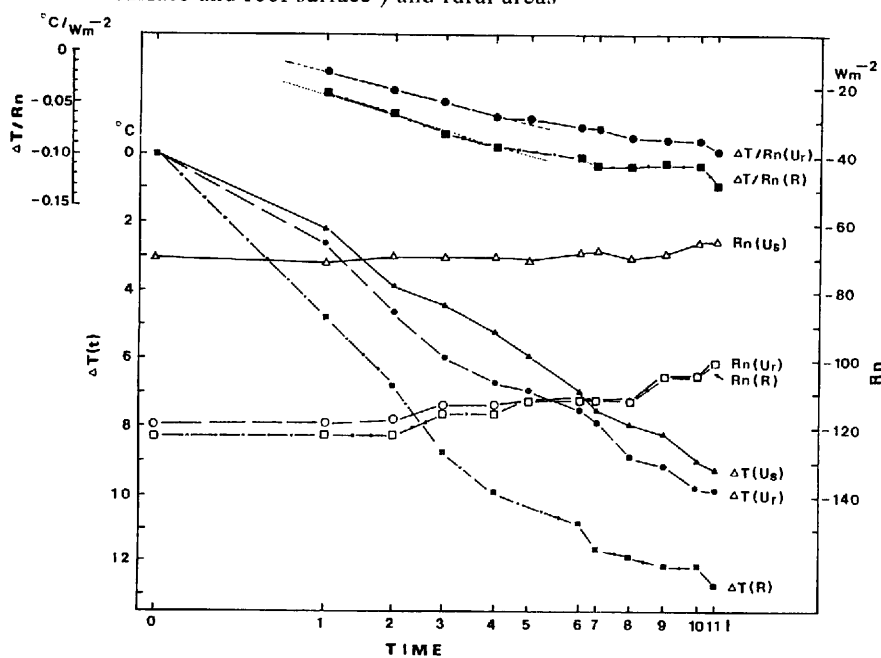


Fig. 21 Variation of surface temperature decrease from sunset, net long-wave radiation at the surface and their ratio, versus time from sunset between urban and rural areas

Based on these results, Equation (25) can be rewritten as the following equation.

$$\frac{\Delta T_{t-s}}{R_n} = - \frac{2}{\pi^{1/2} C_p K^{1/2}} t^{1/2} \quad (27)$$

Then a plot of the ratio $\Delta T_{t-s}/R_n$ versus $t^{1/2}$ has the slope $-(2/\pi^{1/2} C_p K^{1/2})$, which will be constant because the equation represents the physics of cooling. Figure 21 shows the cooling amounts of surface temperatures (ΔT_{t-s}), the net long-wave radiation (R_n) and their ratio, versus time from sunset for the ground surface and roof surface of the urban area and for the ground surface of the rural area. An aim of this study is to assess the cooling of the surface temperatures based only on differences in the component materials of the ground surfaces. Because the ground surface temperatures in an urban area are affected not only by the component materials of its surface but also by the buildings nearby, they are not discussed here. The present study supports the Brunt scheme because $\Delta T_{t-s}/R_n$ versus $t^{1/2}$ is almost exactly linear, at least for the first 3 to 4 hours, as indicated by the following equations.

urban roof surface ;

$$\Delta T_{t-s}/R_n = -0.04 t^{1/2} + 0.02 \quad (r^2 = 0.99) \quad (28)$$

rural ;

$$\Delta T_{t-s}/R_n = -0.05 t^{1/2} + 0.01 \quad (r^2 = 0.99) \quad (29)$$

The slope of the regression line for the urban area is less steep than that for the rural area. This means that the rate of cooling is smaller in the urban area, which has a larger thermal admittance, than in the rural area.

CHAPTER IV

TOPOGRAPHICAL EFFECTS ON THE HEAT ISLAND INTENSITY

4.1 The heat island intensity and city size classification based on topographical factors

As mentioned in the previous chapter, the heat island intensity increases with increases in the size of the city (shown in Fig.3). The relationship between the maximum heat island intensities of cities in a region and the populations of the cities can be represented by a linear regression line. The points representing some cities will be near the line. The points for other cities will be farther from the line. A reason for variation in locations of points is that cities are affected by their geographical conditions. In general, the points of plain cities will be close to the linear regression line while those for coastal and basin cities will be farther away.

If a city is located on flat land where there is not much geographical effect, its heat island intensity can be the difference between the urban temperature (T_u) and the nearby rural temperature (T_r). Then,

$$\Delta T_{u-r} = T_u - T_r \quad (30)$$

On the other hand, the heat island intensities of basin and coastal cities are greatly affected by topography. Considering these, the equation would be

$$\Delta T_r = T_r - T_{rn} \quad (31)$$

If T_{rn} represents the air temperature at a flat surface in a rural area, then ΔT_r is the amount of change caused by the surrounding topography. Considering $\Delta T_r = 0$ on the regression line shown in Fig. 3, the deviation from this regression line is mainly caused by topography. Therefore, ΔT_r in the coastal city is negative, and the heat island intensity (ΔT_{u-r}) is rather small. In the basin city however, ΔT_r is positive and the heat island intensity is rather high.

The effects on the heat island intensity of topography have been investigated by Chandler (1964), Tyson *et al.* (1972), Nkemdirim (1980_a, 1980_b), and Goldreich *et al.* (1981, 1984). However, each of their studies concerned urban heat island intensities within a single type of topography. They did not compare the heat island intensities of cities in different types of topographical zones.

The relationship between the maximum heat island intensities and the populations of Japanese cities in the three types of topographical locations, in basins, on inland plains, and along the coastline, are examined in Fig. 22. This figure shows that for cities with approximately similar size populations, the heat island intensities decrease from basin cities to inland plains cities, and to coastal cities. Therefore, the maximum heat island intensity depends not only on the shape, structure, and function of a city but also on the topographical features of the location of the city.

Now, in order to discuss the influence of topography on the heat island intensity, three cities with populations between 350,000 and 450,000 will be studied in detail. They are Gifu, an inland plains city, Asahikawa, a basin city, and Niigata, a coastal city. These cities meet the conditions mentioned in Chapter II.

4.2 Contrasting phenomena in the heat island intensity among the three types of cities

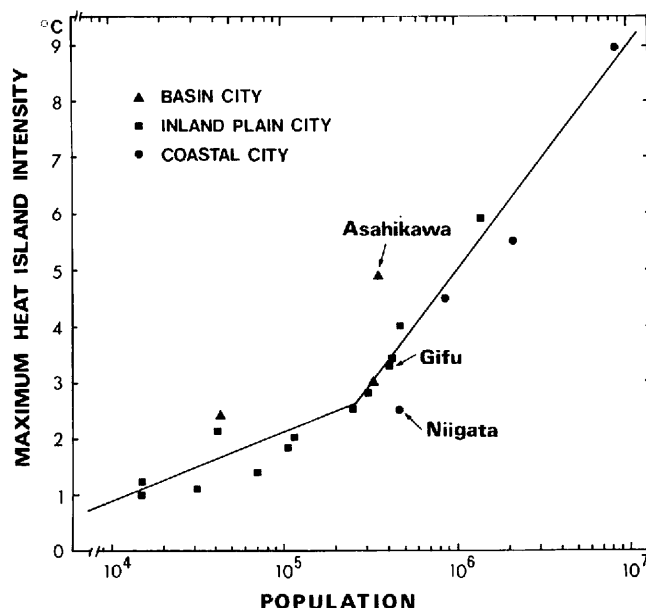


Fig. 22 Relationships between the maximum heat island intensity and the urban population are compared in three categories, basin, inland plain, and coastal cities

In order to compare the diurnal variations of heat island intensities in Gifu, Asahikawa, and Niigata, summer and winter conditions were considered. For each city and each season, AMeDAS data were obtained for a clear (cloud cover < 2/10) and calm day (mean wind speed < 3m/s). The AMeDAS records for the period from January 1, 1981 through December 31, 1984, provided such data.

For each city, one day was selected for January, another for August. The days for January were chosen so that, as much as possible, they had similar conditions of atmospheric pressure distribution, precipitation, cloud cover, and wind speed for all the cities. The days for August were identified in the same way. Figure 23 presents surface weather maps for the days selected for the case studies. On the summer days, the North Pacific Ocean High covered Japan. On the winter days, a Siberian or a migratory high covered Japan. All days were clear and calm in the three cities.

4.2.1 City located on an inland plain

Figure 24 shows the diurnal variations of temperature, cooling and warming rates, heat island intensity, wind speed and direction, and sunshine duration on August 1–2, 1981, at Gifu City. On that day, the sunshine duration during the daytime was nearly one hour per hour (cloud cover 0). The wind prevailed from N to NE during the day. At night the air was calm and so favorable for the formation of a heat island.

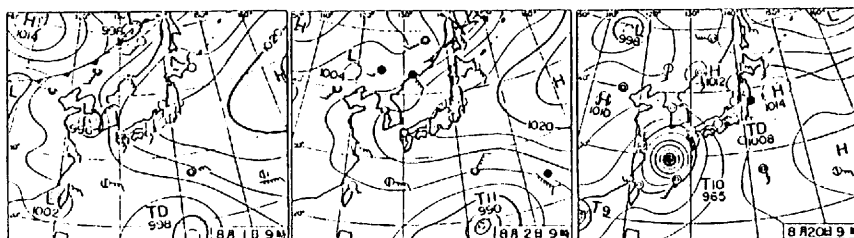
The diurnal ranges of the urban and rural air temperatures were 6.9°C and 8.5°C respectively. The cooling amount of the air temperature (ΔT_{L-N}) between sunset and sunrise was much larger in the rural area. It was 2.9°C for the urban area and 4.6°C for the rural area. The cooling rate ($\Delta T/\Delta t$) was greatest from sunset through midnight in both locations. The maximum heat island intensity reached 3.2°C at 23:00. However, the increase in temperature after sunrise was greater for the ru-

SUMMER

1981.8.1.

1981.8.2.

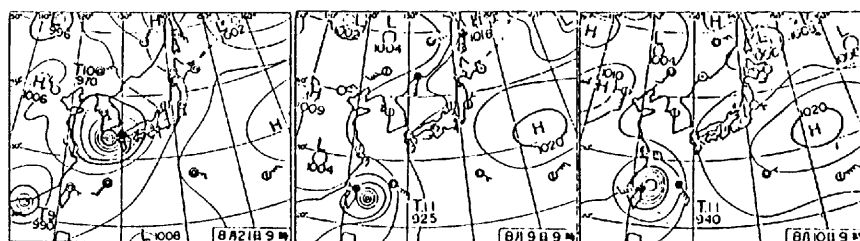
1984.8.20.



1984.8.21.

1982.8.9.

1982.8.10.

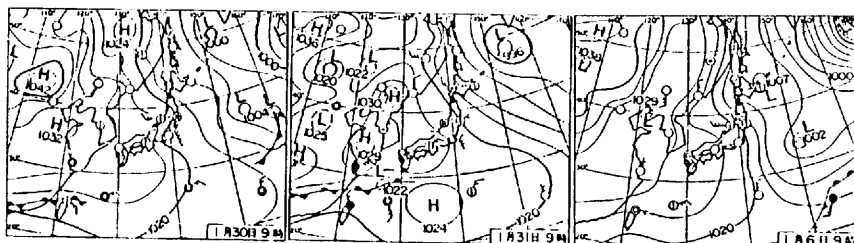


WINTER

1981.1.30.

1981.1.31.

1984.1.6.



1984.1.7.

1983.1.7.

1983.1.8.

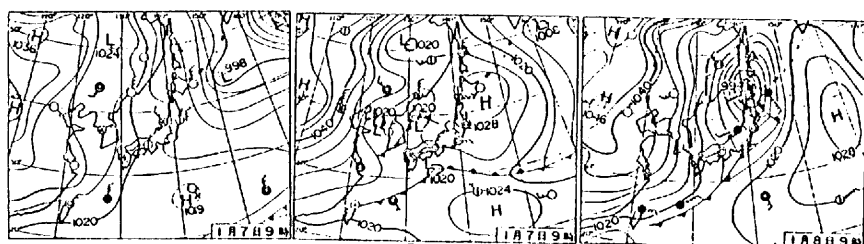


Fig. 23 Surface weather maps of days for which data were collected. Upper is summer and lower is winter

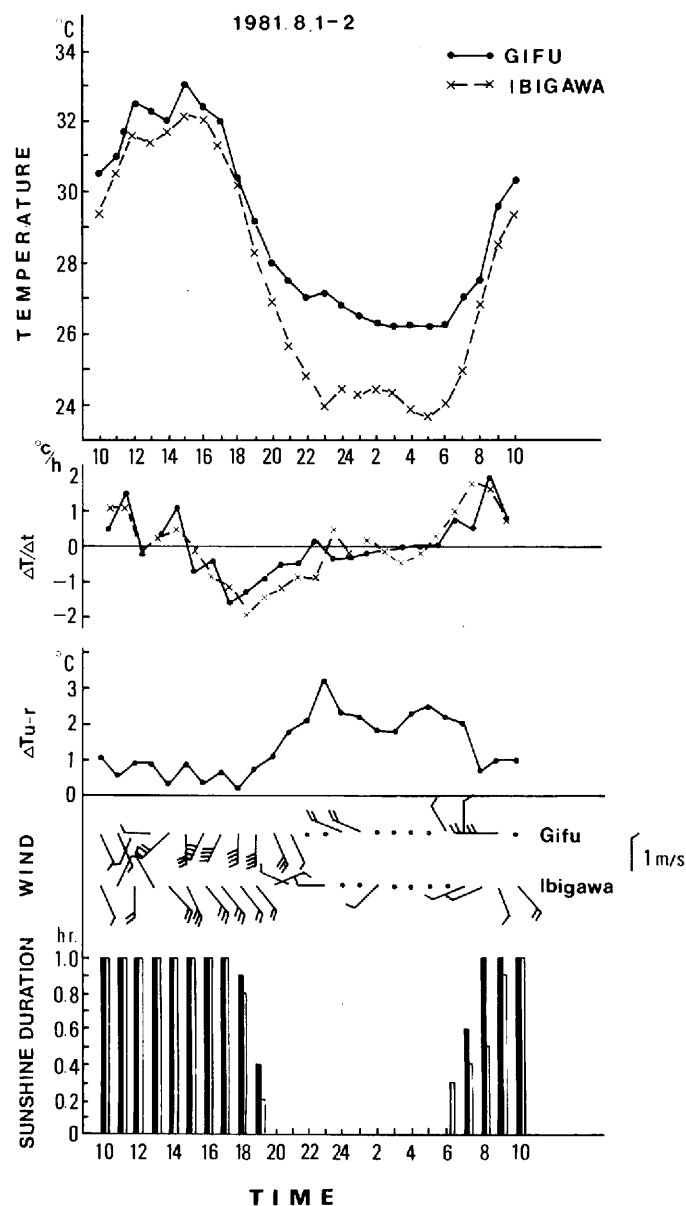


Fig. 24 Diurnal variations of air temperature, cooling and warming rates, heat island intensity, wind, and sunshine duration in Gifu City for Aug. 1-2, 1981

ral area. Moreover, because the rural temperature increased rapidly, the heat island intensity in daytime was smaller than in nighttime. The difference in cooling rates between the urban and the rural area, being large at night, means that the urban area is harder to cool than the rural area. The reason for this, as mentioned in Chapter III, relates to urban activities, the urban geometry and the difference in thermal admittance rates of ground surface materials.

Figure 25 shows the daily variations of temperature, cooling and warming rates, heat island

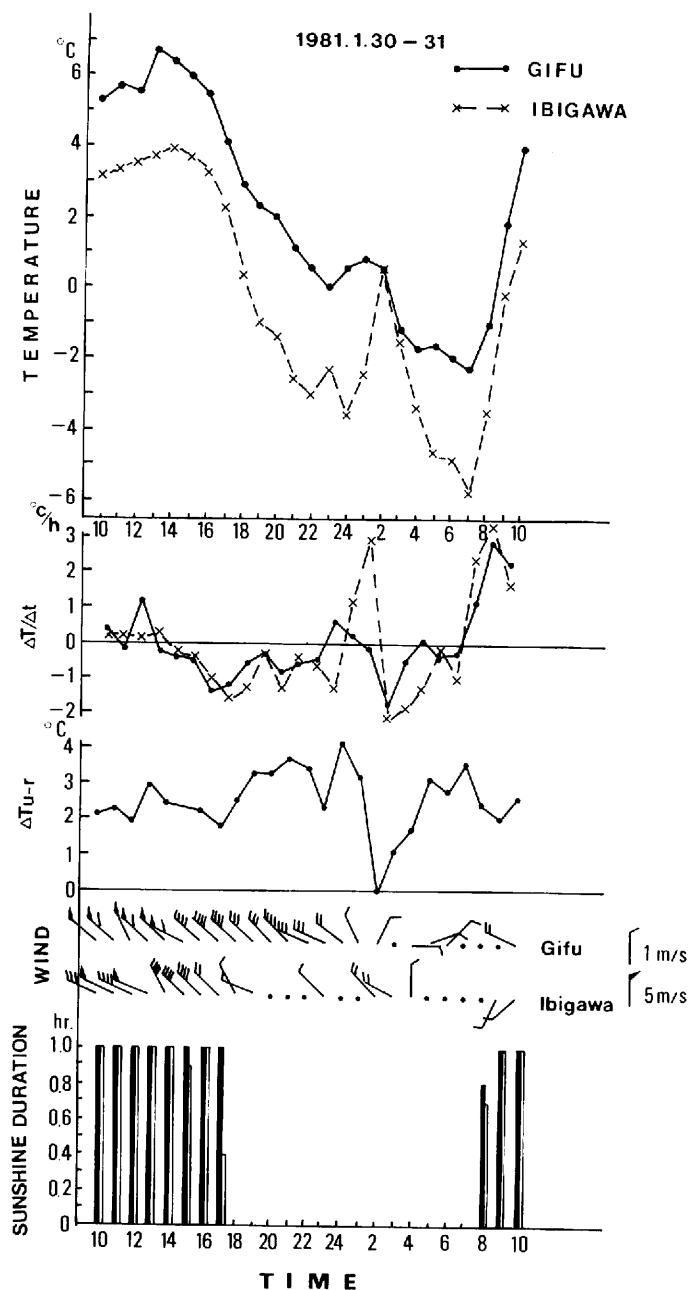


Fig. 25 Same as Fig. 24, but for Jan. 30 – 31, 1981

intensity, wind, and sunshine duration on January 30 – 31, 1981, the winter day selected for Gifu City. On this day, the sunshine duration was nearly one hour per hour (cloud cover 0). During the day, the seasonal wind, a north-west wind, was strong but at night it was calm. The diurnal range of temperatures for the urban area was 9°C, and for the rural area 9.8°C. Compared to summer, it was large. The temperature data for Ibigawa, Gifu City's nearby rural area, show an increase at 02:00. The increase occurred because a 2m/s wind blew at that time, so the nocturnal inversion

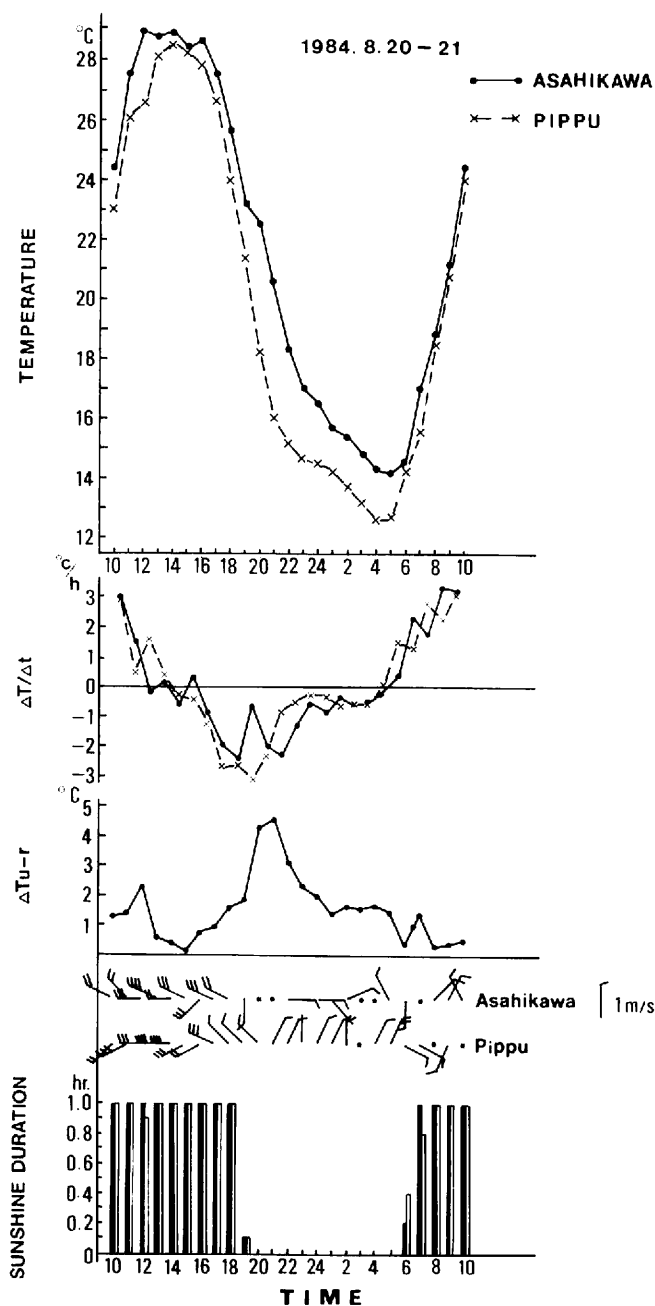


Fig. 26 Diurnal variations of air temperature, cooling and warming rates, heat island intensity, wind, and sunshine duration in Asahikawa City for Aug. 20 - 21, 1984

layer was destroyed. As such, the increase in sensible heat flux due to vertical mixing process could be the reason for the increase in temperature. Afterwards, calm conditions prevailed. The amount of temperature cooling (ΔT_{t-s}) from sunset to sunrise was 6.4°C for the urban area and 8.1°C for rural area, twice the amount of the summer night. The diurnal variations of cooling and

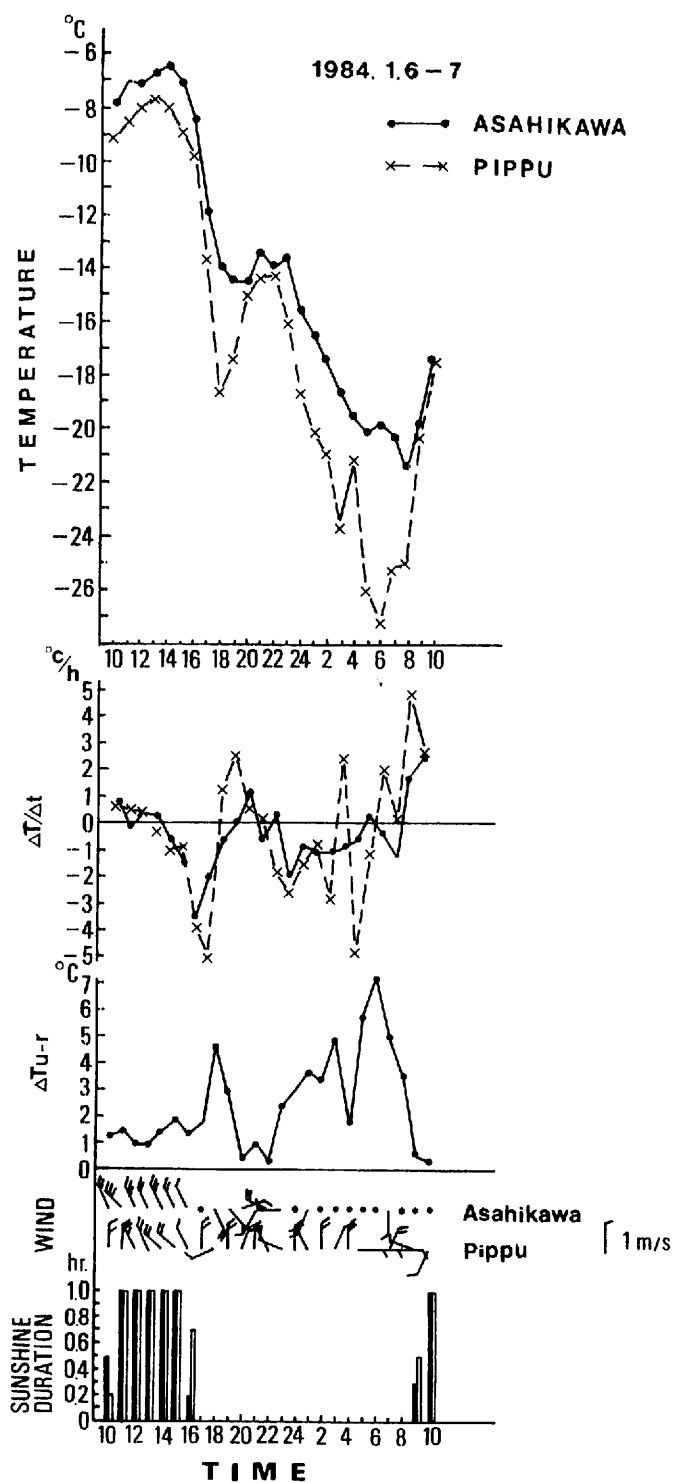


Fig. 27 Same as Fig. 26, but for Jan. 6-7, 1984

warming rates were similar to those during summer, but the difference within the city was larger in winter than in summer, and the heat island intensity was also larger in winter. The maximum heat island intensity was 4.2°C at 24:00.

4.2.2 City located in a basin

Figure 26 shows the diurnal variations of temperature, cooling and warming rates, heat island intensity, wind speed, and sunshine duration of the selected summer day, August 20 – 21, 1984, in Asahikawa City. The weather condition of the day was fine, with an average of nearly an hour of sunshine duration per hour (cloud cover 0). The wind speed of the daytime was 2 – 3m/s, but the air was calm throughout the night. Circumstances were suitable for heat island formation. The diurnal range of temperature in the urban area was 14.8°C and in the nearby rural area of Pippu was 16°C. It is a feature of basin climates that the diurnal range in cities is much larger than in cities on inland plains. The cooling amounts of temperature (ΔT_{t-s}) from sunset until sunrise in the urban area and the rural area were 8.7°C and 9.0°C respectively. The cooling rates ($\Delta T/\Delta t$) both inside and outside the city were extremely large until about 21:00, and became smaller after that. As a result, the heat island intensity also attained its maximum value of 4.6°C at 21:00, but declined thereafter.

Figure 27 shows weather conditions in Asahikawa City on the winter day of January 6 – 7, 1984. The weather was clear, and the air calm all through the day. The diurnal range of temperature was 15°C in the urban area and 18.8°C in the nearby rural area. The range in the rural area was specially large. The temperatures at both places began to cool after reaching their high points at about 13:00 or 14:00 hours, then dropped sharply with sunset between 16:00 and 18:00. However, by 19:00 the temperature decline slowed markedly, then dropped sharply again at about 23:00. But the change slowed again at about 02:00 or 03:00 in the morning, and then increased again at about 04:00, with the lowest temperatures reached between 06:00 and 08:00. Because the cooling rates ($\Delta T/\Delta t$) varied significantly between sunset and early morning, the temperature change curve on the graph in Fig. 27 is undulant. This pattern was probably closely related to the pattern of cold air drainage in the basin at night (Yoshino, 1960, 1975, 1980, 1984 ; Nakamura, 1976, 1978, 1980 ; Kondo, 1982 ; Kondo *et al.*, 1983 ; Kudoh *et al.*, 1982 ; Mori and Kondo, 1984 ; Toritani, 1985). On a clear and calm or nearly calm night, radiative cooling causes cold air drainage from higher to lower elevations in basins. Temperatures fall sharply then at weather stations in the basins as the cool air passes over. Then the temperatures rise slightly as the stations are covered again by the original airmass after the cool air current is gone. As a result, the temperature curve is undulant. In this process, rapid cooling continues until early morning in the basin. However in the urban area, because there is an urban effect, the temperature does not drop as much as in the rural area. The temperature cooling amounts (ΔT_{t-s}) from sunset to sunrise in the urban and the rural areas of the basin were 8.1°C and 11.5°C respectively. Because of this difference, the heat island intensity of the basin city was greater than that of the inland plain city. In the basin city of Asahikawa the maximum heat island intensity was 7.3°C at 06:00.

4.2.3 Coastal city

Figure 28 shows the diurnal variations of temperature, cooling and warming rates, heat island intensity, wind, and sunshine duration of the summer day of August 9 – 10, 1982, in Niigata city. The weather on that day was clear, with about an hour of sunshine duration per hour (cloud cover 0). However, a strong NW sea-breeze developed during daytime. During the night, a land-breeze

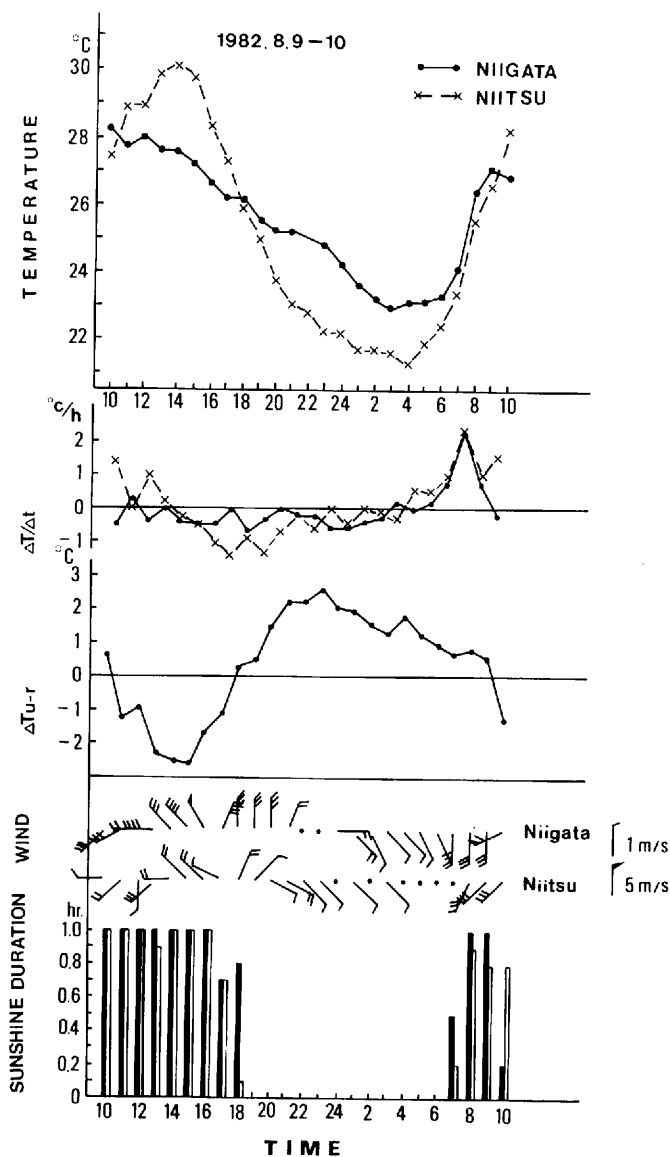


Fig. 28 Diurnal variations of air temperature, cooling and warming rates, heat island intensity, wind, and sunshine duration in Niigata City for Aug. 9–10, 1982

produced a gentle S-SE wind so that conditions were favorable for heat island formation. The diurnal ranges of temperature in the urban area and in the nearby rural area called Niitsu were 5.3°C and 8.8°C respectively. Both those range figure are smaller than the summer figures for the cities on the inland plain and in the basin. The amounts of temperature cooling (ΔT_{i-s}) between sunset and sunrise were also smaller, being 2.4°C in the city and 3.1°C in rural area. Consequently, the heat island intensity was also smaller. The maximum heat island intensity was 2.6°C at 23:00, which was the lowest summer value among the three cities.

A special feature may be noted in Fig. 28. The heat island intensity in the daytime was minus, or negative. This phenomenon, which was not observed in the cities of the inland plain and the basin, was caused by the sea-breeze of the daytime. Niigata City, located on the coast, receives cool SW, W, and NW sea-breezes during the daytime in summer, which lower its temperature. But once that wind blows into the inland, it passes across the warmer land surface and is warmed. As such, the temperature of Niitsu, inland from Niigata, did not fall. Therefore the heat island intensity of Niigata was negative for that portion of the day. However in the night, the heat island intensity became positive because it was not affected by the sea-breeze.

Figure 29 shows the diurnal variations of temperature, cooling and warming rates, heat island intensity, wind, and sunshine duration for Niigata City on January 7 – 8, 1983. The weather was

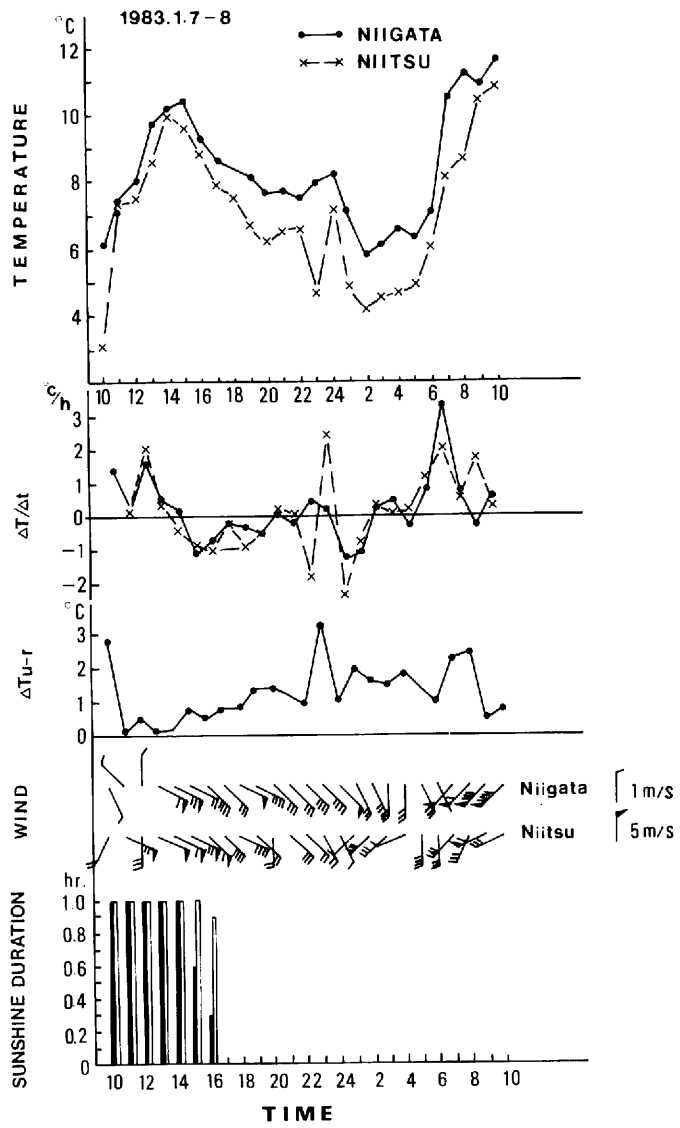


Fig. 29 Same as Fig. 28, but for Jan. 7 – 8, 1983

fine, with almost one hour of sunshine per hour of daylight. Again there was no cloud cover, but a moderately strong SE-SW wind blew (mean wind speed 3.5 – 4m/s) during the daytime. The diurnal range of temperature was very small. That is one of the characteristics of a marine climate. The diurnal range in the city was 4.6°C and for the nearby rural area was 5.8°C. Moreover, the amounts of temperature cooling (ΔT_{t-s}) were small, 2.3°C in the city and 2.9°C outside, and the difference between the inside and outside figures was small. The maximum heat island intensity was only 3.3°C at 23:00. This value was the smallest for winter of the three cities, and only half that of the city in the basin.

The pattern of change in the heat island intensity during the day was very different from that of the summer day. In other words, it was positive rather than negative. This fact is related to the absence of both the sea-and the land-breezes in winter. According to Yoshino et al. (1973_b), who investigated the frequency of appearance of the sea-and land-breezes in Niigata City, the breezes occurred 46% of the time in June, July, and August but did not occur in December, January, and February. Ninomiya (1960) and Fukuda (1970) reported the same finding. The data above suggest that the daily changes in the heat island intensity of coastal cities are strongly affected by the winds of both sea and land.

4.2.4 Comparing the cities from the topographical perspective

Meteorological information related to the heat island intensities of three topographically different cities has been examined for each city. Table 4 presents a summary of the data on the meteorological elements (temperature, wind speed, sunshine duration), the cooling amounts of temperature (ΔT_{t-s}) from sunset until sunrise, and the heat island intensity of the three cities. The diurnal range of temperature was the highest in both season in the basin city with the inland plain and coastal cities following in that order. The diurnal range of temperature in the basin city was 2 to 3 times as large as that of the coastal city. The reason is that the temperature difference between daytime and night is larger in the basin city than the coastal city. The wind speed, however, is strongest in the coastal city. The wind speed of the coastal city is 2 to 3 times stronger than that of the city in the basin. Many days are calm all day long, especially at night, in the both seasons in the basin city. As a result, the basin city seems to be little influenced by advection. On the

Table 4. Diurnal range of temperature, wind speed, sunshine duration, cooling amounts of temperature from sunset till sunrise (ΔT_{t-s}), and the maximum heat island intensity ($\Delta T_{u-r(max)}$) among the three types of cities.

	Summer						Winter					
	Gifu		Asahikawa		Niigata		Gifu		Asahikawa		Niigata	
diurnal range of temperature	urban	rural	urban	rural	urban	rural	urban	rural	urban	rural	urban	rural
	(°C)											
	6.9	8.5	14.8	16.0	5.3	8.8	9.0	9.8	15.0	18.8	4.6	5.8
mean wind speed	(m/s)											
	1.6	1.2	1.4	1.5	2.6	1.4	2.8	1.6	1.1	1.6	3.5	4.0
sunshine duration	(hr)											
	1.0	1.0	1.0	1.0	1.0	1.0	1.0	1.0	1.0	1.0	1.0	1.0
cooling amounts of temperature from sunset till sunrise (ΔT_{t-s})	(°C)											
	2.9	4.6	8.7	9.0	2.4	3.1	6.4	8.1	8.1	11.5	2.3	2.9
maximum heat island intensity ($\Delta T_{u-r(max)}$)	(°C)											
	3.2		4.6		2.6		4.2		7.3		3.3	

other hand, the influence of advection on the coastal city seems to be great all day long. Particularly in summer, when sea and land breezes are common, does the wind speed have a great influence on the heat island intensity of the coastal city. Sundborg (1950), Kawamura (1964), Oke and Hannell (1972), and Park (1986_a, 1986_b) have shown that heat island intensity and wind speed are inversely related. That is the greater is the wind speed, the smaller is the heat island intensity, and the heat island disappears completely if the speed exceeds a certain level. Sunshine duration is one hour per hour (cloud cover 0), so that the days are clear in all three cities. The cooling amounts of temperature (ΔT_{t-s}) from sunset until sunrise vary depending on the location. In particular, the cooling rate of the basin city is large, more than twice that of the inland city and three times that of the coastal city.

This finding agrees generally with the values obtained from Kondo's night cooling equation (1982), though the values from the present study are larger. Kondo explains that the rate of nocturnal cooling when cool air flows from a mountain and accumulates to a thickness of more than 100 – 150m, as in a basin, is approximately 1.3 times as large as that on a plain. Particularly in winter, the cooling rates inside and outside the city depend on topographical conditions. That of the basin city is 3.4°C which is two to six times bigger than those of the inland plain and coastal cities, which are 1.7°C and 0.6°C respectively. The difference in cooling rates between locations inside and outside the city are directly related to heat island formation. Hence, the heat island intensity is greatest in the basin city (Asahikawa), and the value is about 1.7 times as large as of the inland plain city (Gifu) and 2.2 times that of the coastal city (Niigata).

4.3 Spatial and temporal aspects of the heat island intensity in the three types of cities

4.3.1 Diurnal variations of the heat island intensity

The data on the diurnal variations of the heat island intensity suggest that they differ among the cities in the three types of topographical locations. In order to examine this phenomenon more closely, data on temperatures were obtained for additional days of clear (cloud cover < 2/10) and calm (mean wind speed < 3m/s) weather in summer (June, July, August) not only for the three cities but also for other cities in similar topographical locations. Hourly temperature data for the 23 days in which the heat island intensity was strongly noticeable were collected.

Figure 30 shows the diurnal variations of the heat island intensity in Asahikawa, Gifu and Niigata as the averages of those variations during the 23 summer days. The features and the values of the heat island intensity in the cities differ significantly. In Asahikawa, the basin city, the heat island intensity is strongest and has double peaks, between 21:00 and 22:00, and again between 03:00 and 04:00. As mentioned above, it can be assumed that this fact is related to cold air drainage. The double peak in heat island intensities also appears in the basin cities of Yamagata (240,000 inhabitants) and Fukushima (260,000 inhabitants), though theirs reach peaks at slightly different times, between 19:00 and 21:00 and between 04:00 and 05:00. In Gifu, the inland plain city, the value of the heat island intensity is intermediate between that of Asahikawa and Niigata, and it has a single peak at 23:00. The single peak is also seen in the plain cities of Sapporo (1,400,000 inhabitants) and Obihiro (150,000 inhabitants). The peak occurs between 04:00 and 05:00 in Sapporo, and between 01:00 and 02:00 in Obihiro. In Niigata, the coastal city, the heat island intensity is lowest and has a single peak. However, during the day the heat island intensity is negative due to the influence of sea-breezes. The daytime negative heat island intensity can also be seen in other coastal cities. In Shizuoka (460,000 inhabitants), the heat island intensity is lower than -1°C between 10:00 and 13:00.

In general, the heat island intensity in the cities is highest at night and lowest during the day.

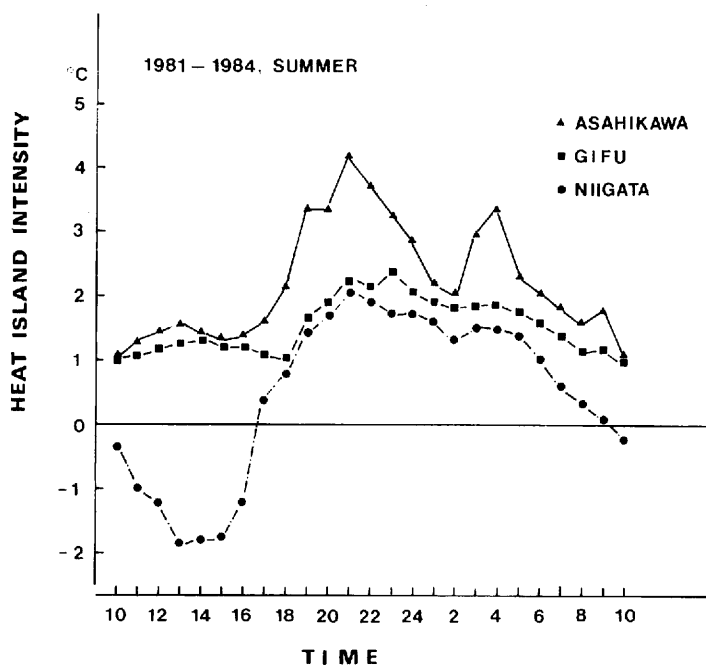


Fig. 30 Diurnal variations of the heat island intensity in Asahikawa, Gifu, and Niigata during the summer (1981 - 1984 ; 23 times)

But the time of greatest intensity and the level of intensity vary. In order to seek clarification of the variations, additional examination of the data is necessary. Figure 31 shows the frequency distribution of the heat island intensity figures for Gifu City in summer. The temperature levels of the heat island intensity figures were classified into units of 1°C . At 01:00, intensity figures of 1 to 2°C occur 14 times, figures of 2 to 3°C appear 7 times, and figures of 4 to 5°C show 2 times. At 02:00 and again at 03:00 the occurrence frequency of 1 to 2°C is 13 times and 0 to 1°C is 4. At 04:00, the heat island intensity becomes high and 3 to 4°C appears 4 times. After 05:00, the heat island intensity decreases and 0 to 1°C appears 6 times. Between 06:00 and 08:00, the occurrences are about the same as at 05:00. After 09:00, the heat island intensity reaches 0°C 2 times ; that means it does not appear. This lasts until 11:00. After 12:00, the heat island intensity appears again 16 times at 0 to 1°C , 7 times at 1 to 2°C , which general pattern continues until 14:00. Between 15:00 and 16:00, 0°C is the intensity figure twice, but after that the heat island intensity increases. After 23:00, it reaches the maximum value and a 4 to 5°C level appears once. The pattern is the same at 24:00 except that the 4 to 5°C figure appears two times. This pattern lasts until 04:00. The peak of frequency distribution of the maximum heat island intensity occurs at the category with the range 3 to 4°C .

Figure 32 shows the frequency distribution of the heat island intensity figures for Asahikawa in summer. At 01:00, the intensity level of 4 to 5°C is reached 11 times and the level of 3 to 4°C attained 9 times. There are no figures under 2°C . Between 02:00 and 05:00, the pattern is generally similar to that of 01:00. At 06:00, the heat island intensity decreases to 1°C . But at 07:00, the maximum value of 6 - 7°C appears. From 08:00 to 09:00, the heat island intensity declines and reaches 0°C 2 times. That means that it does not appear. After 10:00, a 0 to 1°C level appears 11 times and 3 to 4°C appears one time. At about sunset, the heat island intensity again increases. By

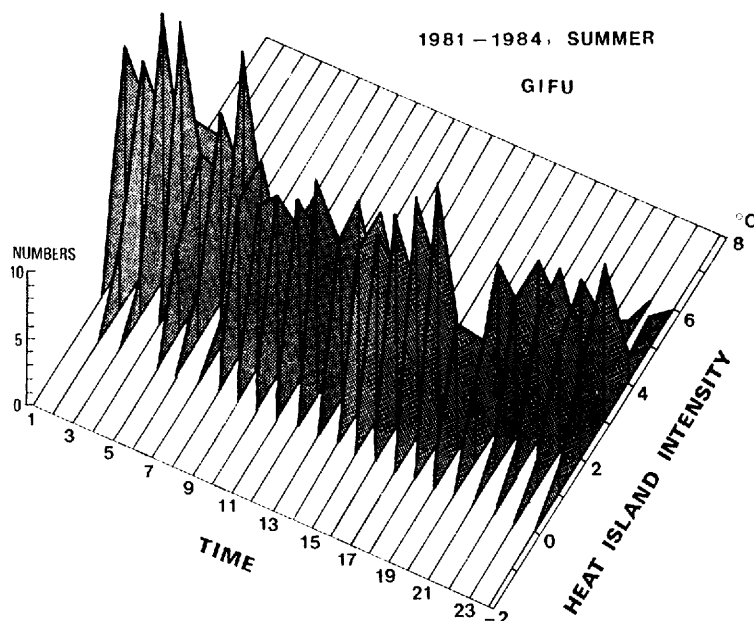


Fig. 31 Frequency distribution of the heat island intensity of Gifu City in summer.
The chosen days same as Fig. 30

17:00, the heat island intensity becomes noticeably higher and the 3 to 4°C figure appears 5 times. After 20:00, the value of 6 – 7°C also appears. Thus, the diurnal variations of the heat island intensity are large. It is apparent that frequency distribution of the maximum heat island intensity reveals patterns that are similar to those identified earlier for the average condition of the heat island intensity for the cities of Gifu and Asahikawa located on an inland and in a basin respectively. The peak of frequency distribution of the maximum heat island intensity shows in the range 4 to 5°C. Further investigation is needed, considering cold air drainage.

Figure 33 shows the frequency distribution of the heat island intensity levels for Niigata City in summer. At 01:00, the 2 to 3°C level occurs 14 times, 1 to 2°C appears 6 times and 0 to 1°C 4 times. This pattern is maintained until 07:00. After 08:00, the heat island intensity becomes negative and continues as such until 18:00. Especially, at 10:00 the – 1 to – 2°C appears 4 times ; at 11:00 3 times ; at 12:00 6 times at 13:00 4 times ; at 14:00 5 times ; at 15:00 3 times ; and at 16:00 3 times. The greatest frequency is of figures between 0 and 1°C, and the heat island intensity becomes very low. After 19:00, the values become positive and 0 to 1°C appears 5 times, 1 to 2°C 12 times and 2 to 3°C 6 times, a pattern that continues through the night. The maximum value appears at 21:00 and 3 to 4°C appears 4 times. The numbers at 22:00 are about the same as those of 21:00. At 23:00 and 24:00, the 2 to 3°C figures are most numerous, showing more than 10 times. The 2 to 3°C range has the peak frequency of the maximum heat island intensity. The fact that the frequency of negative heat island intensity figures is high in daytime is similar to the pattern seen earlier for the average condition of the summer season. Therefore, the values of the heat island intensity and their diurnal variations in coastal cities must be considered in relation to sea-breezes. The same conclusion was reached in a study of Rio de Janeiro (Nishizawa and Sales, 1983).

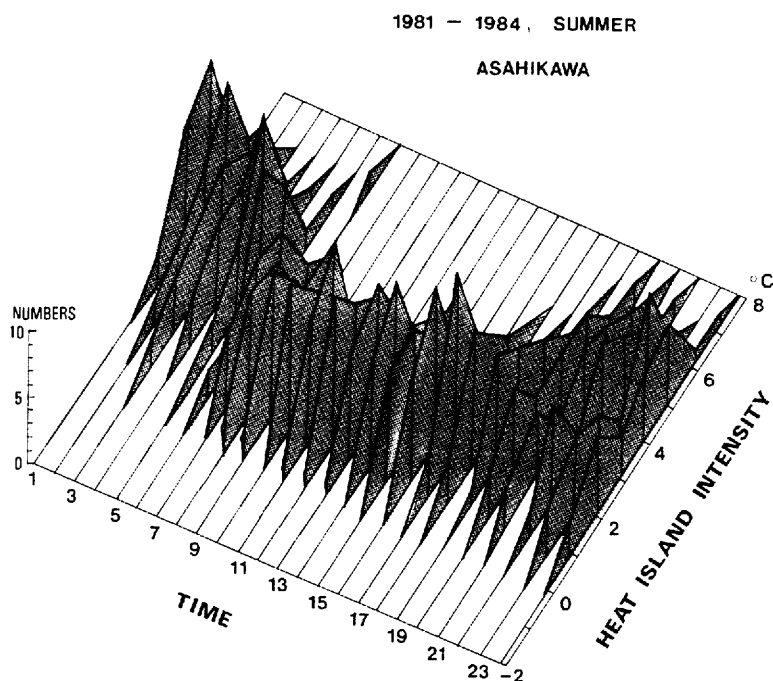


Fig. 32 Same as Fig. 31, but for Asahikawa City

4.3.2 Annual variations of the heat island intensity

In the foregoing section, the hourly changes of the heat island intensity values in summertime and in topographically different circumstances were analyzed. In this section, the annual variation of the heat island intensity will be investigated using data for the years from 1981 to 1984. Data only for clear (cloud cover $< 2/10$) and calm days (mean wind speed $< 3\text{m/s}$) were selected and their average values were calculated for each hour every month.

Figure 34 shows the annual change of the daily variation in the heat island intensity in Gifu City. Through a year, the heat island is formed at all times of the day, but is most prominent at night in winter. The heat island intensity reaches 4.0°C or more between 18:00 and 23:00 in January and at about 19:00 in February. Heat island intensity figures of over 3.0°C appear at night in all seasons except summer. They occur between 17:00 and 18:00 in January, 17:00 and 01:00 in February, 19:00 and 02:00 in March, 18:00 and 22:00 in September, 18:00 and 23:00 in October, 18:00 and 02:00 in November, and 17:00 and 02:00 in December. Furthermore, the heat island intensity figures of over 2.0°C appear at night in summer between 19:00 and 01:00 in June, 20:00 and 01:00 in July, and 21:00 and 01:00 in August. On the other hand, the daytime heat island intensity does not exceed 1.5°C except in winter and is below 1.0°C from 08:00 through 11:00 in June and July.

Figure 35 shows the annual change of the daily variation in the heat island intensity for Asahikawa City. The heat island forms at all times through a year and its values are much larger than those for Gifu City. Quite a strong heat island of over 1.5°C appears even on the summer days. Very strong heat islands of over 5.0°C appear between 17:00 and 18:00 in December, 18:00 and 09:00 in January, 18:00 and 08:00 in February, and 20:00 and 08:00 in March. The highest values,

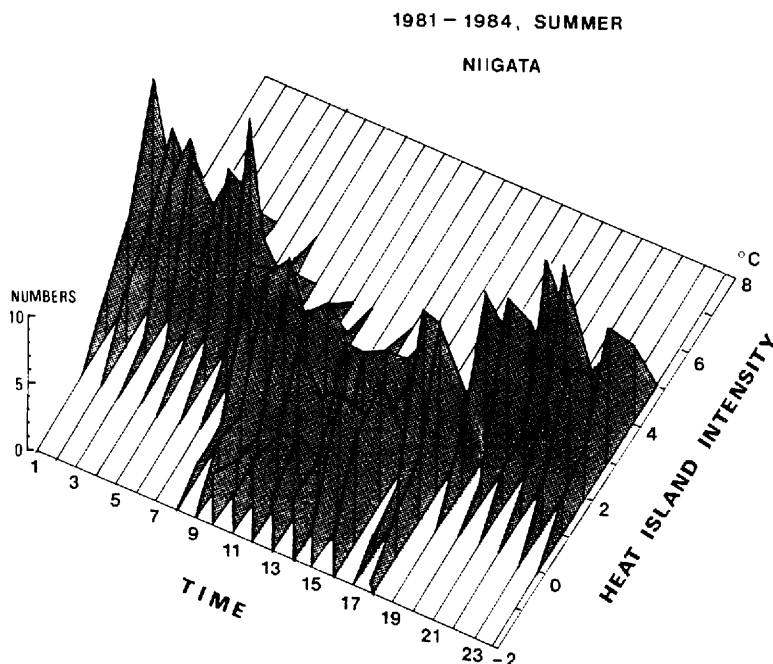


Fig. 33 Same as Fig. 31, but for Niigata City

over 6.0°C , appear at 02:00 and 08:00 in January and between 24:00 and 02:00 in February. It is interesting that highest values appear at night as well as the early morning in winter. This is characteristic of snow covered areas.

In the snow covered areas, transportation of sensible heat and latent heat by turbulence from the atmosphere to the snow-covered surface is extremely limited. Since heat conduction from the soil to the snow-covered surface is much greater than during non snow-covered periods, radiative cooling takes place, and a strong surface inversion layer appears. Inversion destruction usually begins shortly after sunrise, but is delayed in snow covered areas. Whiteman (1982) pointed out that surface inversion intensities are maintained until noon or all day in snow covered valleys. Yet in urban areas, the surface inversion intensity is decreased by urban effects. Therefore, the heat island intensity in snow covered areas is large since the temperature difference of the surface inversion between the urban and the rural areas is large. The maximum heat island intensity may appear in the early morning if the inversion continues after sunrise. Bohm and Gable (1978) indicated that the heat island is formed by the urban effect and topography, based on observation data for Vienna City. They estimated that the urban contribution to the heat island was approximately 30% and the remainder was due to the effect of snow cover. Harimaya *et al.* (1985) pointed out that in Iwamizawa City the heat island intensity in the early morning on a clear day when there is a heavy snow of about 1m is much higher than when the snow is under 20cm deep. Furthermore, Ohata *et al.* (1985) had similar conclusions in their investigation of Nagaoka City. These studies suggest that the heat island intensity is larger when there is a snow cover than when there is none.

Figure 36 shows annual change of the daily variation in the heat island intensity in Niigata City. The heat island is formed at night through most of the year, and the values of the heat is-

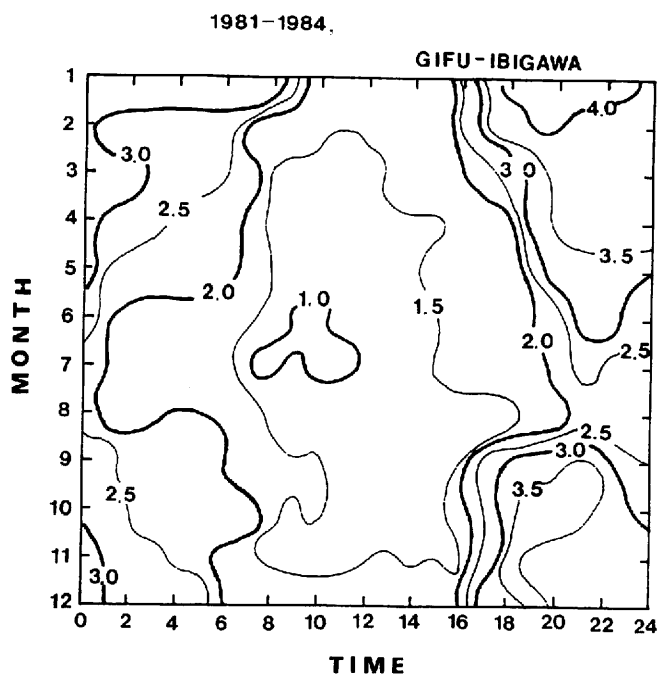


Fig. 34 Annual change of the daily variation in the heat island intensity of Gifu City (1981 - 1984 ; the average value for each hour on selected days in every month ; °C)

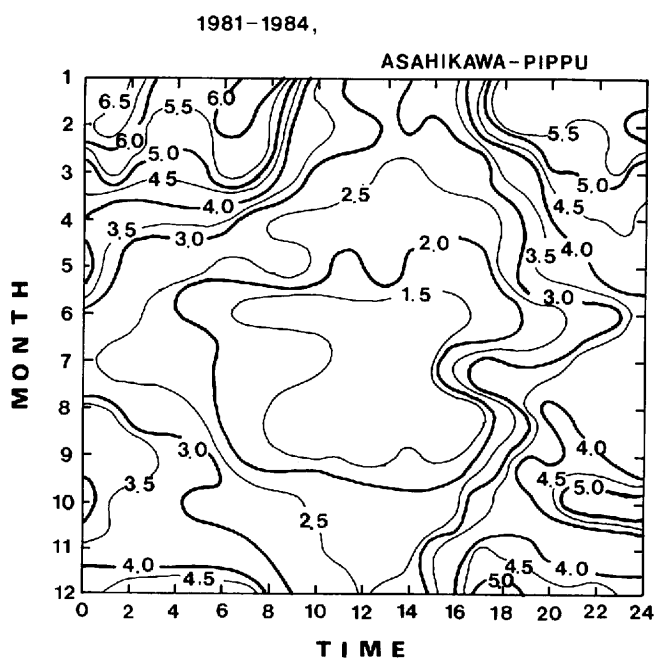


Fig. 35 Same as Fig. 34, but for Asahikawa City (°C)

land intensity are very small compared to those of the other cities. Heat island intensity figures of over 2.5°C appear between 20:00 and 01:00 in January, 19:00 and 06:00 in February, 19:00 and 24:00 in March, at 20:00 in April, between 20:00 and 01:00 in October, 19:00 and 06:00 in November, and 19:00 and 07:00 in December. These data indicate that the heat island appears mostly at night from autumn through spring.

On the other hand, the heat island intensity is small or negative when sea-breezes blow in the daytime from spring through autumn. Negative heat island intensity figures appear between 10:00 and 16:00 in April, 10:00 and 18:00 in May, 09:00 and 18:00 in June, 08:00 and 17:00 in July, 10:00 and 17:00 in August, and 12:00 and 15:00 in September. Especially is the heat island intensity below -1.5°C in the daytime of July and August. These findings indicate clearly that heat island intensity varies over geographic space and through time.

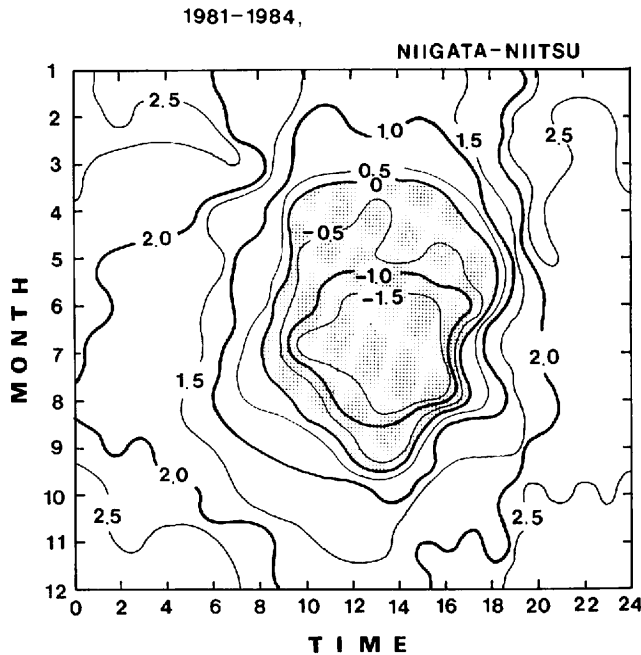


Fig. 36 Same as Fig. 34, but for Niigata City ($^{\circ}\text{C}$)

4.4 Characteristics of the surface inversion layer in two different topographical locations

Differences in the vertical structure of the temperature under the boundary layer between urban and rural areas play an important role for the heat island, as mentioned in Chapter 1. Especially does the formation of the surface inversion layer strongly affect the heat island intensity. On the other hand, the mechanism by which the inversion layer develops is different depending on its topographical circumstances (Clarke and McElroy, 1970 ; Senshu *et al.* 1975). In this section, the appearance, development, and decline of nocturnal surface inversion layers in urban and nearby rural areas are examined by studies of the basin city, Asahikawa, and the coastal city, Akita.

4.4.1 Surface inversion layer in a basin city

Cold air drainage on surrounding mountain slopes and radiative cooling of the ground surface at night in a basin may cause the formation of a strong surface inversion layer over the lower

areas of the basin, as mentioned section 4.2. However, the surface inversion intensity is commonly weak in the urban area of the basin. Especially in the urban area, nearly neutral or unstable conditions can be seen in the temperature profile of a basin city (Nkemdirim and Truch, 1978 ; Sakurai, 1979 ; Nkemdirim, 1980_a, 1980_b ; Goldreich *et al.*, 1981 ; Wanner and Hertig, 1984). An example is shown for Asahikawa city in Fig. 37.

Observations for temperature profiles were made at two stations in Kamikawa Basin, as already mentioned in Chapter II. Weather conditions at the time were favorable for the development of a heat island, as explained in section 4.2 above. The temperature profile at the station called Higashiasahikawa, which is located in a rural area approximately 5km southeast of the center of Asahikawa City, shows a typical surface inversion during nighttime. On the other hand, a surface inversion layer did not exist in the city at night. In the daytime, neither the city nor the nearby rural area had a surface inversion. However, an inversion layer developed aloft from 100m up to 200m, over the rural area at 15:00. The inversion intensity was $1^{\circ}\text{C}/100\text{m}$. The strong surface inversion was formed only after sunset in the rural area. The height of the surface inversion layer was approximately 400m at 18:00. The gradient of the inversion layer between 0 and 100m was steep, and reached to $1.4^{\circ}\text{C}/100\text{m}$. On the other hand, a mixing layer appeared from the ground surface up to 300m in the city at the same time. Furthermore, a neutral condition or weak inversion layer existed between 300 and 500m. The inversion intensity between 0 and 100m was $1.8^{\circ}\text{C}/100\text{m}$ in the rural area at 21:00. At the same time, however, the mixing layer still existed under 200m in the urban area. The atmospheric boundary layer under 600m was composed of several

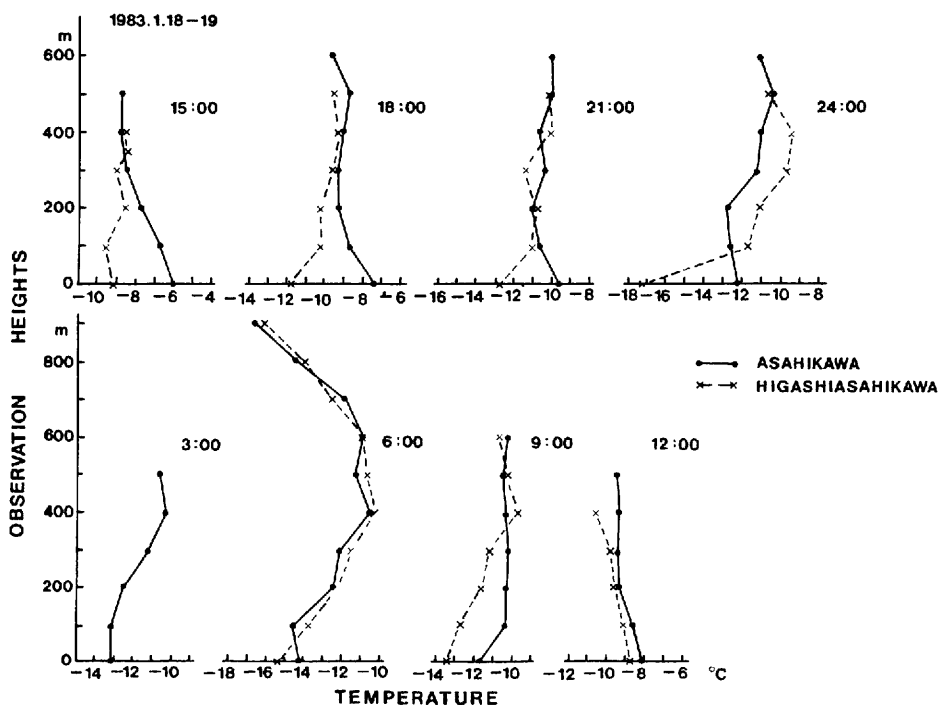


Fig. 37 Comparison of temperature profiles between Asahikawa City and its surrounding area on Jan. 18-19, 1983

mixing and inversion layers in both areas at that time. The surface inversion developed notably in the rural area at 24:00. Its intensity between 0 and 100m was then $5.5^{\circ}\text{C}/100\text{m}$. The rural inversion layer reached up to 400m. Yet there was no surface inversion layer in the urban area. The difference in temperatures between the urban and the rural area was 4.9°C at ground surface (1.5m). It is evident that the heat island was closely related to the surface inversion. The maximum heat island intensity in the city was highest near the ground surface and decreased with increasing height, and was up to -1°C at the 100m level. That fact clearly shows a cross-over phenomenon. Other studies indicate that the heights of cross-overs which are affected by urban influences are about 3 to 5 times the heights of buildings (Kawamura, 1977). Buildings in the center of Asahikawa City are approximately 30m in height. Therefore, the finding of a cross-over for Asahikawa City at about 100m above ground level corresponds well with the findings of other studies. The temperature difference between the urban and rural areas is almost constant above 100m in height, but the constancy disappears above the 500m level.

The surface inversion developed at night and continued until 09:00 in the rural area. In the city, it only appeared in the morning. In the rural area, the height of the surface inversion reached to about 400m, but the inversion intensity was weak at 09:00. The inversion intensity was about $1.3^{\circ}\text{C}/100\text{m}$. On the other hand, in the urban area the surface inversion showed between 0 and 100m ($1.4^{\circ}\text{C}/100\text{m}$), but the isothermal layer appeared above 100m at 09:00. The surface inversion disappeared completely in both areas at noon.

4.4.2 Surface inversion layer in a coastal city

Strong winds commonly blow in coastal areas. Especially do sea breezes prevail on clear days. As a result, the heat island is weakened because the strong winds prevent nocturnal cooling so that the nocturnal surface inversion is weakened. This phenomenon occurs particularly in the warm season. Up to this point in the present study, Niigata has served as an example of a coastal city. However, vertical soundings of meteorological elements were not conducted in the Niigata area. Therefore, Akita City data are used in this section. Akita City and Niigata City are coastal cities in the same climatic region (Sekiguchi, 1959 ; Suzuki, 1966). The data were collected on June 9 and October 14, 1974, by the Japan Meteorological Agency, as mentioned in Chapter II. Figure 38 allows a comparison of temperature and wind profiles between two observation sites, one in the city of Akita, the other in a nearby rural area called Takasu, approximately 30km away from the coast.

The vertical profiles of temperature for summer at both locations do not show a surface inversion layer in the atmospheric boundary layer at any time in the day, except for an inversion layer aloft between 150m and 250m in the rural area at 09:00. Conditions were not appropriate to form a surface inversion layer in the coastal city. This fact is closely related to the wind speed. When winds are fairly strong, a heat-exchange caused by turbulent transport is accelerated and a surface inversion is destroyed while a mixing layer is produced (Bornstein *et al.*, 1985 ; Bornstein, 1986). The mixing layer developed remarkably in daytime in both areas. The depths of the mixing layer were up to 900m at both locations. The air temperature in the coastal city was cooler than that in the nearby area inland from the city. This is due to the influence of sea-breeze in daytime. Sea breezes (WSW, W, WNW, NW) prevailed during daytime in both areas. The air temperature above the sea surface was much lower than that above land during daytime and nighttime, but especially during the daytime. The daily maximum temperature was larger at the inland area than at the coast due to heating from the warm land surface. Air temperatures at the urban, rural and

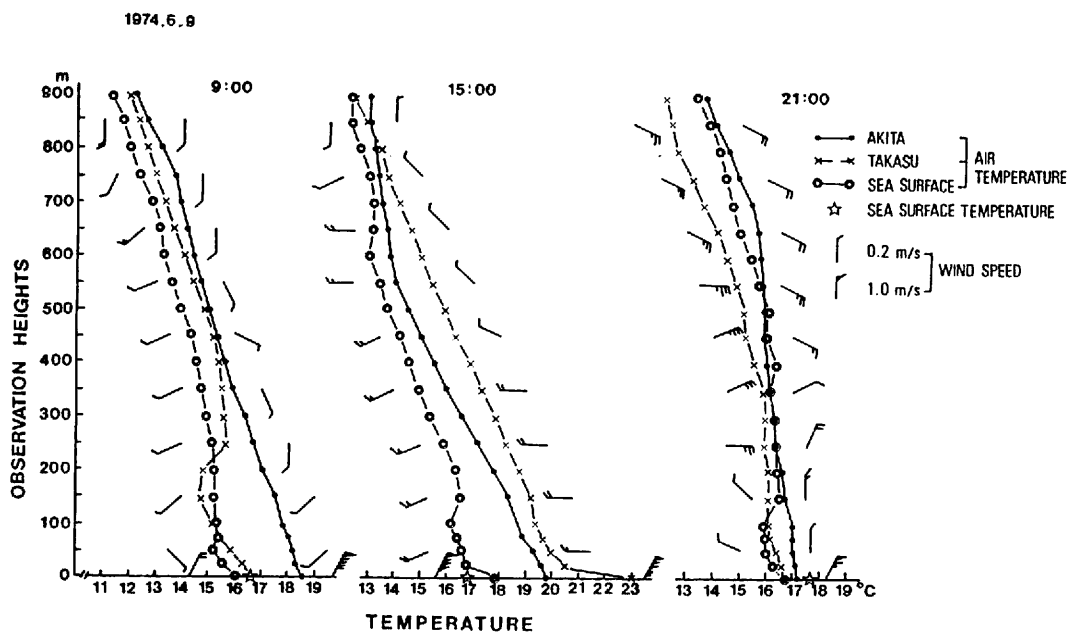


Fig. 38 Comparison of temperature and wind profiles between Akita City and its surrounding area on June 9, 1974

sea surface were 19.8°C , 23.0°C and 17.8°C respectively. Air temperature differences between the sea surface and the urban site, and between the sea surface and the rural site, were 2.0°C and 5.2°C respectively. Therefore, the heat island intensity was negative (-3.2°C). This suggests that an urban area along the coast is affected by the advection effect so that the heat island intensity is negative in the daytime if the rural station is located farther inland than the urban station. Nishizawa and Sales (1983) explained that the influence of heat advection (ΔT_a) is strongest at the coast when a sea breeze blows and that the influence decreases with distance from the coast. However, this phenomenon disappears with land breezes (N, NNE, NE, E, ESE). Therefore, the heat island intensity was positive at night (0.5°C) and continued to be so until morning.

The autumn profiles for both areas do not show a surface inversion layer at all (Fig. 39). There was only an inversion layer aloft that developed from nighttime (100 – 200m) to morning (100 – 400m) in the rural area. The inversion intensities at nighttime and morning were $1.0^{\circ}\text{C}/100\text{m}$ and $0.4^{\circ}\text{C}/100\text{m}$ respectively. In the daytime, the heat island intensity became positive, which was quite different from the summer. Sea and land breezes develop less commonly in this season because it is the beginning of the winter monsoon. The prevailing surface wind was from the north (N) all day in both areas. Therefore, a heat island developed, with the high temperatures of the urban area maintained because the advection effect of the sea breeze was no longer in power. Also, the profile of air temperature above the sea surface was quite different from that of the summer. A comparison of air temperatures between land and sea is as follows. In the morning, the air temperature of the urban area was 15.1°C , in the rural area was 14.1°C and over the sea surface was 15.8°C . Thus, the air temperature over the sea surface was 0.7 to 1.7°C higher than those of the urban and rural areas. The sea surface temperature was much higher (20.2°C). The heat island intensity was 1.0°C . In the daytime, the air temperatures of the urban, rural, and sea surface were 16.9°C , 16.3°C and 18.9°C respectively. The heat island intensity then was 0.6°C .

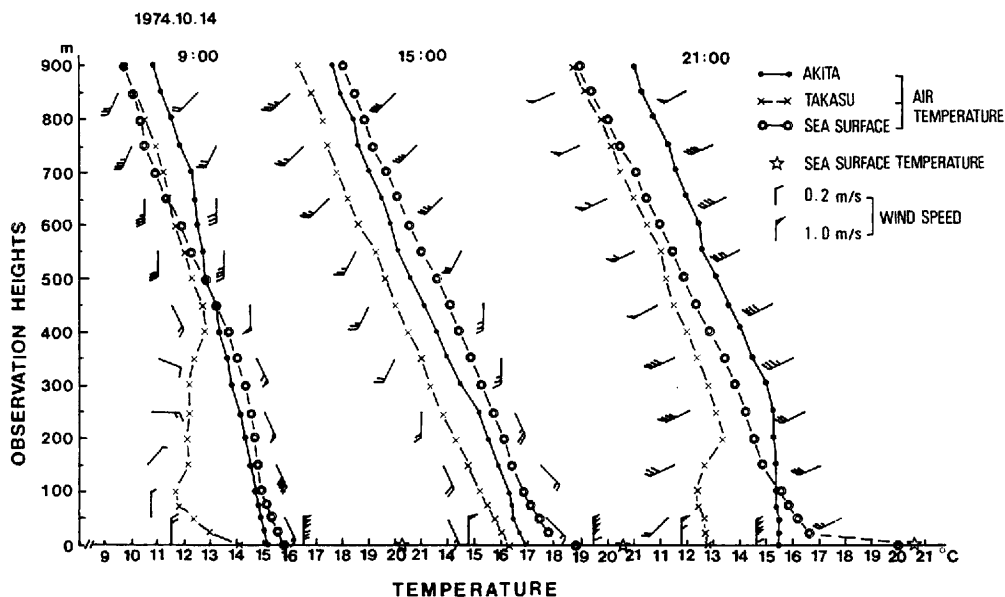


Fig. 39 Same as Fig. 38, but for Oct. 14, 1974

At night, the temperature differences between the urban and rural areas and between the land and sea surfaces were particularly large. The air temperatures of the urban, rural, and sea surfaces were 15.5°C, 12.8°C, and 20.0°C respectively, so that the sea surface value was 4.5 to 7.2°C higher than the land values. The sea surface temperature was higher (20.6°C). The heat island intensity was 2.7°C.

4.4.3 Comparing features of the surface inversion layers in the two cities

As mentioned above, the characteristics of the appearance, development, and decline of a surface inversion layer vary with topographical features. Table 5 summarizes the characteristics of the surface inversion layers in the basin and the coastal areas. The data reveal that in winter in the basin, a strong surface inversion layer was formed in the rural area during the nighttime. On the other hand, in the urban area, there was no surface inversion layer at all except at 09:00. The surface inversion intensity in the rural area was 5.5°C/100m at 24:00. The strong surface inversion layer lasted from night to morning, and its break-out was between 09:00 and 12:00. The vertical lapse rate of air temperature was larger in the urban than the rural area. At night, the rural lapse rate was negative (−5.5°C/100m), compared with the urban which was positive (0.4°C/100m). In that situation, the negative value indicated a stable or inversion condition, a zero value would have been a neutral condition or adiabatic lapse rate, and a positive value would have meant instability. Because the temperature dropped due to the persistence of radiative cooling at the ground surface, the atmosphere was stable in the rural area where the formation of a surface inversion layer was notable in comparison with the urban area during the nighttime (Ludwig, 1970 ; Böhlen, 1978). Because of this process, the temperature difference between the urban and rural areas became greater, and the heat island intensity grew larger in the nighttime. The nocturnal heat island intensity was 4.9°C and the diurnal heat island intensity was 3.1°C.

Table 5. Characteristics of the surface inversion layer, lapse rate of temperature (γ) wind, and the maximum heat island intensity ($\Delta T_{u-r(max)}$) in each city.

	City located in basin (Asahikawa City)			
	winter			
	urban		rural	
	daytime	nighttime	daytime	nighttime
Surface inversion layer ; appearance	×	×	×	○
development				
height				0 – 400m
intensity (maximum value)				5.5°C/100m
break-out				09:00 – 12:00
Lapse rate of temperature (γ) ;	0.54°C/100m	0.4°C/100m	0.4°C/100m	– 0.5°C/100m
Wind ; prevailing direction mean speed (m/s)				
Maximum heat island intensity ; ($\Delta T_{u-r(max)}$)		daytime ; 3.1°C nighttime ; 4.9°C		
(continued)				
	Coastal city (Akita City)			
	summer			
	urban		rural	
	daytime	nighttime	daytime	nighttime
Surface inversion layer ; appearance	×	×	×	×
development				
height				
intensity (maximum value)				
break-out				
Lapse rate of temperature (γ) ;	1.1°C/100m	0.2°C/100m	3.6°C/100m	0.6°C/100m
Wind ; prevailing direction	upper 500m ; W (sca-breeze)	upper 400m ; ESE (land-breeze)	upper 400m ; WNW (sea-breeze) intermediate; E, ENE (land-breeze)	upper 600m ; ESE (land-breeze)
	below 500m ; WSW (sca-breeze)	below 400m ; N (land-breeze)	below 400m ; W (sca-breeze)	below 200m ; NE, WNW
mean speed (m/s)	upper 500m; 0.2 below 500m; 0.9	upper 400m; 0.4 below 400m; 0.5	upper 400m; 0.2 below 400m; 1.0	upper 600m; 0.5 intermediate ;0.6 below 200m; 0.1
Maximum heat island intensity ; ($\Delta T_{u-r(max)}$)		daytime ; – 3.2°C nighttime ; 0.5°C		

(continued)

Coastal city (Akita City)				
autumn				
	urban		rural	
	daytime	nighttime	daytime	nighttime
Surface inversion layer ; appearance development height intensity (maximum value) break-out	×	×	×	×
Lapse rate of temperatre(γ) ;	0.6°C/100m	0.1°C/100m	1.1°C/100m	0.4°C/100m
Wind ; prevailing direction	upper 500m : SW intermediate; S below 300m; SE surface; N	all layer except for surface; WSW surface; N	upper 500m; SW intermediate : SSW below 200m; SSE surface; N	all layer except for surface; WSW surface; N
mean speed (m/s)	upper 500m; 1.0 intermediate; 0.5 below 200m; 0.4 surface; 4.2	all layer except for surface; 0.7 surface; 5.2	upper 500m; 0.6 intermediate; 0.4 below 200m; 0.4 surface; 1.5	all layer except for surface; 0.6 surface; 1.1
Maximum heat island intensity ; ($\Delta T_{u-r(max)}$)	daytime ; 0.6°C nighttime ; 2.7°C			

In the coastal area, surface inversions do not appear in summer or autumn in either the urban or rural area. The lapse rate was 0.4°C/100m in the rural area near the coast in autumn, as compared to the value of - 5.5°C/100m in the rural area of the basin in winter. Although the two figures should not be compared directly because they relate to different seasons, the numbers suggest that the surface inversion layers are very different one from the other because of their topographical differences. In the coastal location, the vertical lapse rate was larger in the rural than in the urban area and the atmosphere of the rural area became unstable during the daytime in summer. The lapse rates were 1.1°C/100m in the urban area and 3.6°C/100m in the rural, so that the rural value was 3 times larger than the urban. This phenomenon of the urban area becoming cooler than the rural area during daytime in summer, was closely related to sea breezes, as mentioned in the daytime. The urban area, located on the coast, had lower temperatures due to the cool sea breeze. By contrast, the rural area located inland had a higher temperature because it was not directly affected by the sea breeze. Therefore, the diurnal heat island intensity was negative(- 3.2°C). At night, however, because of the shift from sea breeze to land breeze, the temperature in the urban area did not fall, but maintained a high level so that the heat island intensity was positive (0.5°C). On the autumn day, the heat island intensity was also positive (0.6°C). This was due to the absence of sea and land breezes during the transition between warm and cool seasons. The prevailing surface wind blew from the north (N) all day long in both regions. The nocturnal heat island intensity was 2.7°C. That intensity level was particularly small as compared with the same feature in the basin area. In summary, in the basin city a surface inversion layer developed caused by radiative cooling and the urban heat island intensity figure was strong. On the other hand, in the coastal city a surface inversion layer did not form because of a strong advection effect caused by the sea breeze, and the heat island intensity level was negative or weakly posi-

tive.

4.5 Schematic models of urban influences and topographical effects on the urban heat island

The conclusions of this chapter are summarized in schematic models (Fig.40).

In a city located on an inland plain, with clear skies and calm air, temperature changes due to heat advection are negligible. Therefore, the heat island intensity is the difference between the urban temperature and a nearby rural temperature, as shown in Equation (30). The heat island intensity (ΔT_{u-r}) is the temperature rise caused by the urban influences.

Differences in the warmth of urban atmospheres as compared to rural atmospheres are related to differences in urban and rural energy sources and to differences in the energy partitioning qualities of the ground surfaces. The energy source difference relates mainly to anthropogenic heat production in the city, which depends on urban activities as mentioned in Chapter III. Consequently, the urban population can be considered an index of anthropogenic heat. Energy partitioning differences are mainly due to the heat storage capacity of the city combined with turbulent transfer characteristics and urban geometry which are related to the radiation and surface energy balance.

In a rural area, a net daytime gain of energy through radiation (R_n) at the earth-atmosphere interface results in a turbulent transfer of heat (sensible heat flux, H) to the atmosphere, conduction of heat (ground heat flux, G_o) to the ground surface, and evaporation (latent heat flux, IE). During nighttime, a net loss of energy through radiation at the interface results in decreased evaporation or condensation, turbulent transfer of heat from the atmosphere, and conduction of heat from the ground.

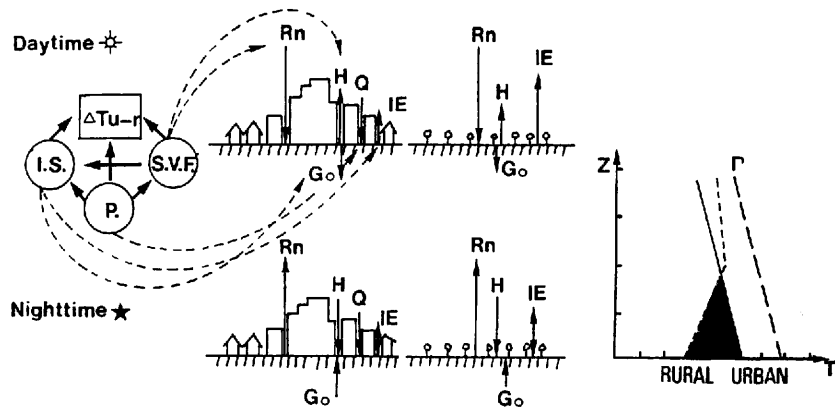
In an urban area, modifications of the above described energy balance can result from any or all of the following : 1) anthropogenic heat created by people (P), 2) the availability of limited amounts of surface moisture because large surfaces are covered by impermeable materials (I.S.), and 3) the urban geometry created by buildings (sky view factor ; S.V.F.).

In daytime, the relative partitioning of energy into latent heat flux (IE), sensible heat flux (H), and ground heat flux (G_o) depends largely on the land-use types. An increase of impermeable surface coverage (I.S.), such as concrete and asphalt-covered areas results in a decrease of evapotranspiration and a loss of latent heat flux (IE), thus increasing the sensible heat flux (H) and ground heat flux (G_o). Therefore daytime temperatures in the urban area are higher than those of the rural area. However, because the difference in the heat balance at the ground surface is small between the urban and rural area, the heat island intensity is small in daytime.

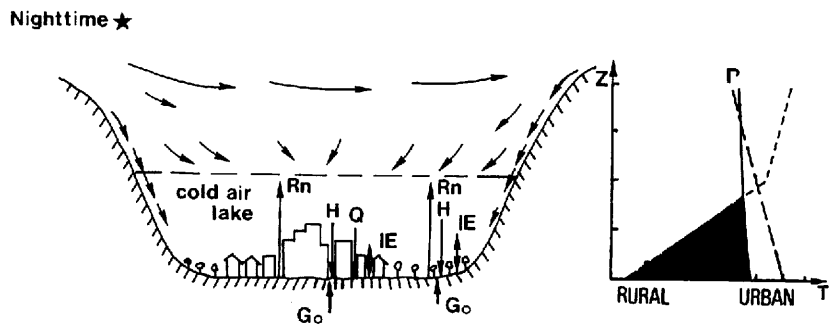
By contrast, during a clear and calm night, the heat balance at the ground surface depends largely on ground heat flux (G_o), which in turn relates closely to the net radiation flux (R_n). Long-wave radiation flux (R_n) should lead to cooling of the ground surface at night. The special observation data based on the long-wave radiation component show that, within the urban canopy layer, the radiative cooling rates at ground surface are much less (about 60%) than above roof surface level. This fact owes largely to the decreased sky view factor (S.V.F.) below the roof surface level, which reduces radiative losses and sensible heat flux (H) in the almost calm canyon air. In addition, thermal properties due to the large heat retention capacity of building and street surfaces and the high heat conductivity related to the ground heat flux (G_o), prevent rapid cooling after sunset thus maintaining a warmer urban area during nighttime. Anthropogenic heat (Q) plays an important role in increasing urban temperature. Therefore, a surface inversion layer is not

SCHEMATIC MODELS

(PLAIN)



(BASIN)



(COAST)

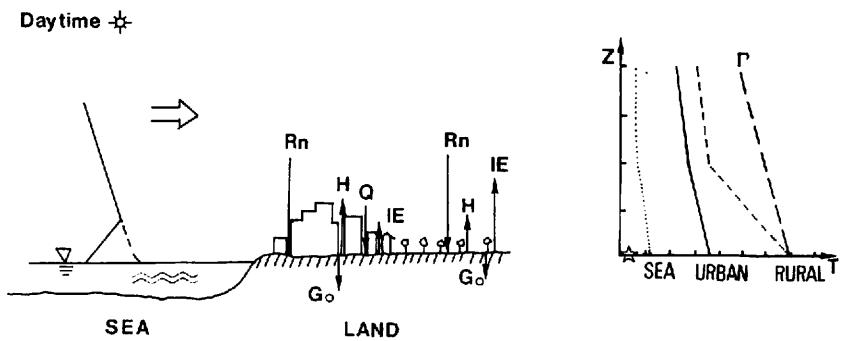


Fig. 40 Schematic models of the heat island phenomenon

formed. However, in rural areas, a surface inversion layer commonly develops because radiative cooling continues from sunset until sunrise. The air above an urban area remains warmer than the air above an adjacent rural area so that the nocturnal heat island intensity increases.

Not all cities are located on flat land, however, temperatures in basin and coastal cities are sometimes greatly affected by their surrounding topographies. Then the difference between the temperature of the rural area in the basin or near the coast (ΔT_r) and the temperature of the rural area on an inland plain is the value of the topographical effect. See Equation (31).

In rural areas around a basin city, cold air drainage on surrounding mountain slopes and radiative cooling of the ground surface can form a strong surface inversion layer, a cold air lake, during the nighttime. On the other hand, the surface inversion intensity will generally be weak in the urban area. Nearly neutral or unstable conditions can be seen in the temperature profile of a basin city. Therefore, the nocturnal heat island intensity is strong when compared to those of inland plain and coastal cities. In daytime, however, the process of the urban heat island formation in a basin city is similar to that in an inland plain city.

In a coastal city, urban heat islands are generally prevented from developing by strong winds and humid air. Cool sea breezes prevail during daylight hours on clear and calm summer days. An urban area along a coast is affected by advection so that the maximum air temperature is lower than the maximum in nearby inland rural areas. Therefore the urban heat island intensity is negative or only slightly positive. However, this phenomenon disappears when land breezes blow at night.

CHAPTER V

CONCLUSIONS

The main objective of this research was to examine the urban influences and the topographical effects on the urban heat island intensity.

First, the influence of urban structures on the heat island intensity was discussed. The relationship between the maximum heat island intensity and the urban population was examined and its regional differences were statistically observed using automobile observation data. The analyses yielded the following conclusions.

The heat island intensity increases with growth of the urban population in every country. However, there are regional differences in the relationship. In North American and European cities, the relationship is generally proportional and linear, and their regression lines can be represented as straight lines. By contrast, for Japanese and Korean cities, the regression relationship is better represented by two straight lines. In other words, the regression lines bend at around 300,000 in population. The increment of the maximum heat island intensity in cities that have populations over 300,000 is larger than in the cities that have less than 300,000 people. That suggests that the functions and structures of Japanese and Korean cities with under 300,000 people are different from those with over 300,000 people.

In order to relate the differences of urban function and structure to the heat island intensity, the sky view factor and impermeable surface coverage ratio were employed as indices of the factors. The sky view factor decreases with an increase in the urban population, demonstrating a negative correlation. This means that the sky view factor decreases due to an enlargement of the urban area and to an increase in the number of tall buildings. The sky view factor regression lines for the Japanese and Korean cities did not bend at the 300,000 population level. Yet among countries and regions the relationships are different. The slope for North American cities is larger than that for European cities. This is similar to the relationship between population and the maximum heat island intensity. On the other hand, Japanese cities can be divided into two groups. One includes cities which have sky view factors in accordance with their populations and the other includes cities which have larger sky view factors than predicted from their populations (*i.e.*, cities in Hokkaido).

The relationship between the impermeable surface coverage ratio and the urban population in Japanese and Korean cities is a positive one, for the ratio increases with growth of the urban population. The relationship is represented by a biphasic regression line in both countries, with a slope transition occurring at the 500,000 population level. This is similar to the relationship of urban population to the maximum heat island intensity. Thus, the impermeable surface coverage ratio is one of the indices which explains why the relationship of the heat island intensity to urban population can be represented by two regression lines rather than by one simple regression line. Although the impermeable surface coverage ratio is probably not the only factor involved in this biphasic correlation, it is a key to understanding it.

Special observation data for Mitsukaido City, based on the heat balance model at the ground surface, allowed further examination of the roles of the sky view factor and the impermeable surface coverage ratio as indices of urban function and structure. The interruption of long-wave

radiation into the urban ground surface by buildings was discussed using the sky view factor as an index of the topography of the ground surface. Then, the thermal features of the impermeable materials composing much of the urban surface were discussed for an understanding of the use of the impermeable surface coverage ratio as an index of the structure of the ground surface. The idea is based on an equation formulated by Brunt (1941) which shows the cooling during night.

The ground surface of an urban area where the sky view factor is small can maintain a high temperature during both daytime and nighttime due to the presence of the buildings which absorb short-wave radiation in daytime and decrease long-wave radiation in nighttime on the ground surface. Also, the cooling rate is smaller in the urban area than in the rural area because the urban area has a large thermal admittance. The sky view factor and the impermeable surface coverage ratio are, then, closely correlated with long-wave radiation which is related to radiative cooling during the night. Therefore, these are appropriate indices of urban structure, which are the main factors causing the nocturnal heat island phenomenon.

Secondly, the influences of topographical factors on the heat island intensity were discussed using the AMeDAS data. Examinations of the heat island intensity occurred for Gifu City located on an inland plain, for Asahikawa City located in a basin, and for Niigata City located on a coastline. The spatial and temporal aspects of the heat island intensity were analyzed in the context of each topographical location.

The diurnal ranges of temperatures in the basin city in both winter and summer were the largest, followed by those for the inland city and the coastal city in that order. The diurnal ranges of temperature in the basin city were two to three times as large as those of the coastal city. Wind speed, however, was strongest in the coastal city. The wind speed of the coastal city was two to three times stronger than that of the city in the basin. As such, the basin city did not seem to be influenced much by advection. In the coastal city, the sea breeze strongly influenced advection during the daytime in summer. In winter, the rates of cooling inside and outside of the city differed depending on the topographical features. The cooling rate of the basin city was two to six times larger than those of the inland and coastal cities. The difference in the cooling rates between the inside and the outside of the city was directly related to the heat island formation. The heat island intensity was the highest in the basin city, its value about 1.7 times as large as the inland city's and 2.2 times the coastal city's.

Regarding the climatic analysis, the diurnal changes of the heat island intensity in summer were related to the topography in which the cities are located. In the basin city, Asahikawa, the heat island intensity was very high and there were two peaks during the day. It can be assumed that the double peaks owe to cold air drainage. The most common maximum heat island intensity levels were in the 4 to 5°C range. In the inland city, Gifu, the heat island intensity was intermediate and had a single peak. The most frequent maximum heat island intensity levels occurred in the 3 to 4°C range. In the coastal city, Niigata, the heat island intensity was low and had a single peak. But during the daytime, the heat island intensity was negative due to the influence of sea breezes. The most common maximum heat island intensity levels were in the 2 to 3°C range. In the inland city (Gifu), the heat island formed at all times through the year but most prominently on winter nights. In the basin city (Asahikawa), the heat island not only always formed, but also had the highest values. In the coastal city (Niigata), the heat island intensity was small or negative when the sea breeze blew in daytime from spring through autumn.

The special observation data allowed examination of the variations of the heat island intensity in relation to the intensity of the nocturnal surface inversion layer in the rural area near each city.

In the rural area near the basin city, a strong surface inversion layer was formed on winter nights. On the other hand, in the city itself a surface inversion layer did not form except in the morning. The intensity of the rural surface inversion was very strong ($5.5^{\circ}\text{C}/100\text{m}$ at 24:00) and lasted until morning, its break-out being between 09:00 and 12:00. The lapse rate of temperature was larger in the urban ($0.4^{\circ}\text{C}/100\text{m}$) than in the rural area ($-5.5^{\circ}\text{C}/100\text{m}$). Because of low temperatures due to radiative cooling at the ground surface, the atmosphere was stable in the rural area and there was a surface inversion layer at night. As a result, the temperature difference between the urban and rural areas was larger, and the heat island intensity was larger at night.

In the coastal city, a surface inversion layer did not appear during summer or autumn in either the urban or the rural area because strong winds and high humidity prevented nocturnal cooling. However, the inland rural area maintained a high temperature because it was not directly affected by the sea breeze. Therefore, the heat island intensity was negative or weakly positive in the coastal city.

In summary, rural areas mean a basin city have a strong surface inversion layer caused by radiative cooling so that the heat island intensity is strong. On the other hand, in the coastal city, a surface inversion layer is not formed because there is much advective effect from cool sea breezes so that the heat island intensity is negative or a weak positive.

ACKNOWLEDGEMENT

The author wishes to express her sincere gratitude to her academic adviser, Professor Takeshi Kawamura, the Institute of Geoscience, the University of Tsukuba, Japan, for his guidance and support in this study. Special thanks are extended to Professors Masatoshi M. Yoshino and Toshie Nishizawa, the Institute of Geoscience, the University of Tsukuba, Japan, for their suggestions and discussions.

The author gratefully acknowledges guidance and encouragement from Professors Yeon Ok Kim, the Department of Geography, the Ewha Womans University, Korea, and Shuji Yamashita, the Department of Geography, the Tokyo Gakugei University, Japan. In addition, the author wishes to acknowledge the kind assistance provided by Dr. Mamoru Kobayashi, Dr. Tetsuzo Yasunari, Dr. Shuji Yamakawa, Mr. Rikie Suzuki and Mrs. Taiko Kurihara, the Institute of Geoscience, the University of Tsukuba, Japan.

The author is grateful to Professor Takeshi Kawamura, Director of the Environmental Research Center of the University of Tsukuba, for kind permission to publish this manuscript and to provide instruments, and the members of the Environmental Research Center of the University of Tsukuba, the Sapporo Meteorological Observatory, Asahikawa City Office, and Japan Geographical Survey Institute for providing special observation data, and to the Mitsuikaido Rotary Club for its helpful cooperation.

Thanks are due to Dr. Canute VanderMeer, Miss Yuki Morinaga, and Miss Takako Sugiyama for support in preparing this thesis.

REFERENCES

- *Aida, M. and Koto, K. (1978) : Urban albedo (1) : model estimation and simulation ; in *Urban Atmospheric Environment*, Kawamura, T. (ed.), Tokyo Univ. Press, 92-93.
- Arakawa, H. (1937) : Increasing air temperatures in large developing cities. *Beitr. Geophys.*, **50**, 3 - 6.
- *Arakawa, H. (1968) : Drying effect and temperature condition due to urbanization in Tokyo. *Tenki*, **16**, 23 - 24.
- Atkinson, B. W. (1983) : Numerical modelling of thermally-driven mesoscale airflows involving the planetary boundary layer. *Prog. Phy. Geog.*, **7**, 177 - 209.
- Bach, W. (1970) : An urban circulation model. *Arch. Biokl. Ser. B*, **18**, 155 - 168.
- Bader, D. C. and McKee, T. B. (1983) : Dynamical model simulation of the morning boundary layer development in deep mountain valleys. *J. App. Met.*, **22**, 341 - 351.
- Bärring, L. and Mattsson, J. O. (1985) : Canyon geometry, street temperature and urban heat island in Malmö, Sweden. *J. Climatology*, **5**, 433 - 444.
- Bohm, R. and Gabl, K. (1978) : Die Wärmeinsel einer Grosstadt in Abhängigkeit von Verschiedenen Meteorologischen Parametern. *Arch. Met., Geophy. Biokl.*, **B, 26**, 219 - 237.
- Böhlen, T. (1978) : The influence of aerosol particles on the warming of urban and rural atmospheres. *Met. Rundsch*, **31**, 87 - 91.
- Bornstein, R.D., Klotz, S., Pechinger, U., Salvador, R., Street, R., Shieh, L. J., Ludwig, F. and Miller, R. (1985) : Application of linked three-dimensional PBL and dispersion models to New York. Preprint Vol., *15th NATO/CCMS Con.*, St. Louis, Mo., U.S.A., 16 - 20 April, 21pp.
- Bornstein, R. D. (1986) : Urban climate models : Nature, limitations, and applications. *WMO No. 652*, 237 - 276.
- Brunt, D. (1941) : *Physical and dynamical meteorology*. Cambridge Univ. Press, London, 428pp.
- Carlson, T. B., Dodd, J. K., Benjamin, S. G. and Cooper, J. N. (1981) : Satellite estimation of the surface energy balance, moisture availability and thermal inertia. *J. App. Met.*, **20**, 67 - 87.
- Chandler, T. J. (1964) : City growth and urban climates. *Weather*, **19**, 170 - 171.
- Chandler, T. J. (1970) : Selected bibliography on urban climate. *WMO No. 276*, 383pp.
- Chandler, T. J. (1976) : Urban climatology and its relevance to urban design. *WMO Tech. Note*, **149**, 62pp.
- Clarke, J. F. and McElroy, J. L. (1970) : Experimental studies of the nocturnal urban boundary layer ; in *Urban Climatology*, *WMO Tech. Note*, **108**, 108 - 112.
- Dabberdt, W. F. and Davis, P. A. (1974) : Determination of energetic characteristics of urban-rural surface in the greater St. Louis area. Preprint, *Symp. Atmos. Diffusion and Air Pollut.*, Santa Barbara, 133 - 141.
- Duckworth, F. S. and Sandberg, J. S. (1954) : The effect of cities upon horizontal and vertical temperature gradients. *Bull. Amer. Met. Soc.*, **35**, 198 - 207.
- Eagleman, J. R. (1974) : A Comparison of urban climatic modifications in three cities. *Atmos. Environ.*, **8**, 1131 - 1142.
- East, C. (1971) : Chaleur urbaine à Montreal. *Atmosphere*, **9**, 112 - 122.
- Fuggle, R. F. and Oke, T.R. (1976) : Long-wave radiative flux divergence and nocturnal cooling of the urban atmosphere. I Above roof-level. *Boundary - Layer Met.*, **10**, 113 - 120.
- *Fukuda, K. (1970) : On the sea and land breeze at Niigata. *Tenki*, **17**, 599 - 602.

- Fukui, E. (1957) : Increasing temperature due to the expansion of urban areas in Japan. *J. Met. Soc. Japan*, **75**, 336 – 341.
- *Fukui, E. (1968) : Recent rise of temperature in Japan. *Geog. Rev. Japan*, **41**, 477 – 490.
- Fukui, E. (1969) : Recent rise of temperature in Japan. *Sci. Rep.*, Tokyo Kyoiku Daigaku, Sec. C., **10**, 145 – 164.
- Fukuoka, Y. (1983) : Physical climatological discussion on causal factors of urban temperature. *Memoirs of the Faculty of Integrated Arts and Sciences*, **8**, Hiroshima Univ., 157 – 178.
- Goldreich, Y., Tyson, P. D., Gogh, R. G., and Venter, G. P. N. (1981) : Enhancement and suppression of urban heat plumes over Johannesburg. *Boundary-Layer Met.*, **21**, 115 – 126.
- Goldreich, Y. (1984) : Urban topoclimatology. *Prog. Phy. Geog.*, **8**, 336 – 364.
- *Hariyama, T., Taniguchi, T., Ohira, T. and Hiramatsu, C. (1985) : The urban heat island during the snow cover period (I). *Geophy. Bull. Hokkaido Univ.*, **45**, 1 – 14.
- *Hattori, K. (1979) : Changing form of small scale cities ; in *Urbanization of Modern Japanese Cities*, Aokie, Nagano, Shirasaka and Fukuhara. (ed.), Kokonshoin, 213 – 227.
- *Ishimizu, T. (1965) : Considerations on the classification of urban functions in Japanese cities. *Ehime Univ. Kiyō*, **4**, Ehime Univ., 89 – 115.
- *Ito, K. (1977) : *Manual sunshine data for building design*. Ohm Pub. Co., 140pp.
- Ingersoll, L., Zobel, R. J. and Ingersoll, A. C. (1948) : *Heat Conduction*. McGraw-Hill, New York, 278pp.
- Jauregui, E. (1986) : Tropical urban climates : Review and assessment. *WMO No.* **652**, 26 – 45.
- *Joo, K. S. (1982) : Urbanization and urban system of Korea : 1960 – 1980. *Geog. Rev. Japan*, **55**, 1 – 20.
- *Kawamura, T. (1964) : Some considerations on the cause of city temperature at Kumagaya City. *Geog. Rev. Japan*, **37**, 560 – 565.
- *Kawamura, T. (1968) : Urban climate ; Particularly urban heat island. *Kisho-Kenkyu Note*, **98**, 142 – 157.
- *Kawamura, T. (1975) : Urban climatic change ; Human existence and natural environment, Tokyo Univ. Press, Tokyo, **3**, 16 – 27.
- *Kawamura, T. (1977) : Causes of city climate and its modeling. *Kisho-Kenkyu Note*, **133**, 226 – 238.
- *Kikuchi, H. (1974) : A study of urban climate : Relation between the increase in population and urban temperature at Sapporo. *J. Met. Res.*, **26**, 417 – 425.
- # Kim, I. (1976) : A study of the distribution of summer air temperature in Taegu City. M. S. Thesis. Dep. Geog., Kyungpook Univ., Korea (unpublished), 65pp.
- *Kobayashi, M. (1979) : Comparative observation of long-wave radiation balance on ground-surface and on roof-level in the urban area. *Geog. Rev. Japan*, **52**, 251 – 260.
- *Kondo, J. (1982) : Preliminary theoretical study on nocturnal cooling over complex terrain. *Tenki*, **29**, 935 – 949.
- *Kondo, J., Yasuda, N., Satoh, T., Haginoya, S., Miura, A., Yamazawa, H. and Kawanaka, A. (1983) : The nocturnal stable layer "cold air lake" formed in the basin. *Tenki*, **30**, 327 – 334.
- *Kudoh, T., Tanaka, H., Toritani, H. and Hwang, S. (1982) : Formation of cold air lake in Sugadaira basin. *Geog. Rev. Japan*, **55**, 849 – 856.
- Kung, E. C., Bryson, R. A. and Lenschow, D. H. (1964) : Study of a continental surface albedo on the basis of flight measurements and structure of the earth's surface cover over North America. *Mon. Wea. Rev.*, **92**, 543 – 564.

- Landsberg, H. E. (1972) : Climate of the urban biosphere. *Biomet.*, II, 71 – 81.
- Landsberg, H. E. (1979) : Atmospheric changes in a growing community. *Urban Ecology*, **4**, 53 – 82.
- Landsberg, H. E. (1981) : *The urban climate*. Academic Press, New York, 275pp.
- Landsberg, H. E. and Maisel, T. N. (1972) : Micrometeorological observations in an area of urban growth. *Boundary-Layer Met.*, **2**, 365 – 370.
- Lee, D. O. (1984) : Urban climates. *Prog. Phy. Geog.*, **8**, 1 – 31.
- Lundwig, F. L. (1970) : Urban temperature fields ; in Urban Climates, *WMO Tech. Note*, **108**, 80 – 112.
- Lunde, B. K. (1977) : Seasonal and wavelength dependence of urban /rural radiance in Iowa. *J. App. Met.*, **16**, 103 – 105.
- Macjima, I., Nogami, M., Aoyama, T., Oka, S., Tagami, Y., Hohgetsu, T., Sugihara, Y., Yamakawa, S., Nishiyama, Y. and Umemoto, T. (1980) : Recent climatic change and urban growth in Tokyo and its environs. *Geog. Rep.*, Tokyo Metropolitan Univ., **14/15**, 27 – 48.
- Mitchell, J. M. (1953) : On the causes of instrumentally observed secular temperature trends. *J. Met.*, **10**, 244 – 261.
- Mitchell, J. M. (1961) : The temperature of cities. *Weatherwise*, **14**, 224 – 229.
- Moffitt, B. J. (1972) : The effects of urbanization on mean temperatures at Kew Observatory. *Weather*, **27**, 121 – 129.
- *Mori, Y. and Kondo, J. (1984) : Nocturnal radiational cooling at the mountainous district taking accumulation and efflux of cooled air into consideration. *Tenki*, **31**, 45 – 52.
- Myrup, L. O. and Morgan, D. L. (1972) : Numerical model of the urban atmosphere. Vol. 1: The city-surface interface. *Contributions in Atmos. Science*. No. **4**. Univ. of California, Davis, 237pp.
- *Nakamura, K. (1976) : The nocturnal cold air drainage and distribution of air temperature on the gentle slope. *Geog. Rev. Japan*, **49**, 380 – 387.
- *Nakamura, K. (1978) : Appearance and drainage areas of the cold air stream on the slope of Mt. Omatsu, Sugadaira, central Japan. *Geog. Rev. Japan*, **51**, 793 – 803.
- *Nakamura, K. (1980) : Radiative cooling and ground inversion on the slope of Mt. Omatsu, Sugadaira, central Japan. *Geog. Rev. Japan*, **53**, 758 – 768.
- *Ninomiya, K. (1960) : The sea and land breeze at Niigata. *J. Met. Res.*, **12**, 719 – 723.
- *Nishizawa, T. (1958) : The influence of buildings on the urban temperature. *Misc. Rep. Res. Inst. Natural Resources*, **48**, 40 – 48.
- *Nishizawa, T. (1973) : Urban climate, with special reference to heat island. *Kagaku*, **43**, 487 – 494.
- Nishizawa, T. and Sales, J. A. (1983) : The urban temperature in Rio de Janeiro, Brazil. *Latin American Studies*, **5**, Univ. Tsukuba, 29 – 37.
- Nkemdirim, L. C. (1980_a) : T test of a lapse rate/wind speed model for estimating heat island magnitude in an urban airshed. *J. App. Met.*, **19**, 748 – 756.
- Nkemdirim, L. C. (1980_b) : Cold air drainage and temperature fields in an urban environment : a case study of topographical influence on climate. *Atmos. Environ.*, **14**, 375 – 381.
- Nkemdirim, L. C. and Truch, P. (1978) : Variability of temperature fields in Calgary, Alberta. *Atmos. Environ.*, **12**, 809 – 822.
- Nunez, M. and Oke, T. R. (1976) Long-wave radiative flux divergence and nocturnal cooling of the urban atmosphere. *Boundary-Layer Met.*, **10**, 121 – 135.

- Nunez, M. and Oke, T. R. (1977) : The energy balance of an urban canyon. *J. App. Met.*, **16**, 11 – 19.
- Nunez, M. and Oke, T. R. (1980) : Modelling the daytime urban surface energy balance. *Geographical Analysis*, **12**, 373 – 389.
- *Ogasawara, Y. (1954) : Urban areas of Japan. *Surugadaigakushi*, **4**, 107 – 130.
- *Ohata, T., Watanabe, O. and Higuchi, K. (1985) : Heat island of a city in snow-covered area. *Tenki*, **32**, 87 – 95.
- Oke, T. R. (1973) : City size and the urban heat island. *Atmos. Environ.*, **7**, 769 – 779.
- Oke, T. R. (1974) : Review of urban climatology 1963 – 73. *WMO Tech. Note*, **134**, 132pp.
- Oke, T. R. (1976) : The distinction between canopy and boundary layer urban heat islands. *Atmosphere*, **14**, 268 – 277.
- Oke, T. R. (1978) : Advectively-assisted evapotranspiration from irrigated urban vegetation. *Boundary-Layer Met.*, **17**, 167 – 173.
- Oke, T. R. (1979) : Review of urban climatology 1973 – 76. *WMO Tech. Note*, **169**, 100pp.
- Oke, T. R. (1981) : Canyon geometry and the nocturnal urban heat island : Comparison of scale model and field observations. *J. Climatology*, **1**, 237 – 254.
- Oke, T. R. (1982) : The energetic balance of the urban heat island. *Quar. J. Roy. Met. Soc.*, **108**, 1 – 24.
- Oke, T. R. and Hannell, F. G. (1972) : The form of the urban heat island in Hamilton, Canada. *WMO Tech. Note*, **108**, 113 – 126.
- Oke, T. R. and Maxwell, G. B. (1975) : Urban heat island dynamics in Montreal and Vancouver. *Atmos. Environ.*, **9**, 191 – 200.
- Oke, T. R., Kalanda, B. D. and Steyn, D. G. (1981) : Parameterization of heat storage in urban areas. *Urban Ecology*, **5**, 45 – 54.
- *Omoto Y. and Hamotani, K. (1982) : On the decrease of relative humidity observed at urban meteorological observatories of Japan. *Tenki*, **29**, 73 – 80.
- Park, H. S. (1986_a) : Features of the heat island in Seoul and its surrounding cities. *Atmos. Environ.*, **20**, 1859 – 1866.
- *Park, H. S. (1986_b) : A climatological study of the heat island in Seoul and its surroundings. *Geog. Rev. Japan*, **59**, 695 – 711.
- *Park, H. S. and Kawamura, T. (1986) : A consideration of the cause of heat island : a relationship between the heat island and sky view factor. *Bull. Environ. Res. Cen., Univ. Tsukuba*, **10**, 27 – 38.
- Parry, M. (1967) : The urban "Heat-Island". *Biomet.*, **II**, 616 – 624.
- Paterson, R. D. and Hage, K. D. (1979) : Micrometeorological study of an urban valley. *Boundary - Layer Met.*, **17**, 175 – 186.
- Preston-Whyte, R. A. (1970) : A spatial model of an urban heat island. *J. App. Met.*, **9**, 571 – 573.
- Sakurai, K. (1979) : Relation between the air pollution and the meteorological condition at Asahikawa : On the heat island effect. *J. Faculty Sci., Hokkaido Univ. Ser. VII (Geophy.)*, **6**, 115 – 125.
- *Sekiguchi, T. (1959) : A climatic classification of Japan. *Sci. Rep., Tokyo Kyoiku Daigaku*, **3**, 65 – 78.
- *Senshu, T., Nishinomiya, S., and Akai, Y. (1975) : On the temperature inversions in the lower atmosphere. *Denryokuchuokenkyuhoukoku*, **275006**, 1 – 49.
- Smith, H. R. T. (1965) : Methods and purpose of functional town classification. *A. A. A. Geog.*

- Summers, P. W. (1965) : An urban heat island model ; its role in air pollution problems, with applications to Montreal. *First Canadian Conference on Micrometeorology in Toronto*, 1 – 32.
- Sundborg, A. (1950) : Local climatological studies of the temperature conditions in an urban area. *Tellus*, **2**, 222 – 228.
- *Sung, J. Y. (1977) : The urban system in Korean cities. *Geog. Rev. Japan*, **50**, 381 – 401.
- *Suzuki, H. (1966) : Climate and climatic classification of Japan ; in *Climatology*, Yoshino, M. M., Taimeido, 350pp.
- Terjung, W. H. and Louie, S. S-F. (1973) : Solar radiation and urban heat islands. *A. A. A. Geog.*, **63**, 181 – 207.
- *Tonuma, K. (1980) : *An index of population*. Shoukoku Pub. Co., 337pp.
- *Toritani, H. (1985) : Formation of cold air lake and cold air drainage in the Sugadaira basin, Nagano Prefecture, Japan. *Geog. Rev. Japan*, **58**, 67 – 79.
- Torrance, K. E. and Shum, J. S. W. (1976) : Time-varying energy consumption as a factor in urban climate. *Atmos. Environ.*, **10**, 329 – 337.
- Tyson, P. D. du Toit, W. J. F. and Fuggle, R. F. (1972) : Temperature structure above cities : review and preliminary findings from the Johannesburg urban heat island project. *Atmos. Environ.*, **6**, 533 – 542.
- Wanner, H. and Hertig, J. A. (1984) : Studies of urban climates and air pollution in Switzerland. *J. App. Met.*, **23**, 1614 – 1625.
- White, J. M., Eaton, F. D. and Auer, A. H. Jr. (1978) : The net radiation budget of the St. Louis metropolitan area. *J. App. Met.*, **17**, 593 – 599.
- Whiteman, C. D. (1982) : Breakup of temperature inversions in deep mountain valleys : Part I. Observations. *J. App. Met.*, **21**, 270 – 289.
- Whiteman, C. D. and McKee, T. B. (1982) : Breakup of temperature inversions in deep mountain valleys. Part II : Thermodynamic model. *J. App. Met.*, **21**, 290 – 302.
- *Yamashita, S. (1975) : A note on the radiation balance of an urban environment. *Geog. Rev. Japan*, **40**, 731 – 741.
- *Yamashita, S. (1981) : Casual factors of the urban heat island ; in *An applied climatological study on the urban climate formation*. Yamashita, S. (ed.), *Monbusho-kagakukenyuhiho-jokin-shikenkenkyu* (1), 88 – 94.
- Yamashita, S., Sekine, K., Shoda, M., Yamashita, K. and Hara, Y. (1986) : On relationships between heat island and sky view factor in the cities of Tama river basin, Japan. *Atmos. Environ.*, **20**, 681 – 686.
- Yap, D. and Oke, T. R. (1974) : Sensible heat fluxes over an urban area-Vancouver, B. C. *J. App. Met.*, **13**, 880 – 890.
- *Yoshino, M. M. (1960) : Recent researches on cold air drainage and cold air lakes. *Agr. Met.*, **15**, 161 – 165.
- Yoshino, M. M. (1975) : *Climate in a small area*. Tokyo Univ. Press, 549pp.
- *Yoshino, M. M. (1980) : Research on drainage due to cold air drainage from the view point of local climatology. *Saigai-no-kenkyu*, **11**, 124 – 135.
- Yoshino, M. M. (1981) : Change of air temperature distribution due to the urbanization in Tokyo and its surrounding regions. *Sci. Rept. Inst. Geoscience, Univ. Tsukuba, Sect. A*, **2**, 45 – 60.
- Yoshino, M. M. (1984) : Thermal belt and cold air drainage on the mountain slope and cold air lake in the basin at quiet, clear night. *Geojournal*, **8**, 235 – 250.

- *Yoshino, M. M. and Kai, K. (1973_a) : Change of air temperature in Japanese cities in the recent years and its relation to the synoptic weather patterns and population. *Tenki*, **20**, 489 – 497.
- *Yoshino, M. M., Kudoh, T. and Hoshino, M. (1973_b) : On the sea and land breeze at the Sea of Japan region. *Geog. Rev. Japan*, **46**, 205 – 210.

* In Japanese

In Korean

Environmental Research Center Papers

- No. 1 (1982) Kenji KAI: Statistical characteristics of turbulence and the budget of turbulent energy in the surface boundary layer. 54p.
- No. 2 (1983) Hiroshi IKEDA: Experiments on bedload transport, bed forms, and sedimentary structures using fine gravel in the 4-meter-wide flume. 78p.
- No. 3 (1983) Yousay HAYASHI: Aerodynamical properties of an air layer affected by vegetation. 54p.
- No. 4 (1984) Shinji NAKAGAWA: Study on evapotranspiration from pasture. 87p.
- No. 5 (1984) Fujiko ISEYA: An experimental study of dune development and its effect on sediment suspension. 56p.
- No. 6 (1985) Akihiko KONDOH: Study on the groundwater flow system by environmental tritium in Ichihara region, Chiba Prefecture. 59p.
- No. 7 (1985) Chong Bum LEE: Modelling and climatological aspects on convective boundary layer. 63p.
- No. 8 (1986) Kazuo KOTODA: Estimation of river basin evapotranspiration. 66p.
- No. 9 (1986) Abdul Khabir ALIM: Experimental studies on transient behavior of capillary zone. 76p.
- No. 10 (1987) Michiaki SUGITA: Evaporation from a Pine forest. 61p.
- No. 11 (1987) Hye-Sook PARK: Variations in the urban heat island intensity affected by geographical environments. 79p.

発行 昭和62年3月31日

編集・発行者 筑波大学水理実験センター

〒305 茨城県新治郡桜村天王台1-1-1

TEL 0298 (53) 2532

印刷 朝日印刷株式会社

〒308 茨城県下館市中館186